MICROCOPY RESOLUTION TEST CHART
NATIONAL BUREAU OF STANDARDS-1963-A

DAVID W. TAYLOR NAVAL SHIP RESEARCH AND DEVELOPMENT CENTER

Bethesda, Maryland 20084

DTNSRDC THREE COMPONENT LASER
DOPPLER VELOCIMETRY:
TOWING TANK SYSTEM MEASUREMENT ERRORS

DTIC
ELECTE
FEB 27 1986
S D

D

DAVID J. FRY

SHIP PERFORMANCE DEPARTMENT

DTIC FILE COPY

APRIL 25,1985

SPD-1163-03

MAJOR DTNSRDC ORGANIZATIONAL COMPONENTS

DTNSRDC

COMMANDER 00

TECHNICAL DIRECTOR 01

OFFICER-IN-CHARGE CARDEROCK 05	OFFICER-IN-CHARGE ANNAPOLIS 04
SHIP SYSTEMS INTEGRATION DEPARTMENT 12	
SHIP PERFORMANCE DEPARTMENT 15	AVIATION AND SURFACE EFFECTS DEPARTMENT 16
STRUCTURES DEPARTMENT 17	COMPUTATION, MATHEMATICS AND LOGISTICS DEPARTMENT 18
SHIP ACOUSTICS DEPARTMENT 19	PROPULSION AND AUXILIARY SYSTEMS DEPARTMENT 27
SHIP MATERIALS ENGINEERING DEPARTMENT 28	CENTRAL INSTRUMENTATION DEPARTMENT 29
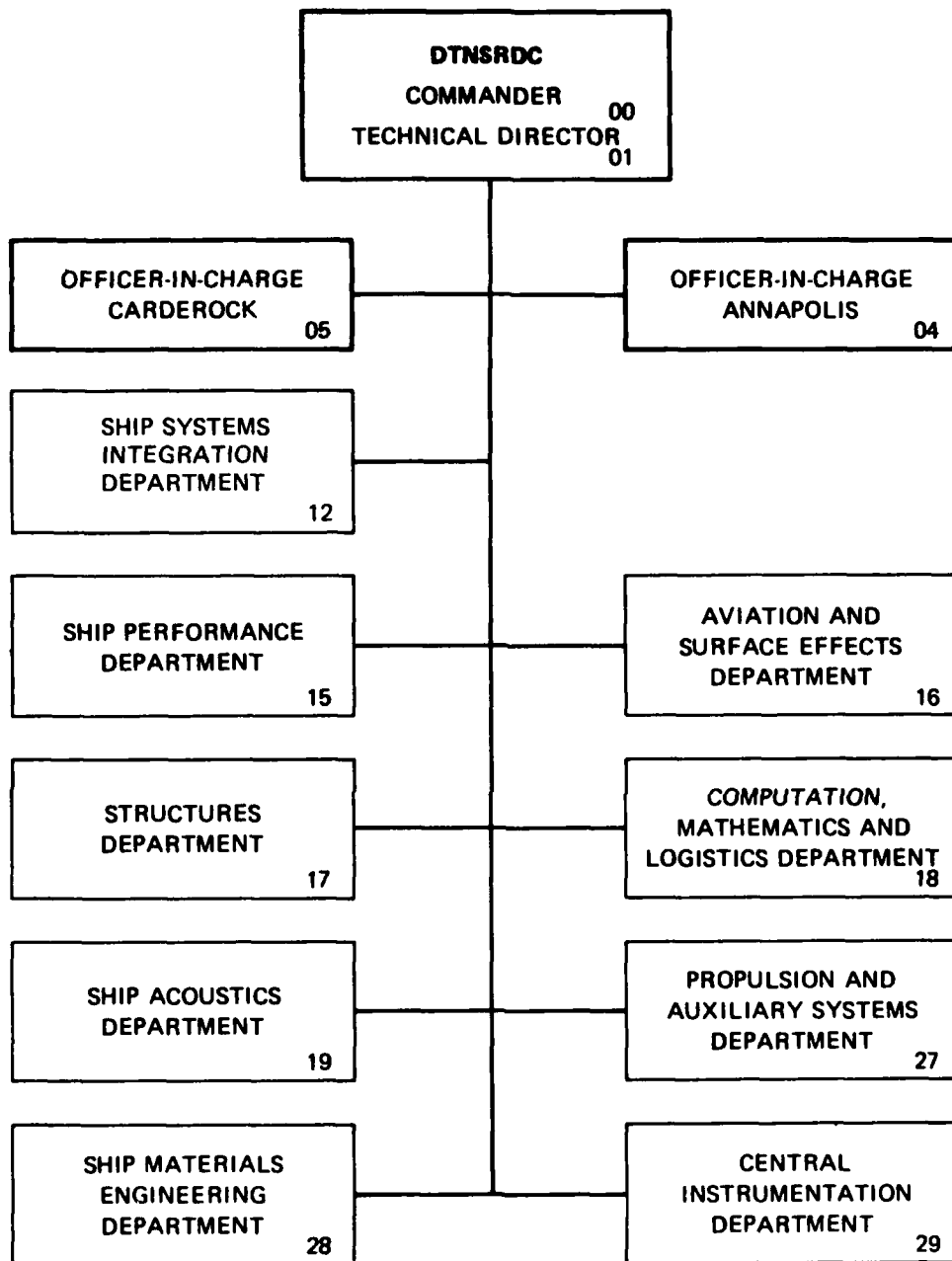
REPORT DOCUMENTATION PAGE

1a. REPORT SECURITY CLASSIFICATION Unclassified		1b. RESTRICTIVE MARKINGS			
2a. SECURITY CLASSIFICATION AUTHORITY		3. DISTRIBUTION / AVAILABILITY OF REPORT Approved for Public Release: Distribution Unlimited			
2b. DECLASSIFICATION / DOWNGRADING SCHEDULE					
4. PERFORMING ORGANIZATION REPORT NUMBER(S) DTNSRDC		5. MONITORING ORGANIZATION REPORT NUMBER(S)			
6a. NAME OF PERFORMING ORGANIZATION David W. Taylor Naval Ship Research and Development Center	6b OFFICE SYMBOL (If applicable) Code 1542	7a. NAME OF MONITORING ORGANIZATION			
6c ADDRESS (City, State, and ZIP Code) Bethesda, Maryland 20084-5000		7b. ADDRESS (City, State, and ZIP Code)			
8a. NAME OF FUNDING / SPONSORING ORGANIZATION Naval Sea Systems Command	8b OFFICE SYMBOL (If applicable) 05R24	9. PROCUREMENT INSTRUMENT IDENTIFICATION NUMBER			

8c ADDRESS (City, State, and ZIP Code) Dept. of Navy Washington, D.C. 20362	10. SOURCE OF FUNDING NUMBERS			
	PROGRAM ELEMENT NO. 62543N	PROJECT NO	TASK NO. SF43-421	WORK UNIT ACCESSION NO DN178066

11. TITLE (Include Security Classification)

Three Component Laser Doppler Velocimetry: Towing Tank System Measurement Errors

12. PERSONAL AUTHOR(S)
Fry, David J.

13a. TYPE OF REPORT Final	13b. TIME COVERED FROM _____ TO _____	14. DATE OF REPORT (Year, Month, Day) 1985, October, 1	15. PAGE COUNT 130

16. SUPPLEMENTARY NOTATION

17.　　　COSATI CODES			18. SUBJECT TERMS (Continue on reverse if necessary and identify by block number)
FIELD	GROUP	SUB-GROUP	Laser Velocimeter; Three Component Velocity Measurement; Towing Tank; Bias Errors

19. ABSTRACT (Continue on reverse if necessary and identify by block number)

A three - component Laser Doppler Velocimetry (LDV) system for the David Taylor Naval Ship Research and Development Center's towing carriages became operational in mid 1984. This is one in a series of reports to help experimenters efficiently use the new instrumentation. The series also serves as a repository for a large volume of information gathered while purchasing, testing, and optimizing this velocity measurement system. This particular report deals with mean velocity measurement errors: both minimizing them and quantifying what remains.

> Thirteen measurement errors are quantified in terms of: velocity field characteristics, LDV equipment design, and user - chosen system operating parameters. Operating parameter effects on measurement error are emphasized because usually they are the only way an experimenter can control errors.

Background sections and appendixes explain in considerable detail, the origin of these measurement errors. First, the operating parameter choices for the towing tank LDV (cont.)

20. DISTRIBUTION / AVAILABILITY OF ABSTRACT ☒ UNCLASSIFIED/UNLIMITED ☐ SAME AS RPT ☐ DTIC USERS	21. ABSTRACT SECURITY CLASSIFICATION UNCLASSIFIED	
22a. NAME OF RESPONSIBLE INDIVIDUAL David J. Fry	22b. TELEPHONE (Include Area Code) 301-227-5417	22c. OFFICE SYMBOL Code 1542

DD FORM 1473, 84 MAR
83 APR edition may be used until exhausted
All other editions are obsolete

system are listed with a description of how they affect measurements. Then, each of the measurement errors is discussed, and this helps establish a functional relationship to operating parameters, LDV equipment design, and flow field characteristics. Various appendixes support and amplify the information given.

Three user reference sections are included in this report. The first provides guidance in making operating parameter choices and measurement - error estimations prior to an experiment. The second describes how, during an experiment, the user can determine if proper parameter choices have been made. The last section details how final error estimates can be made after an experiment, for inclusion in written reports.

TABLE OF CONTENTS

TABLE OF CONTENTS

TABLE OF CONTENTS

LIST OF FIGURES

LIST OF TABLES

NOTATION

A,B,K	Constant factors
D	Diameter
D_{mv}	Diameter of LDV measurement volume
D_{e-2}	Standard laser beam diameter measurement
E	Error standard deviation
E_a	Velocity component directional error
E_c	Carriage speed measurement error
E_d	Timing digitization error
E_f	Fringe spacing determination error
E_{FrB}	Fringe bias error
E_{FiB}	Filter bias error
E_i	Flow disturbance error
E_L	Particle lag error
E_n	Signal noise error
E_s	Frequency shift value error
E_t	Velocity error due to traverse bending
E_v	Velocity fluctuation error
E_{VB}	Velocity bias error
F	Frequency
FS	Frequency shift
G	Function
M_f	Timed fringe crossings
N	Number of independent measurements
n	Particles per unit volume
N_f	Fringe crossings in measurement volume
P_x	Vertical positioning error
P_y	On-Axis positioning error
P_z	Streamwise positioning error
S	Fringe spacing
SG_p	Particle specific gravity
SNR	Signal - noise ratio parameter
T	Velocity component across D_{mv}, $(U^2 + V^2)^{0.5}$
T_{avg}	Measurement averaging time

T_B	Particle residence time in measurement volume
T_{d1}	Measurement electronic downtime
T_{d2}	Measurement particle downtime
$\vec{U}$	Water velocity vector
U	Streamwise velocity component
U_o	Towing speed
V	Vertical velocity component
Vol	Volume of LDV measurement region
W	On-Axis velocity component
x,y,z	Vertical, On-Axis, Streamwise coordinate direction
δ	Boundary layer thickness
λ	Light wavelength
σ	Standard deviation of velocity or frequency fluctuation
ν	Kinematic viscosity

SUBSCRIPTS

avg	Average measurement
B,G	Blue, green laser beams
f	Fringe
i	Individual measurement or realization
p	Particle
r	Raw data
Sig	Doppler signal
U	Streamwise component
V	Vertical component
Vel	Velocity
W	On-Axis component
x	Any component

SUPERSCRIPTS

$-$	Time averaged quantity
$\rightarrow$	Vector quantity

ABBREVIATIONS

CONT	Continuous measurement mode
DMA	Direct Memory Access
HDL-VAX	Harry Diamond Lab. VAX 11-780 Computer
KHz	Kilohertz
LDV	Laser Doppler Velocimetry
MHz	Megahertz
m	Meter
m/s	Meters per second
ms	Milliseconds
mV	Millivolt
ns	Nanoseconds
s	Seconds
SM/B	Single measurement per burst mode
SNR	Signal to noise ratio
TBC	Total burst count mode
TBM	Total burst measurement mode
μm	Micrometer
μs	Microseconds

ABSTRACT

A three - component Laser Doppler Velocimetry (LDV) system for the David Taylor Naval Ship Research and Development Center's towing carriages became operational in mid 1984. This is one in a series of reports to help experimenters efficiently use the new instrumentation. The series also serves as a repository for a large volume of information gathered while purchasing, testing, and optimizing this velocity measurement system. This particular report deals with mean velocity measurement errors: both minimizing them and quantifying what remains.

Thirteen measurement errors are quantified in terms of: velocity field characteristics, LDV equipment design, and user - chosen system operating parameters. Operating parameter effects on measurement error are emphasized because usually they are the only way an experimenter can control errors.

Background sections and appendixes explain in considerable detail, the origin of these measurement errors. First, the operating parameter choices for the towing tank LDV system are listed with a description of how they affect measurements. Then, each of the measurement errors is discussed, and this helps establish a functional relationship to operating parameters, LDV equipment design, and flow field characteristics. Various appendixes support and amplify the information given.

Three user reference sections are included in this report. The first provides guidance in making operating parameter choices and measurement - error estimations prior to an experiment. The second describes how, during an experiment, the user can determine if proper parameter choices have been made. The last section details how final error estimates can be made after an experiment, for inclusion in written reports.

1

ADMINISTRATIVE INFORMATION

The work described in this report was done at the David W. Taylor Naval Ship Research and Development Center (DTNSRDC) under a project for Laser Doppler Velocimeter System Development. The project was funded by the 6.2 Ship and Submarine Technology Program, Program Element 62543N, Task Area SF 43421, and DTNSRDC Work Unit 1506-253 (FY-84) and 1506-130 (FY-85).

INTRODUCTION

In the last quarter of fiscal year 1981 (FY-81), work began on a three-component Laser Doppler Velocimeter (LDV) system for all towing basins at DTNSRDC. It was envisioned that the primary use of the system would be to do ship wake surveys and measure mean velocities. A contract was awarded* to TSI Inc. to build the optics system.

Appendix 1 details the optical configuration. The optics system was completed and delivered to DTNSRDC in June 1982 for inspection and checkout. The system met all contract specifications.

A new contract was awarded** to TSI Inc. to develop a traversing system and data analysis system for the Towing Tank LDV.

The completed system was delivered and installed in July 1983. However, several performance specifications were not met. TSI took the system back, made modifications, and redelivered the system in March 1984 (Figures 1 and 2). This time the system was accepted.

The procedures and skills of aligning and setting up the system are not covered here. This information is available from:

1. Previous system users
2. DTNSRDC Departmental Report[1] ***
3. TSI Inc. manuals[2-7]

2

TYPICAL APPLICATIONS:
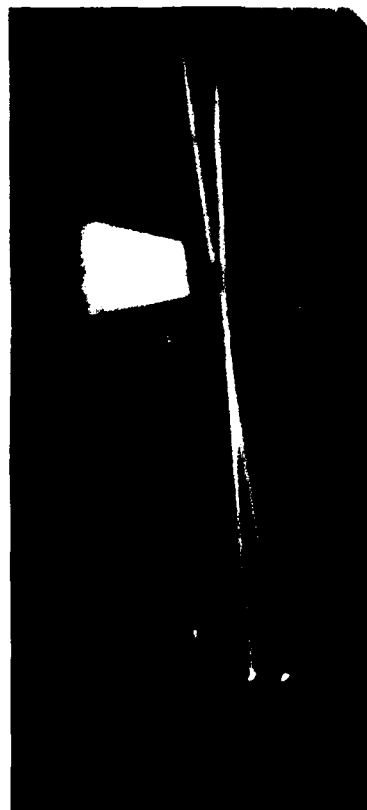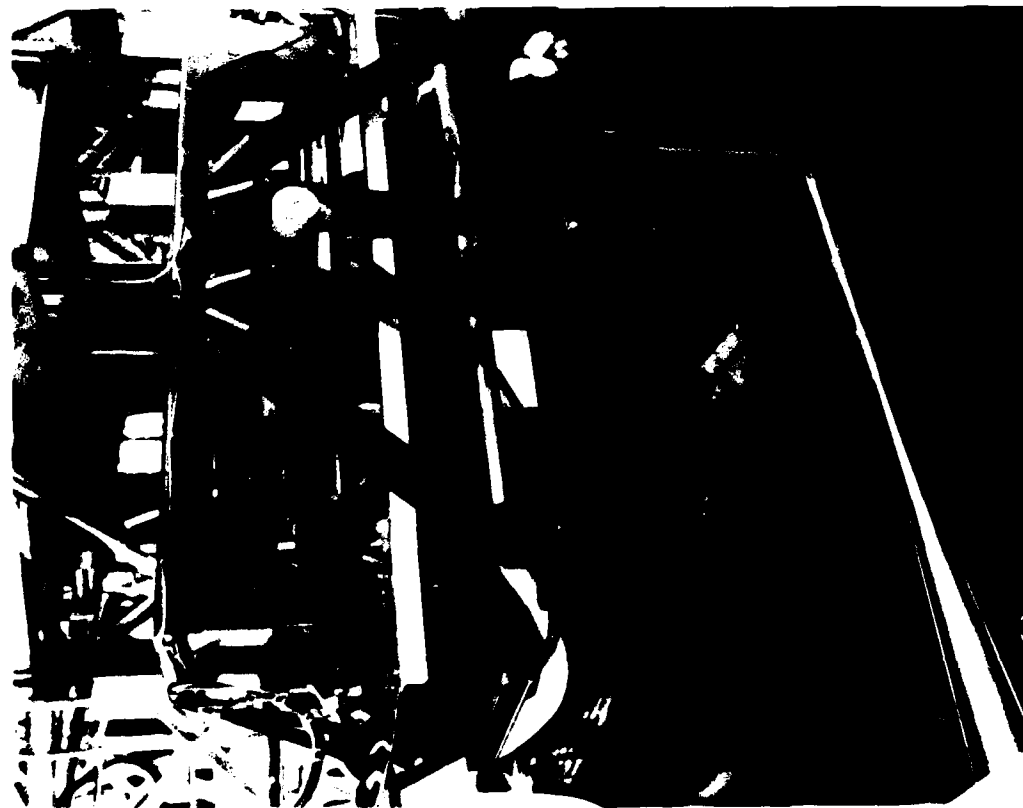
STERN - PROPELLER FLOW
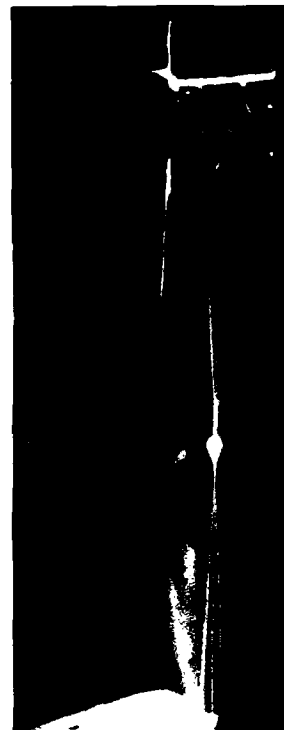
BULBOUS BOW FLOW

Figure 1: LDV Towing Tank System.
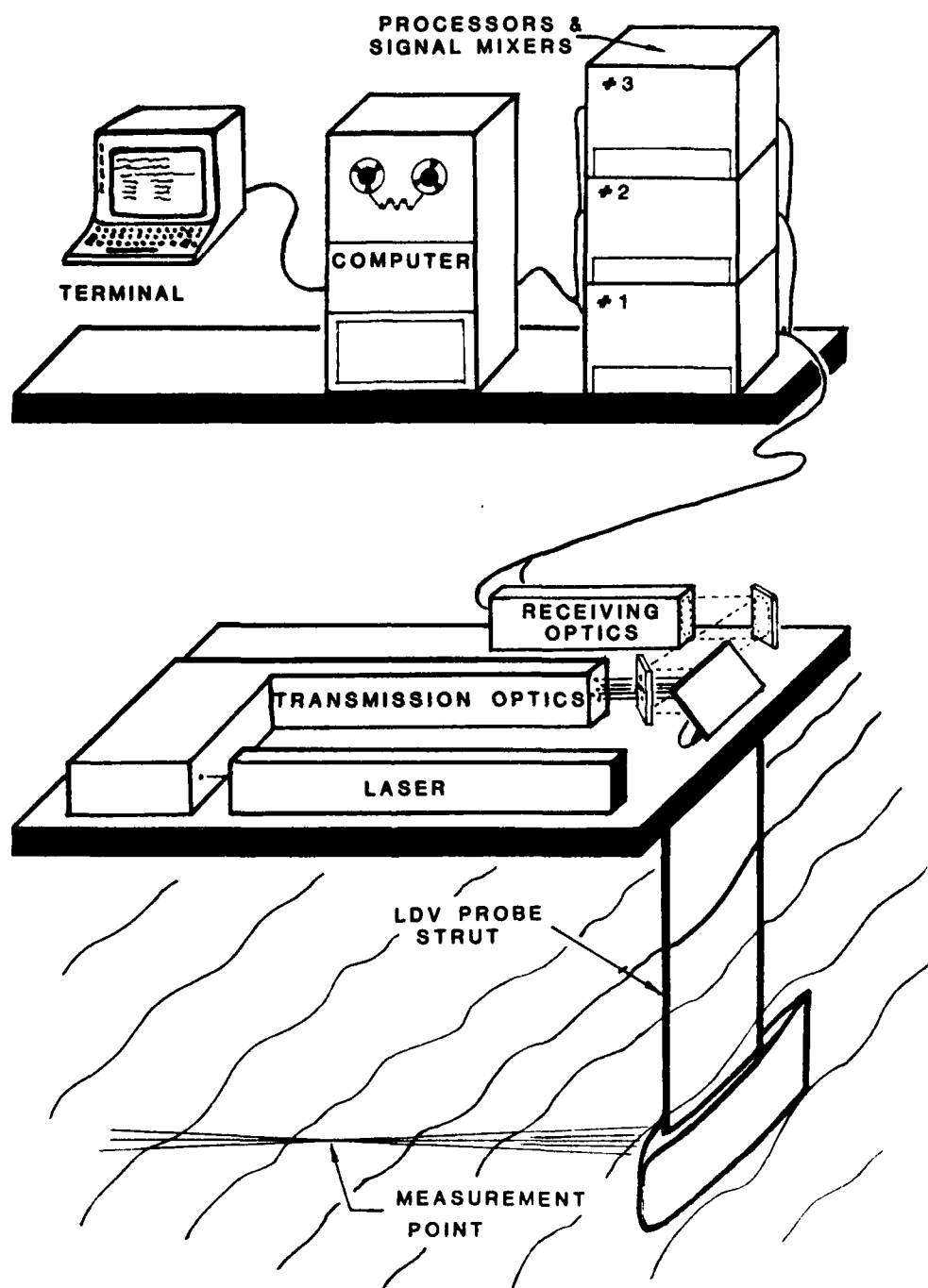
Figure 2: Towing Tank LDV System Schematic

There is essentially only one way to physically set up the system. However, once the LDV system is in place, users are confronted with many operating parameter choices before taking any data.

This report will guide users in making operating parameter choices as well as enable them to quantify the errors present in their measurements. Capabilities and errors are a function of the LDV equipment design and flow field characteristics. However they are also highly dependent on operating parameters chosen by users.

The sections of this report are comprised of two types:

1. Background Information
2. Reference Information

The following two sections supply background information. The first lists the operating parameter choices for the towing tank system and describes how they affect LDV measurements. The second lists possible measurement errors and establishes their functional relationship to operating parameters, LDV equipment design, and flow field characteristics. Various appendixes support and amplify the information given.

Three reference sections follow. The first provides guidance in making operating parameter choices and measurement error estimations prior to an experiment. The second describes how, during an experiment, the user can determine if proper parameter choices have been made. The last section details how final error estimates can be made after an experiment, for inclusion in written reports.

LDV OPERATING PARAMETERS

PRINCIPLES OF LDV MEASUREMENTS

Before the choice of various operating parameters can be made, the basics of the LDV measurement technique must be understood. The principles behind dual beam, LDV measurements are described in great detail in many publications[8,9,10]. The technique description that follows will be much briefer and less detailed.

Measurement Basics

LDV systems typically focus and cross a number of laser beams at a measurement "point". The towing tank system has five separate beams of two colors. Particles in the water, passing through the beam crossing region scatter light that the LDV system collects and utilizes in determining the particle and fluid velocity (if the particle "follows" the flow).

The determination of particle velocity is best understood in terms of interference "fringes" of light effectively set up within the beam crossing region. The fringes are a series of parallel, alternating light and dark planes. The intensity of the scattered light changes as the particle moves between light and dark fringes. The fringes have a uniform and accurately determinable spacing (fringe spacing, S, is a function of laser beam wavelength and beam crossing angles). A photomultiplier and an electronic signal processor determine the time required by the particle to cross a given number of fringes (Figure 3). This time is passed to the LDV system's computer for storage. Later, the computer is used to calculate a component of the particle's velocity by multipling the known fringe spacing and the fringe crossing frequency (obtained from stored time data). By looking at scattered light from different sets of beams, all three velocity components are determined.

Simple, stationary fringes allow determination of velocity component magnitudes. But there is still a need to distinguish between particles traveling at the same speed but in opposite

6

A. PARTICLE TRAVERSING MEASUREMENT VOLUME

B. ENLARGEMENT

C. PHOTOMULTIPLIER SIGNAL

PARTICLE IN LIGHTED PLANE

PARTICLE IN DARK PLANE

VOLTAGE

TIME

D. PROCESSOR SIGNAL AFTER HIGH PASS FILTERING

VOLTAGE

TIME

TIME FOR FOUR FRINGE CROSSINGS
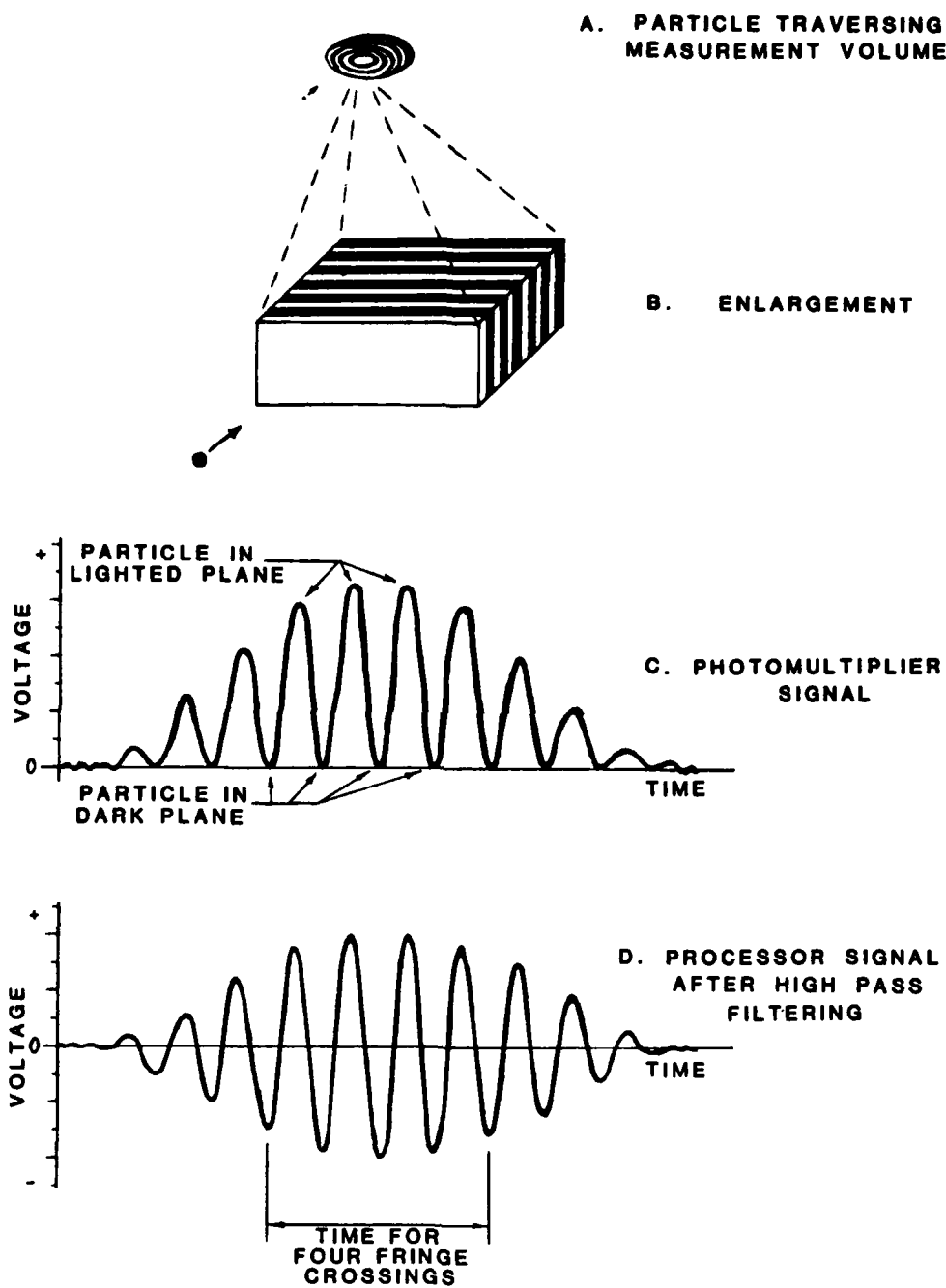
Figure 3: Signal Bursts in LDV Measurements

directions. If fringes could move and move fast enough, they would always sweep across particles in the same direction, regardless of the particle's direction of motion. A fringe speed greater than the fastest particle moving in the same direction would be required.

The towing tank LDV system effectively allows fringes for each component to move past a fixed point at frequencies (called a frequency "shift" or FS) between .002 and 10 MHz, inclusive. This frequency is precisely the frequency of scattered light intensity changes that the LDV system will measure for a stationary particle. Particles moving against the fringes will have higher frequencies. Particles moving in the same direction as the fringes will have lower frequencies. In data processing, the shift frequency must be subtracted from the measured frequency before multiplication by the fringe spacing yields the particle velocity. Any resulting negative velocities indicate particles moving with the fringes, while positive velocities indicate motion in the opposite direction.

Spatial Resolution

The LDV measurement signals only occur when a particle simultaneously scatters light from at least two laser beams. Thus, it is apparent that LDV measurements are particle velocities that occur somewhere within the laser-beam crossing region (henceforth called the "measurement volume"). Spatial resolution is at least as good as these measurement volume dimensions*. It should be noted that the scattered light from different sets of beams are used in determining each of the three components of velocity. Figure 4 indicates which beams are involved and the measurement volume dimensions for each component.

Laser beam cross-sections have no sharply defined edges. One

----

* Some LDV systems have scattered light receiving optics focused only on portions of the beam crossing region and therefore get better spatial resolution.

8
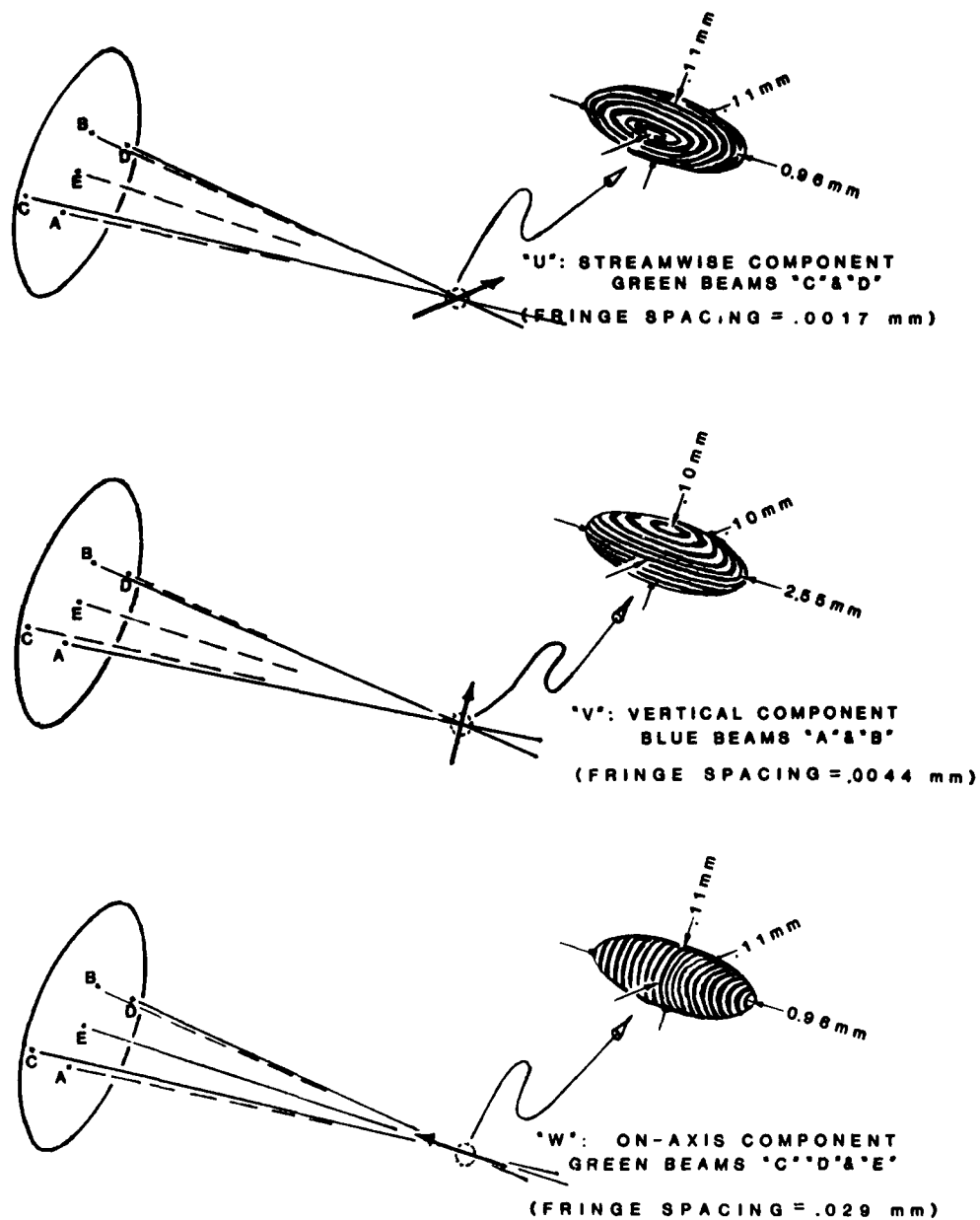
Figure 4: Measurement Volume Dimensions

9

beam diameter definition, "D_{e-2}," is based on the circle of points where the light is 13.5% of the intensity found at the beam center. Beams with a circular cross-section of diameter D_{e-2} are used in the geometric calculation of the measurement volume dimensions (Figure 4). A more meaningful definition of measurement volume boundaries is where some average sized particle has a scattered light signal just above detection thresholds.

Measurement Response Time

The signal processors and computer of the towing tank LDV system determine the particle and water velocity on the basis of timing "M_f" fringe crossings. Velocity changes that occur during the crossing of M_f fringes cannot be detected but are averaged together.

$$T_{avg} = M_f * S_U / (FS * S_U + U) \qquad (1)$$

where   U: measured velocity component[**]

S_U: component fringe spacing

Note that this averaging time is a function of both particle (or water) velocity and the operating parameter of frequency shift.

The signal processors also have an "electronic downtime" after each measurement due to the fringe timing circuits and the transmission of data to the computer. The manufacturer, TSI Inc. lists this downtime as:

$$T_{d1} = 8 \text{ } \mu s \qquad (2)$$

Separate velocity measurements cannot be made at time intervals less than $T_{d1} + T_{avg}$.

The response of the LDV system is limited also by the type of

---

[**] U is negative in the direction of moving fringes

10

signal processors used in the towing tank system. These counter type processors work best when only one particle is in the measurement volume at a time. Randomly arriving particles can only satisfy this condition if the measurement volume is frequently void of particles for periods longer than:

$$T_{d2} = D_{mv} / (U^2+V^2)^{0.5}$$ (3)

where D_{mv}: short axis dimension of LDV Meas. Vol.
U,V: velocity components (see Figure 4)

This period might be called a particle "downtime."

Velocity fluctuation frequencies greater than $1/(2*T_{d2})$ are not detectable by the LDV system under even optimal particle arrival rates. The towing tank system usually sees much slower particle arrival rates that greatly reduce the upper frequency limit (50 Hz or less) on detectable velocity fluctuations. However, if the fluctuations are repetitive (such as those due to a propeller rotating at constant RPM) velocity, change frequencies of $1/(2*T_{avg})$ are obtainable for data collected and averaged over repeated fluctuation cycles.

FREQUENCY SHIFT OPERATING PARAMETERS

This section describes the operating parameter choices allowed by the frequency shift components of the towing tank LDV system. These parameters are set by the orientation of Bragg cells in the LDV optics system and by push button controls on the accompanying electronic control boxes. The design and operation of the Bragg cells and their signal mixing electronics is covered extensively in TSI manuals.[5,6]

Different frequency shifts are not obtained by actually changing the speed of the moving fringes. The LDV optics system can use Bragg cells operating at only a single, unadjustable frequency. However, the LDV photomultiplier output signal (fixed frequency shift) can be

11

electronically mixed with a signal of different and adjustable frequency. The voltage signal obtained behaves like an LDV signal with a frequency shift equal to the difference between the Bragg cell and mixing signal frequencies [5]. This derived LDV signal, with its "effective" frequency shift, is used by the towing tank LDV signal processors.

Effective frequency shifts are available in the range of .002 to 10 MHz. Obtainable values are in discrete steps of .002,.005,.010,.02,.05,.10,.... The effective direction of fringe motion is also selectable. One additional fringe motion frequency is available for each velocity component when the mixing circuitry is bypassed (100 MHz for the streamwise component, 40 MHz for the vertical component, 20 MHz for the on-axis component). The direction is unchangeable in this case.

The frequency shift for each velocity component is chosen according to the range of expected velocities. The lowest frequency shift that allows M_f fringe crossings for these velocities is the choice that will usually minimize overall measurement error.

COUNTER PROCESSOR OPERATING PARAMETERS

The counter processors for the towing tank LDV are manufactured by TSI Inc. (Model 1990). There is a separate processor for each of the three velocity component channels. The LDV signal input into the processor is a voltage that varies almost sinusoidally (under noise-free conditions). Positive voltage peaks occur when the particle is passing through a light fringe and negative voltage peaks occur when a dark fringe is crossed. The magnitudes of the peaks are modulated by the position of the particle in the measurement volume. The largest magnitudes occur when the particle is illuminated most intensely, near the center of the measurement volume. A typical LDV signal (called a signal "burst") input to the processors is shown in Figure 3. The processor output is a digital signal containing the count of clock cycles (1 ns each) occurring while the particle crosses M_f fringes.

The counter processors have many different parameters that must be set. They can basically be divided into those that change the input signal and those that affect the fringe counting method. A very complete description of the processor and parameter settings is found in Reference 3. This section will provide only the details needed for later estimation of velocity measurement errors.

Signal Conditioning

A selected high pass and low pass filter are first applied to the LDV signal. Twelve settings are possible for each of the high and low pass filters[3]. Each setting has a minimum roll off of 30 dB/octave. These filters should be set to eliminate as much signal noise as possible and, yet, not filter out any of the expected signal frequencies.

A continuously variable gain control (-31 dB to +34 dB) is available. Signal voltage amplitudes must exceed counter thresholds of +/- 50 mV to trigger the timing circuitry. The upper limit on an acceptable gain setting is controlled by the necessity of keeping signal noise amplitudes well below the counter thresholds (to avoid spurious counts). Smaller signal gains and, hence, noise amplitudes reduce errors in the processor's timing of M_f fringe crossings.

Larger particles tend to produce more scattered light and, therefore, higher voltage input signals. An amplitude limit control throws away processor timings done on signals exceeding a maximum voltage. A good choice of this maximum voltage parameter can eliminate data from large particles not following the water flow.

Processor Operating Method

Three types of timings can be done by the processor on the LDV signal. A "primary fringe timing" counts the processor clock cycles over a set number, M_f, of fringe crossings. A "secondary fringe timing" counts the clock cycles over a smaller number of fringe crossings. The primary and secondary fringe timings occur simultaneously. Finally, a "burst timing" counts clock cycles over all of the fringe

13

crossings that a single particle makes as it crosses the measurement volume.

There are four "modes" of processor operation that can be chosen. Each uses the three timings in a different way. In continuous (Cont) mode, as many sets of primary and secondary fringe timings as possible are made on each particle (or signal burst). In each set, primary and secondary timings are compared for consistency. If consistent, the primary fringe timing and fringes counted (M_f) are the outputs.

In the single measurement per burst (SM/B) mode, only one primary and secondary fringe timing is made for each particle. They are compared for consistency. The single primary fringe timing and the fringes counted (M_f) are the outputs.

Total burst count (TBC) mode also has an output of a single primary fringe timing (if consistent with the secondary fringe timing); but instead of M_f, the total number of fringes encountered (as used in burst timing) is the output.

Finally, in the total burst mode (TBM) the burst timing and the total number of burst fringe crossings (if less than 256) are the outputs. There is no consistency check.

Separate from the mode selection switch is a fringe count setting. This sets the M_f value for primary fringe timing in the Cont, SM/B, and TBC modes. Values of 2, 4, 8, 16, 32, 64, or 128 can be selected. Secondary timings are done for $1/2$ M_f fringe crossings when M_f is less than 8. Otherwise 5/8 M_f fringe crossings are used. In the TBM mode the fringe count setting is the minimum number of fringe crossings for the burst timing measurement to be accepted as valid.

A "comparison %" control sets the allowable velocity difference when primary and secondary timings are checked for consistency. Greater differences cause the data to be thrown out. A comparison % value of 0 (indicating no consistency check) must be chosen for the TBM mode where no consistency check is possible.

The timer exponent control should be set on automatic for

14

maximum timing accuracy. Processor timings consist of a clock cycle count digitally stored as a 12-bit mantissa and a 4-bit exponent. The automatic setting insures that the mantissa count is as high as possible (and the exponent count is as low as possible). Conceivable timing errors of +/- 1 in the mantissa then have the least possible effect on measurement accuracy.

COMPUTER SYSTEM OPERATING PARAMETERS

This section describes the operating parameter choices encountered when transforming counter processor outputs into estimates of the three components of mean velocity. Some parameters deal with which and how many of the three counter processor outputs are accepted and stored (i.e., data acquisition). Other choices concern whether data corrections are made based on experimental calibrations (i.e., data correction). The rest of the parameters in this section deal with how the stored data is later manipulated to give the best possible estimate of the mean velocity (i.e., data manipulation).

Reference 4 details parameter selection and the operation of the DEC computer interface used in the towing tank LDV. Reference 7 gives a brief, global description of standard TSI software ("DRP-3") for data acquisition and manipulation. The software for the towing tank system is a modified version of DRP-3.

Data Acquisition

The control of the data flow from the counter processors to computer storage is done by Interface Modules (TSI Inc., Model 1998) and a direct memory access (DMA) board. This interface can operate in the random or in the coincidence mode. In random mode, data from any processor is sent as soon as it is ready. All processible signals received by each counter are stored except those that are ready

during the time of data transmission from a processor (a period of 8 μs^*). Coincidence mode data storage requires valid data points from all three counter processors at the "same time". The "same time" is arrival within a coincidence time window that can be set anywhere between 10 μs and 10 ms. The time window starts with the first valid data point from any processor. If data from the other two processors arrives within the time window period, all three data points are transmitted and stored.[**]

A computer interface option allows transfer of the time between measurements. An additional 16-bit word is sent with each measurement. It contains (when properly decoded) the time delay between valid measurements.

The final operating parameter in data acquisition is the number of valid measurements accepted at each measurement location. The sum of the contributions from each processor (or velocity component channel) can be set in computer software. Operation in a purely random transfer mode usually yields more measurements of some components than others. However, a device in the interface insures that 256, 512, 1024, or 2048 data points from each channel are transferred. An equal number of measurements in each channel (i.e., for each velocity component) is also assured if operation is in the coincidence mode. However, in this mode, finite - time windows mean some data points will be thrown away because of noncoincidence. Therefore, the rate of data transfer to the computer will be lower.

Data Correction

The collected data should usually be corrected in one or more ways based on calibration tests performed after the LDV system is in place. A few measurements taken before a test begins (and after

----

* Reflects instantaneous storage rate during the filling of certain finite buffers (32K 16-bit words)
** A required processor order can also be set.[4]

16

every subsequent LDV optics realignment) can yield corrections for
the effects of:

1. Velocity component directional alignment
2. LDV probe strut flow disturbance
3. Frequency shift and signal mixing accuracy

The LDV user can choose to later adjust his experimental results using these corrections.

Experience has shown that checking the directional alignment of
the on-axis component is especially important. Even very careful
optical alignment may allow directional errors of as much as 3°.

It is desirable to correct mean velocity estimates for the flow
disturbance of the LDV probe strut on the ship model flow field (Figure 2). Undisturbed velocity values are always sought in towing tank
tests. The actual flow disturbance will be different for every
experiment and for every measurement location. However, a first
order correction is possible. It is based on the measured velocity
disturbance induced at the measurement volume by towing only the LDV
probe strut.

The effective frequency shift may not always be exactly as
indicated by the shift controller. However in calculating
velocities, the computer software uses the indicated shift exactly.
This results in possible errors if no correction is made.

All of the above corrections are possible from calibration
velocities taken when the probe strut is towed alone. Then any
non-zero, mean velocity (in the vertical or on-axis direction) is due
to these uncorrected effects. Streamwise mean velocity differences
from the tow speed are also due to these same effects along with
fringe spacing measurement error.

Data Manipulation

The straight-forward arithmetic mean of measurements is not
always the best way to get accurate mean velocity estimates from
counter processor data. Because processor measurements are not

17

random samples of the water velocity, certain data biases affect arithmetic means of the data.

Processor measurements occur only when "measureable" (a minimum number of strong fringe crossings must be timed for a valid measurement) particles arrive at the measurement volume. The rate of particle arrival is a function of the velocity direction and magnitude (velocity bias). The "measureability" of any particle is a function of the particle velocity direction (fringe bias). Selected processor frequency filters may attenuate and reduce "measureability" of some valid LDV signal frequencies more than others (filter bias).

The LDV system computer software contains an option that through data manipulation can correct for velocity bias. The key to the correction is information on the measurement volume transit time for each particle. Thus, this correction can be done only if the processors are operated in TBC or TBM modes. Another method of bias correction[11] can eliminate both velocity and fringe bias if all three velocity components are measured coincidentally (i.e. within a time window shorter than that needed for significant velocity changes). Also, both fringe and filter bias can effectively be eliminated by proper choice of operating parameters already mentioned (particularly the channel frequency shift and counter processor input filter settings).

Finally, when large amounts of LDV measurements are taken, a small number of invalid measurements are sometimes also stored. Usually these invalid measurements (often caused by signal noise) are detectable because of their marked disparity with the overwhelming majority of the rest of the measurements. Measurement error analysis often assumes a Gaussian distribution of measurements about a mean and then applies "Chauvenets' Criterion"[12]. This eliminates data values that are too many standard deviations from the data mean and therefore unlikely to be part of the distribution of data. The computer software has data manipulation routines that allow such "invalid" data values to be found and eliminated.

OPERATING PARAMETERS SUMMARY

The operating parameter choices described in this section have come under three headings. Table 1 lists all the parameters under their appropriate heading for easy refeᵣence. Certain parameter choices should always be the same for towing tank LDV system setups. These choices are listed in Table 1 and will be assumed in the sections to follow.

TABLE 1 - TOWING TANK LDV SYSTEM PARAMETER CHOICES

```
FREQUENCY SHIFT OPERATING PARAMETERS:
    I-A     Frequency Shift.......................................    -
COUNTER PROCESSOR OPERATING PARAMETERS:
    II-A    Input Frequency Filters...............................    -
    II-B    Input Gain............................................    -
    II-C    Amplitude Limit.......................................    -
    II-D    Mode of Operation.....................................    -
    II-E    Mf or Fringe Crossings Counted........................    -
    II-F    Count Comparison Accuracy.............................    -
    II-G    Timer Exponent Control ..........................Automatic
COMPUTER SYSTEM OPERATING PARAMETERS:
    III-A   Random or Coincident Transmission.................. Random
    III-B   Time Between Measurements....................Not Stored
    III-C   Total Measurements per Location.......................    -
    III-D   Distribution of Measurement Among Components......... Equal
    III-E   Velocity Component Direction Correction...............    -
    III-F   LDV Probe Strut Flow Disturbance Correction..........    -
    III-G   Frequency Shift - Signal Mixer Correction............    -
    III-H   Velocity Bias Correction..............................    -
    III-I   Fringe Bias Correction...............................  None
    III-J   Filter Bias Correction...............................  None
    III-K   Erroneous Data Elimination............................    -
```

VELOCITY MEASUREMENT ERRORS

In this section, contributors to towing tank LDV velocity measurement error will be examined and quantified. They are divided into three groups. The first group of errors affect the accuracy of individual particle velocity component measurements. The second group of errors affect the accuracy of transforming those particle measurements into fluid mean velocity estimates. The third group enters through the manipulations necessary to obtain final (with corrections), dimensionless (based on towing speed), undisturbed (by LDV probe strut), mean velocities.

Error magnitudes cannot be discussed as if they have a certain value. Rather sets of individual measurements and sets of mean measurements will have a distribution of values about the true mean value. Error magnitudes (|measurement - true mean value|) have a related distrubition. This section will characterize velocity-component error distributions by calculating their standard deviations (nondimensionalized by the towing speed).

ERROR CHARACTERISTICS

Individual error characteristics suggest how they can be combined into an overall measurement error estimate. How often an error changes in value is one such characteristic. Errors are classified as "fast" or "slow changing", depending on how frequently their value at a location changes significantly during a typical measurement time (5 to 20 s).

The contribution of "fast changing" errors to the mean measurement error gets smaller as the set of averaged measurements grows larger. If the probability density function of the "fast" errors form a Guassian distribution about a mean of zero, then the Central Limit Theorem of classical statistics applies. The standard deviation of error from averaged measurements can be simply related to the standard deviation of individual measurements and the number of measurements averaged, as follows:

$$E_{avg} = E_{ind} / (N)^{0.5} \tag{4}$$

where   N   :   number of independent measurements averaged

E_{avg}: Std. Dev. of error *from averaged measurements*

E_{ind}: Std. Dev. of individual measurements

"Slow changing" errors have one value for all individual measurements taken at a given location. The error for measurement averages is the same as the individual measurement errors and is independent of the number of individual measurements averaged.

Errors are also classified as "position dependent" or "position independent" according to whether their magnitude changes significantly within the measured flow field. Accuracy effects of position dependent errors can often be reduced if regions of large error can be anticipated or detected. LDV operating parameters can be changed to values (not applicable to the flow field as a whole) which will enhance accuracy in a particularly troublesome region.

Table 2 lists possible measurement errors, their classification, and the inputs that determine their magnitude. All three sets of inputs are required for analysis of measurement errors. These inputs are:

1. Operating Parameters
2. Flow Field Characteristics
3. LDV Equipment Characteristics

INDIVIDUAL PARTICLE VELOCITY ERRORS

LDV measurement systems really measure the speed of small particles traveling with a fluid. The following four sources of error can affect the accuracy of the particle velocity component measurements.

Signal Noise Error

Random noise in the scattered light signal will cause velocity measurement errors. A noise-free signal leaving the system

21

TABLE 2 - TOWING TANK LDV SYSTEM ERROR DETERMINATION

MEASUREMENT ERRORS	CHARACTERISTICS				ERROR INPUTS		
	Fast	Slow	Pos. Dep.	Pos. Indep.	Operating Parameters	Flow Field	Equip-ment
INDIVIDUAL PARTICLE VELOCITY ERRORS:							
1. Signal Noise	X		X		I-A,II-A,II-B, II-D,II-E,II-F, III-K	d,e	-
2. Time Digitization	X			X	I-A,II-D,II-E	a	-
3. Fringe Spacing		X		X	-	-	3
4. Freq. Shift Value		X		X	I-A,III-G	-	1
MEAN FLUID VELOCITY ERRORS:							
5. Particle Lag	X		X		II-C	b,d	-
6. Velocity Fluctuation	X		X		II-D,III-C	a	-
7. Velocity Bias		X	X		II-D,III-A,III-H	a	-
8. Fringe Bias		X	X		II-B,II-D,II-E, III-A,III-I	a	-
9. Filter Bias		X	X		I-A,II-A,III-J	a	-
FINALIZED FLUID VELOCITY DATA ERRORS:							
10. Carriage Speed		X		X	-	-	2
11. Velocity Component Direction		X		X	III-E	-	3
12. Flow Disturbance		X	X		III-F	c	4
13. Traverse Positioning Error		X	X		-	c	5

KEY TO ERROR INPUTS:

Operating Parameters:
(See Table 1.)

Flow Field Characteristics:
a. Velocity fluctuation at measurement
b. Local velocity gradients
c. Towed model velocity field
d. Light scattering seed particles
e. Solid surface proximity to measurement point

Equipment Characteristics:
1. Frequency shift - signal mixer calibration
2. Carriage towing speed measurement
3. Angle measurement of laser beams
4. Fringe pattern size and shape
5. LDV traversing accuracy

photomultiplier has nearly a sinusoidal voltage variation (Figure 3).
Real signals have random noise (mean value of zero) added from vari-
ous light and electronic sources. The LDV system signal processors
time M_f fringe crossings where a fringe is assumed crossed when the
voltage signal is zero. Errors result when the first or last of the
timed "zero-crossings" is advanced or retarded by the signal noise.

Only random noise signals that change during the M_f fringe count
will cause this error. So this error must be considered "<u>fast chang-
ing</u>". Because a portion of the random noise is derived from noise in
the received scattered light this error source is "<u>position
dependent</u>". Measurement points near solid surfaces, for example, can
be expected to have more scattered light noise.

Every LDV signal burst measured has its own SNR or
"signal-to-noise ratio", which is defined here to be the ratio of the
LDV signal amplitude (peak) to the standard deviation of the imposed
random noise. Error distributions for both starting and for stopping
the timing of M_f fringe crossings are equal and independent. If the
LDV signal is assumed to be sinusoidal, then the resulting error in
particle velocity component has a zero mean and dimensionless
standard deviation of:

$$E_n = |(F_{Sig}*S_x/U_o) * (1.41 * sin^{-1}(1/SNR)) / (2*\pi*M_f)| \qquad (5)$$

where F_{Sig}: measured signal frequency
   S_x : U, V, or W component fringe spacing
   U_o : towing speed

Note that increased SNR and increased fringe counts (M_f) will
reduce this error. However, simply increasing the frequency shift to
allow counting more fringes generally does not reduce the error.
There is a canceling effect between increased M_f values possible and
the increased signal frequency, F_{Sig}.

Towing tank LDV signal-to-noise ratios have a wide distribution
due to different particle sizes and trajectories. They also differ

between velocity components and depend on counter processor adjustment (Table 2). Thus this formula will not be used to directly estimate signal noise error. Rather, experimental particle velocity component data (discussed in the time digitization error section) will allow a calculation of typical towing tank SNR values from measured error standard deviations. Table 3 lists the results.

TABLE 3 - DETERMINATION OF TYPICAL COMPONENT SNR VALUES

Variable	Streamwise Component "U"	Vertical Component "V"	On-Axis Component "W"
$(E_n^2 + E_d^2)^{0.5}$	0.0099	0.0048	0.0460
Timing Digitization Error: E_d	0.0002	0.0002	0.0011
Signal Noise Error: E_n	0.0099	0.0048	0.0460
$F_{Sig} * S_x / U_o$	1.000	0.683	4.78
Typical SNR Values (eq.# 5)	2.9	4.0	1.6

Timing Digitization Error

The digital data transferred from the LDV signal processors to the data processing computer is 16-bits long with a 12-bit mantissa and a 4-bit exponent. The 16-bit word represents the time needed for a particle to pass M_f fringes in the measurement volume. The processor insures (with automatic exponent control) that the 12-bit

24

mantissa is a number somewhere between 2048 and 4096[*] with an accuracy of +/- 1.

The digitization error changes with every particle measurement ("fast changing"). The error is purely random and independent of fluid mean velocity and measurement volume location ("position independent").

A mantissa error that is equally likely to be +1, 0, or -1 is assumed. The mantissa value is equally likely to take on any value between 2048 and 4096. Then the digitization error in particle velocity components has a mean of zero and dimensionless standard deviation of:

$$E_d = (2/3) * (\sum_{I=2048}^{4096} (1/I) / 2048) * (F_{Sig} * S_x / U_o) \qquad (6)$$

$$= 2.3 * 10^{-4} * (F_{Sig} * S_x / U_o)$$

This error and the signal noise error are the only two "fast changing" errors affecting particle velocity component measurements. Thus in a steady flow, the scatter of measured particle velocities about the true mean is a result of only these errors. Typical values for the standard deviation of particle velocity components appear in Table 3. These were taken when no towed model was present to disturb the flow or introduce noise from reflected laser beams. The towing speed was 3 m/s and there were fixed frequency shifts on all components (U: 0.0 MHz; V: 0.5 MHz; W: 0.5 MHz). After reducing the error due to digitization effects (insignificant), typical component SNR can be calulated using Equation (5). These also appear in Table 3. Note that the following operating parameter choices help increase these SNR values and are recommended for general use:

1. Fringe counts, $M_f > 4$
2. Count comparison = 1%

----

[*] For measured frequencies, F_{Sig}, less than 3.9 MHz

3. Signal gain holds interburst noise to within +/- 25 mV

4. Erroneous data eliminated by Chauvenet's criterion

Fringe Spacing Determination Error

Particle speed determination require an accurate value for the fringe spacing. For a properly aligned LDV system[*], fringe spacing is uniform and depends only on the laser light wavelength in water and the laser beam crossing angle. The laser light wavelengths are known to within +/- .04% (Appendix B). Determination of the beam crossing angle will not be as accurate.

A new beam crossing angle is possible only when the LDV optics are realigned. The optics should not be realigned during the course of an experiment. Thus, this error is "slow changing" and "position independent".

The suggested fringe spacing determination technique is to measure a solid surface speed (spinning wheel) underwater. The wheel is spun by a precisely controlled stepper motor (Figure 5a) and has a rim speed of 0.2815 +/- .0001 m/s. This error estimate results from wheel diameter measurement inaccuracies (0.001 in. or 0.05% of the diameter). LDV signal noise also contributes to the fringe spacing error. The average of at least 750 frequency measurements (with no effective frequency shift) are recommended for the vertical and streamwise spacing determination.

$$S_U = 0.2815 \ (m/s) \ / \ F_U \ (Hz) \tag{7a}$$

$$S_V = 0.2815 \ (m/s) \ / \ F_V \ (Hz) \tag{7b}$$

The determination of on-axis fringe spacing is calculated based on the streamwise fringe spacing and green beam wavelength (λ_G = $0.3859*10^{-6}$ meter for 18° C.; see Appendix B) underwater.

----

[*] Fringe spacing can change across the measurement volume if beam focal points and crossing points do not coincide.

Alignment Block:
- 1.5 m from Lens
- Reflected Beam
  Coincidence Accuracy .5mm

$S_x = \lambda / 2 \sin X$

λ: beam pair wavelength
   in water

S_x: fringe spacing

Lens:
- 600 mm
  focal length

Mirror:
- Range = 15°
- Accuracy = .014

360 mm

Mirror

Mirror:

Figure 5b: Alternate Fringe Spacing Measurement Scheme

$X = .2815(m/s)/f_x \text{ (Hz)}$

Vertical
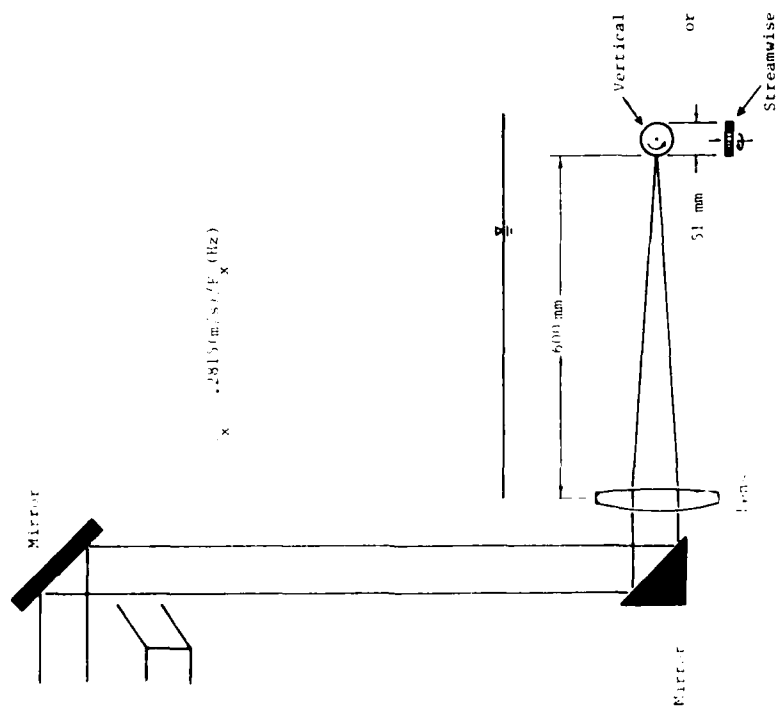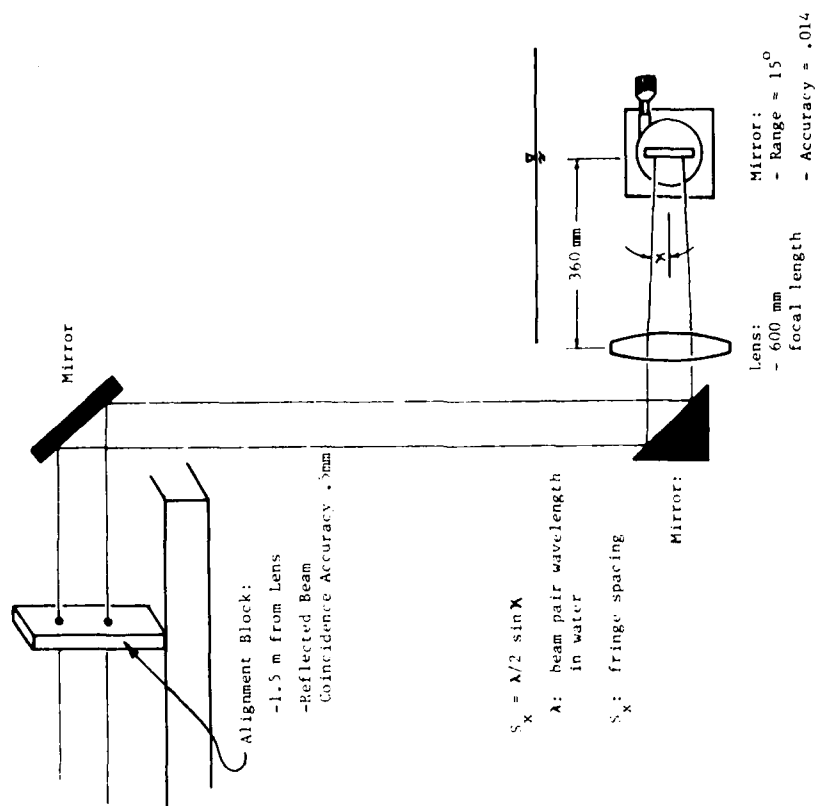
or

Streamwise

600 mm

51 mm

Mirror

Mirror

Figure 5a: Suggested Fringe Spacing Measurement Scheme

Figure 5 – Fringe Spacing Measurement Schemes.

27

$$S_W = \lambda_G \; / \; (2*\sin(\; \sin^{-1}(\; \lambda_G/2S_U)/2 \;))^2 \hspace{2cm} \text{eq.\#7c}$$

The wheel-speed error and exhibited measured frequency repeatability (standard deviation of 0.06% of mean) suggest a fringe-spacing-determination error with mean of zero and standard deviation of:

Streamwise or "U" Component:
$$E_f = 7*10^{-4} * U/U_o \hspace{4cm} (8a)$$

Vertical or "V" Component:
$$E_f = 7*10^{-4} * V/U_o \hspace{4cm} (8b)$$

On-Axis or "W" Component:
$$E_f = 14*10^{-4} * W/U_o \hspace{4cm} (8c)$$

An alternate scheme for determining fringe spacings is to directly measure beam crossing angles as illustrated in Figure 5b. The magnitude of error in the angular measurement is the same for green and blue beam pairs. So, fringe spacing determinations for the streamwise direction (larger χ value) are more accurate than for the blue beams. This method for vertical fringe spacing is inadequate because angular determination errors on the order of 1% are possible. In a test, the streamwise (or green beam) fringe spacing determined in this way was only 0.2% different from the spacing found from the spinning wheel. In the same test, the vertical fringe spacing determinations differed by 0.5%.

Frequency Shift Value Error

TSI, Inc. (the LDV system manufacturer) rates their effective frequency shifts to be accurate to within +/- 0.01%. The frequency shift must be subtracted from the measured signal frequency before the remainder is multiplied by the fringe spacing to obtain the particle speed.

It is uncertain how fast the frequency shift error changes. It will be assumed to be "slow changing" because of aging electronic

components. The error is "position independent" because it is purely a result of electronic component operation.

Assuming a uniform error distribution between +0.01% and -0.01%, the frequency shift error in particle velocity components has a mean of zero and a standard deviation of:

$$E_s = (.0001/1.73) * (F_{Sig}*S_x/U_o) \qquad (9)$$
$$= 5.8*10^{-5} * (F_{Sig}*S_x/U_o)$$

Summary of Particle Velocity Errors

The four particle velocity component errors of this section are independent. Three of the errors depend similarly on signal frequency measured and the component fringe spacing term $(F_{Sig}*S_x/U_o)$. This is because these errors directly affect the measured signal frequency, F_{Sig} and not the frequency directly proportional to particle velocity, $(F_{Sig}-FS)$.

Two of the errors are "fast changing" and will be reduced by taking the mean of multiple samples of the particle velocity. The two "slow changing" errors will not be reduced in multiple sample means. In most situations E_n and E_f will far outweigh the other two errors. Table 4 conveniently displays this information.

MEAN FLUID VELOCITY ERRORS

The towing tank LDV system was intended to obtain the 3 component, mean water velocity in the flow field around ship models. This section describes additional errors introduced when turning the particle velocity measurements of the previous section into mean water velocity estimates.

Particle "Lag" Error

This error represents the difference between particle velocity and the local water velocity. The ability of a particle to "follow" precisely the local flow field is a function of the particle's size

TABLE 4 - PARTICLE VELOCITY COMPONENT ERROR FORMULAS

| | Character | | Component Velocity Errors | | |
	Fast	Slow	Streamwise	Vertical	On-Axis
E_n:	X		$0.132*F/(U_0*M_f)$	$0.230*F/(U_0*M_f)$	$4.42*F/(U_0*M_f)$
E_3:	X		$.0004*F/(U_0*M_f)$	$.0010*F/(U_0*M_f)$	$.0066*F/(U_0*M_f)$
E_f:		X	$.0007*\|U/U_0\|$	$.0007*\|V/U_0\|$	$.0014*\|W/U_0\|$
E_s:		X	$.0001*F/U_0$	$.0003*F/U_0$	$.0017*F/U_0$

KEY:

F : component signal frequency in MHz

U_0: towing speed in m/sec

M_f: signal processor fringe count

and weight and of water accelerations near the measurement point. Figure 6 shows the density and size distribution of the seed particles initially chosen for towing tank LDV measurements.

The amount of particle lag, at a given measurement location, can change as fast as the velocity field ("fast changing"). However, in the presence of some persistant fluid flow structures (e.g., a trailing vortex from a lifting surface, the expected value of the error is not zero ("slow changing"). Particle lag errors are "position dependent" because they result from the local fluctuating and/or mean water velocity.

Several analyses concerning particle lag are done in Appendix C. The first analysis considers the particle's local velocity to have a steady mean and a sinusoidal variation with time. Particles tend to
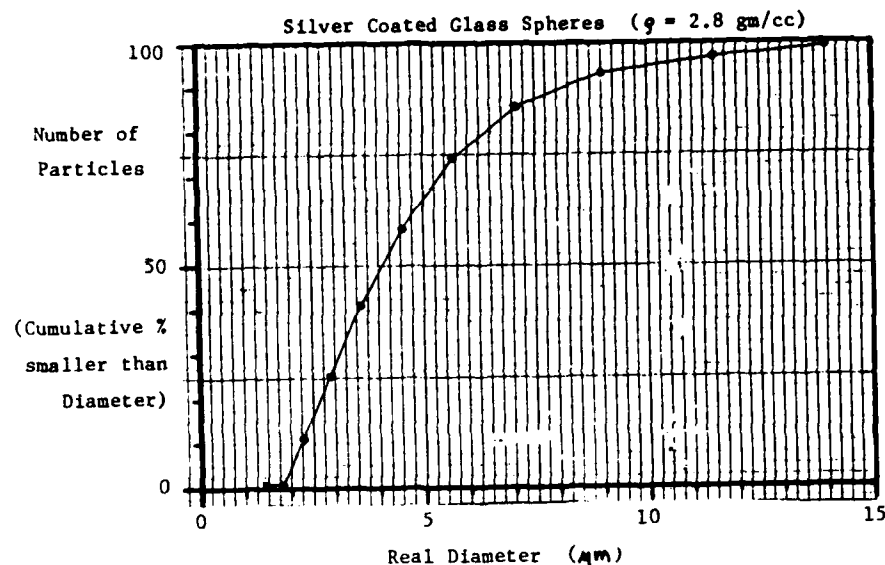
Figure 6 Diameter Distribution of Seed Particles

follow this fluctuation due to viscous forces*. Stoke's flow about a spherical particle is assumed. The particle follows the flow with a sinusoidally varying velocity that differs in amplitude and phase from the water velocity. The difference is a function of the particle size and density. Figure 7 shows the amplitude error (E_{L1}) for an assumed fluctuation magnitude and a fluctuation frequency of 1 KHz. It is based on the following equation derived in Appendix C.

$$E_{L1} = 3.88*10^{-2}*F_{Vel}^2* SG_p^2 * D_p^4 * \sigma_x / (U_o * \gamma^2) \tag{10}$$

where F_{Vel}: frequency of velocity fluctuations
SG_p : particle specific gravity
D_p : particle diameter
σ_x : std. dev. of velocity fluctuation
γ : kinematic viscosity of water

----

* Low Reynold's numbers result from the particle size.

31

Assumptions:
SG_p = 2.8
σ_x/U_o = 0.1
f_x = 1000 Hz
U_o = 3.0 m/s
δ = .15 m

E_{L2}/U_o

E_{L1}/U_o

E_{L1}/U_o or E_{L2}/U_o

TOWING TANK SEED SIZE DISTRIBUTION

1% 11% 15% 15% 17% 16% 12% 7% 3%
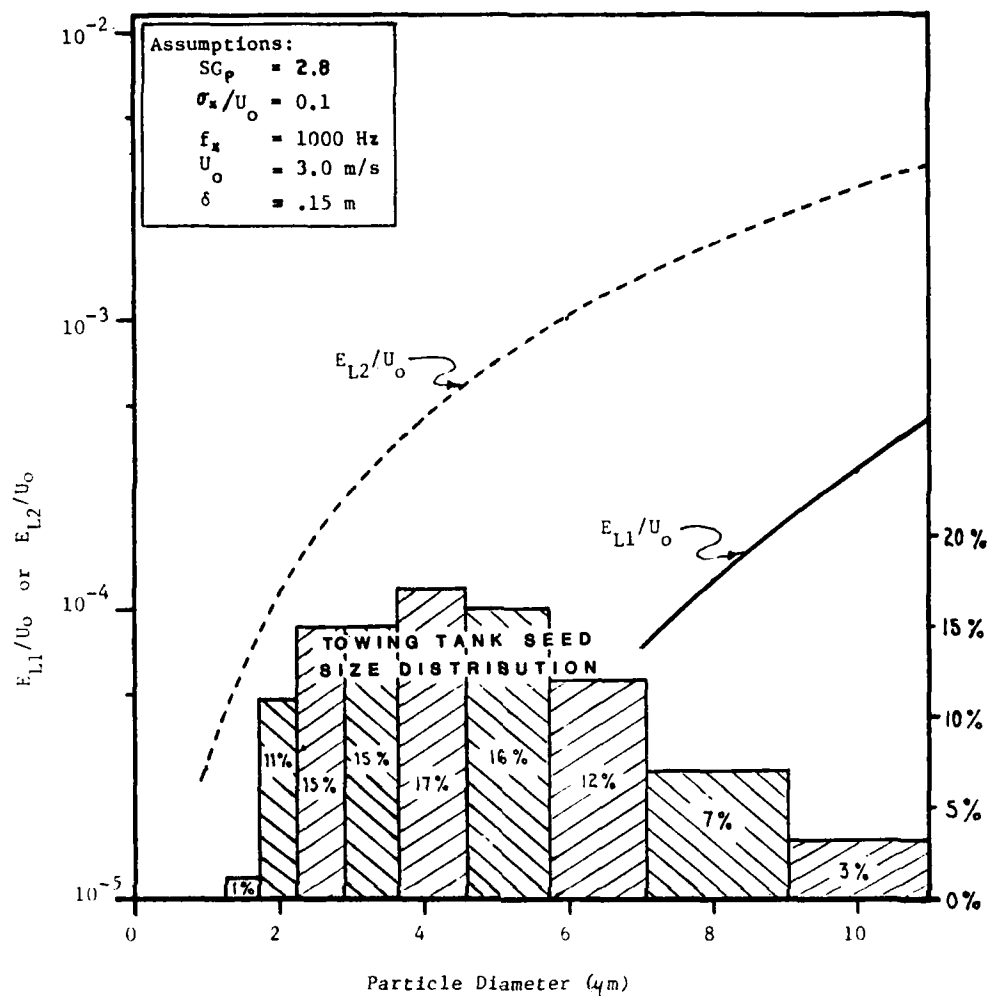
Particle Diameter (μm)

Figure 7: Estimates of Particle Lag Error

A second analysis (Appendix C) examines particle lag in vortical flows where the difference in fluid and particle velocities is found as a function of expected particle seed accelerations. The acceleration due to large scale eddies (length scale of wake boundary layer thickness and velocity scale of the towing speed) and the smallest detectable eddies (length scale of LDV measurement volume are both considered. It is shown that the smaller scale eddies in this analysis cause the most particle lag. Figure 7 contains curves showing the results of the lag error calculation for certain assumptions.

32

It is based on:

$$E_{L2} = (U_O * SG_p * D_p^2) / (18 * \gamma * (\xi^2 * 2 * D_{mv})^{0.33})$$ (11)

where ξ : boundary layer thickness

No estimate of error is made for persistant, large vortices. These can be evaluated only after some velocity measurements of the particular flow structure have been taken. Also, note that because of this centrifugal effect, the inner radii of vortices will have fewer and smaller particles. This could be a source of "bias" in addition to those listed in Table 2.

A generally applicable estimate of particle lag error magnitude can be made by arbitrarily combining the two separate lag error estimates:

$$E_L = (E_{L1}^2 + E_{L2}^2)^{0.5}$$ (12)
$$= ((3.9 * 10^{-4} * \sigma_x / U_O)^2 + (3.4 * 10^{-4} * U_O)^2)^{0.5}$$

where U_O, σ_x: velocities in m/s
         F_{Vel} = 1000 Hz
         D_p = 6.0 um
         SG_p = 2.8
         ξ = 0.15 m

Velocity Fluctuation Error

This error occurs because the LDV averaging time, T_{avg} is shorter than the time needed for significant velocity fluctuations. Velocity measurements differ from the desired mean value because of turbulence and blade rate fluctuations near ship propellers. This error is "fast changing" because velocity fluctuations are expected to occur much faster than the measurement period (2 - 10 seconds).

Both the frequency and magnitude of velocity fluctuations will change with measurement position ("position dependent").

An estimate of the error standard deviation must come from knowledge of the local velocity fluctuations.

$$E_v = \sigma_x / U_o \tag{13}$$

where σ_x: standard deviation of fluctuating velocity component

Bias Errors

The towing tank LDV, as a measurement technique, samples the water velocity only when a particle passes through the measurement volume and crosses M_f fringes. This complicates the determination of mean velocities because some velocity magnitudes and directions will tend to offer up measureable particles at a greater rate than others. The result is that in a fluctuating velocity field, a simple average of particle measurements is biased from the true mean velocity toward these more "favorable" velocity magnitudes and directions.

Because bias errors are errors in mean velocity estimates, they are "slow changing". Their dependence on the magnitude of velocity fluctuations and the distribution of particles makes them "position dependent".

Much bias is eliminated if the particles are distributed uniformly in the measured fluid. The degree to which particle uniformity is achieved in the towing basin under standard operating procedures (i.e., seeding only on return passes and 15 minute towing cycles) is not quantitatively known. Seed is sprayed uniformly over a 0.5 m. wide strip centered in the range of measurement locations and reaching the length of the basin. Seed is sprayed nearly every return pass, so that seed falling from the measurement region is gradually replaced and not introduced in large concentrations. Observations of seed across the entire basin width have been made after only 4 seeding cycles. It is believed that these procedures

34

and observations ensure uniform seed distribution vertically and streamwise. There probably is a measureable seed concentration from side to side, but not a significant one over the central meter wide volume of water that can conceivably pass through the LDV measurement volume. Aquisition data rates (away from solid surfaces) have not shown any noticeable dependence on measurement location.

Even if particle distribution biases are insignificant, potentially important biases remain. Dimotakis[11] derives an expression for the mean rate that particles moving with a given velocity will produce an LDV measurement. Appendix D extends Dimotakis' work to the 3 component, frequency shifted LDV towing tank system. That mean measurement rate, calculated by knowing instantaneously all three components of velocity, can be used to weight individual particle velocity measurements. The weighting allows an unbiased estimate of the mean fluid velocity (if all occurring velocities are measureable to some extent).

The calculated mean measurement rate of Reference 11 is conveniently split into the product of two functions of the particle velocity. The first function $G_v(\vec{U})$ is the mean number of particles passing through the measurement volume per unit time. The second function, $G_f(\vec{U})$, is the fraction of the arriving particles that produce a measureable signal (i.e., those that cross a minimum of M_f fringes). Velocity measurements normalized by G_v are free of what is usually called "velocity bias". Velocity measurements normalized by the second function, G_f, are free of what has been called "fringe bias".

$$\bar{U} = \frac{(U_i /(G_v(\vec{U}) * G_f(\vec{U})))}{(1/(G_v(\vec{U}) * G_f(\vec{U})))} \tag{14}$$

A third type of bias results if frequency filters (on the counter signal processors) attenuate some valid LDV scattered light signals more than others. The counter processor will record

proportionately a greater number of unattenuated signal measurements than attenuated signal measurements. A simple arithmetic mean of the recorded measurements will be biased toward the unattenuated signal measurements.

Velocity Bias Estimation In a given measurement situation the amount of velocity bias depends entirely on the degree and manner in which the velocity field fluctuates and not on LDV system parameters. Velocity bias errors were caluculated based on the formulation derived in Appendix D. Figure 8 presents these calculations for a
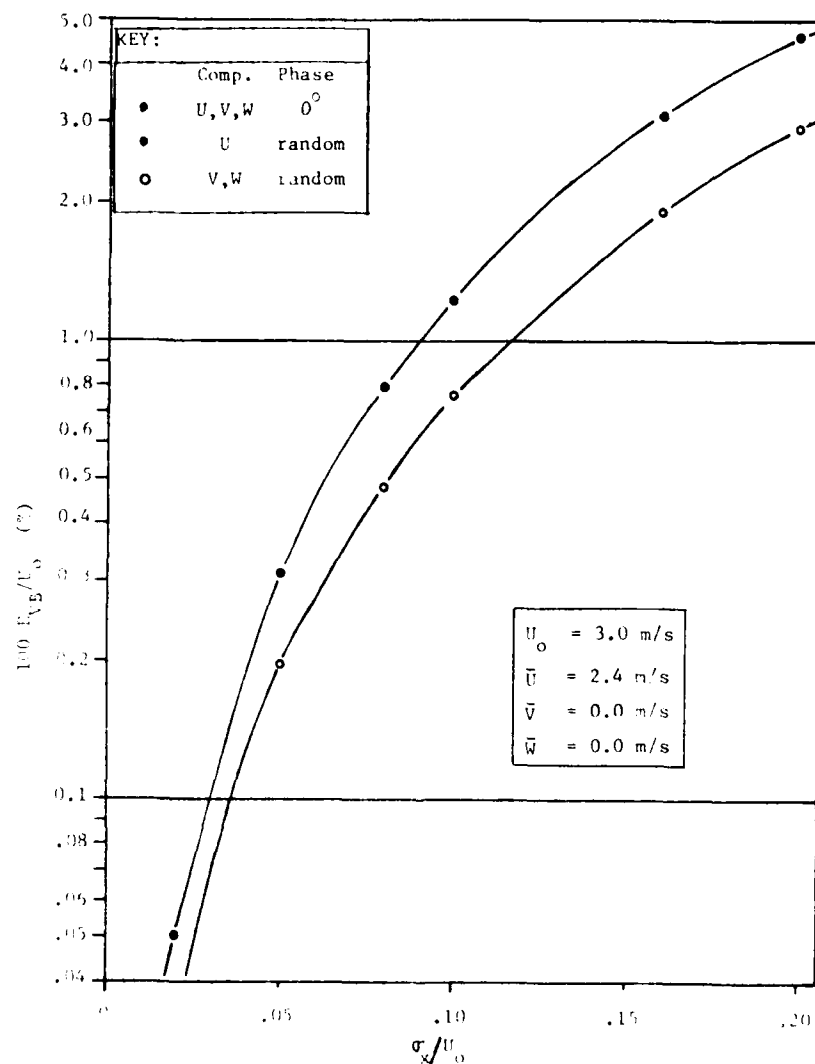

Figure 9 Example Velocity Bias Calculations

particular set of mean velocities and a range of velocity fluctuation magnitudes. The velocity fluctuation for each component is assumed to be a sinusoidal variation on top of the mean velocities listed in the figure. Random phase means that the phase difference between the velocity fluctuations of the streamwise component ("U") and the transverse components ("V" and "W") was varied from 0° to 360°. The average error was graphed. When there was no phase difference between components, the errors for all components are close to the random phase error for the streamwise component ("U").

Velocity bias can be eliminated by weighted data averages as shown in Appendix D and Reference 11. The weighting function, G_v, is the average particle arrival rate for the measured velocity. However, to maximize the data acquisition rate, the towing tank LDV system is not operated to acquire all three velocity components simultaneously. Thus it is not possible to calculate G_v which requires the value of all components at the time of measurement.

However, proper selection of counter processor parameters allows another estimator of average particle arrival rate. The rate at which particles, with a particular velocity, move through the measurement volume is equal to:

$$\text{Particle Rate} = n * \text{Vol} / \overline{T}_B(\vec{U}) \tag{15}$$

where   n   :   particles per unit volume

        Vol   :   volume of measurement region

        $\overline{T}_B(\vec{U})$:   average residence time of particles with velocity $\hat{U}$ in the measurement volume

Since the particle density and measurement region volume are constants, velocity bias can also be eliminated by using a weighting function of "$1/\overline{T}_B(\vec{U})$". The towing tank LDV processors can record the particle residence time T_{Bi} for each measurement U_i if operated in TBC or TBM modes. TSI Inc. suggests its use as a weighting function in the elimination of velocity bias.[10]

37

$$\bar{U} = \sum_i U_i * T_{Bi} \Big/ \sum_i T_{Bi} \tag{16}$$

similarly for "V" and "W"

The processors detect the particle residence time by counting fringe crossings. Random noise spikes can easily cause the processor to prematurely think that a particle has exited the measurement volume. Residence time measurements or total fringe counts will show more low fringe counts if this effect is important. Figure 9 shows the distribution of measured total fringe counts (streamwise component) and the distribution expected from gaussian laser beams, the seed particle distribution (Figure 6 and scattered light intensity proportional to particle diameter squared) and measurement volume geometry. The large number of extra low fringe counts is obvious. It appears that as many as half of the total fringe counts are mistakenly low. The velocity bias correction essentially has no effect on these measurements, so a reasonable assumption (for Figure 9 data) is that as much as half of the velocity bias is not removed by the correction.

It is shown in Appendix E that $T_{Bi}(U)$ has a standard deviation about $\bar{T}_B(U)$ of as much as $0.35\bar{T}_B$. Appendix E also shows that this results in a standard deviation of weighted velocity measurements about U that is as much as 6% larger than the true $(\bar{T}_B)$ weighted velocity. So, velocity bias correction by the T_{Bi} weighting method increases velocity fluctuation standard deviations by a factor of 1.06 and eliminates one half (arbitrarily chosen based on Figure 9) of the errors graphed in Figure 8.

$$E'_v = 1.06 * \sigma_x / Uo \tag{17}$$
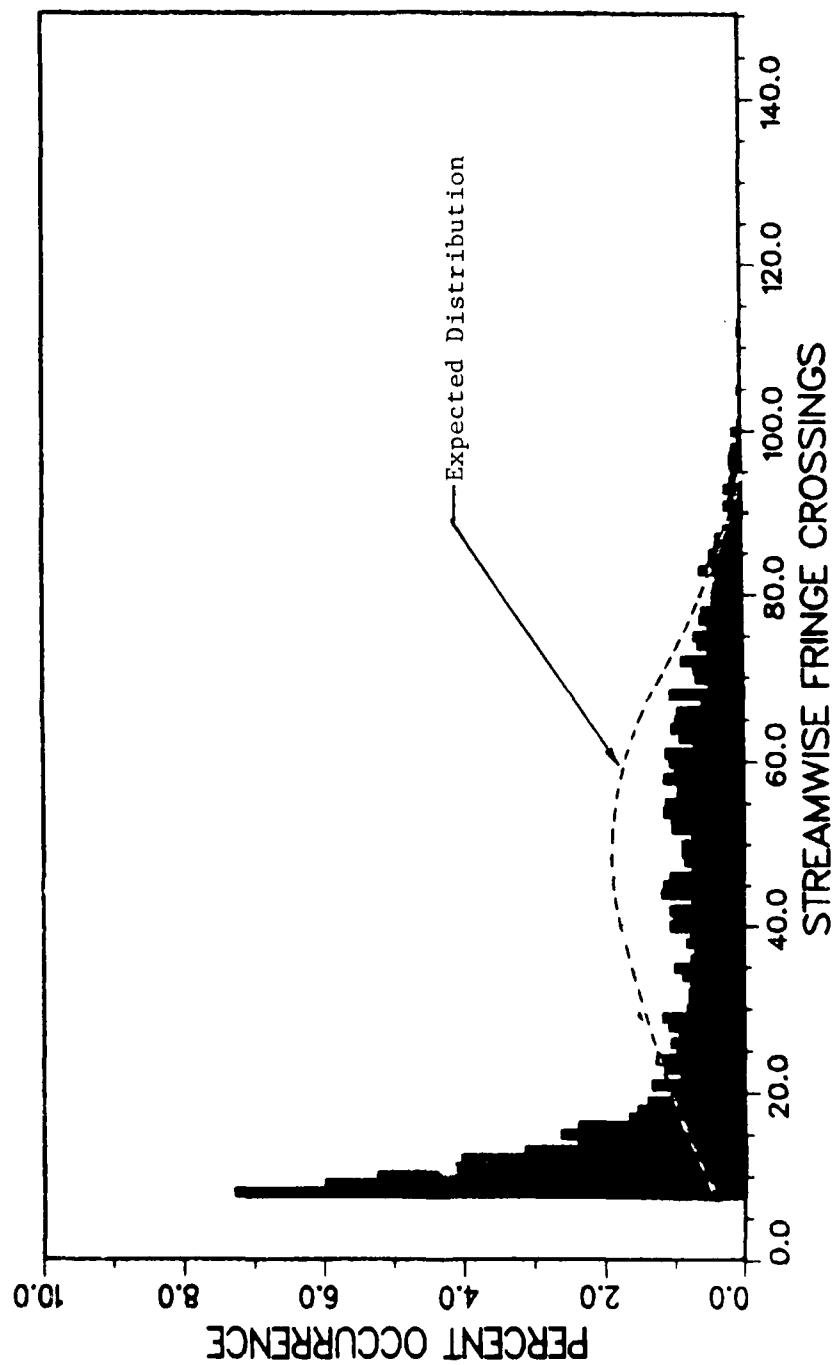$$ = 1.06 * E_v$$

38

Figure 9: Total Detected Fringe Crossings in Measurement Volume (Streamwise Component)

Fringe Bias Estimation In a given measurement situation, fringe bias occurs because certain velocities are more likely to result in valid processor measurements than other velocities. A simple mean of valid measurements is biased toward the more "measureable" velocities. The measureability of any velocity is reflected by the ratio $M_f/N_f(U_x)$ where $N_f(U_x)$ is the number of fringe crossings for a particle with velocity U_x and passing through the measurement volume center. Approximately:

$$N_f(U) = D_{mv}*(FS + U/S_U) / (U^2 + V^2)^{0.5} \tag{18a}$$

$$N_f(V) = D_{mv}*(FS + V/S_V) / (U^2 + V^2)^{0.5} \tag{18b}$$

$$N_f(W) = D_{mv}*(FS + W/S_W) / (U^2 + V^2)^{0.5} \tag{18c}$$

where D_{mv}: diameter of component's measurement volume
FS : effective frequency shift of component
S : fringe spacing of subscripted component

Appendix D formulas for fringe bias require measurement volume dimensions. These can be arbitrarily set by calculated D_{e-2} points (Figure 4). However, when correctly set, the boundaries are points where the particle scattered light just produces a signal above processor thresholds. The boundaries are therefore really functions of particle size and processor signal gain (as controlled by signal noise amplitude).

An experimental determination of the streamwise measurement volume diameter was made by recording the total number of detected fringe crossings for an essentially streamwise towing tank velocity (LDV probe strut was towed without a model). Figure 9 displays a histogram of the results. Signals with less than 8 fringe crossings were not recorded. Also, signals with noise that interrupted the total fringe count appear as low fringe counts. Most importantly however, an upper limit to the number of fringe crossings is

40

apparent.

Boundaries of D_{e-2} would result in a maximum of 64 fringe crossings ($D_{mv} = 0.11$ mm; $S_U = 1.72$ um). The figure shows as many as 113 fringe crossings. However, one might choose 71 fringe crossings as the maximum for an average sized particle (90% of the data fall at or below 71 fringe crossings).

The experimental data indicates a "detectable" measurement volume 11% larger than that calculated based of D_{e-2}. Though the experimental data is only for the streamwise component, it is assumed that the measurement volume dimensions (D_{mv} and L_{mv}) for the all components are 1.11 times greater than the calculated D_{e-2} dimensions of figure 4.

Figure 10 displays calculated fringe bias errors as a function of velocity fluctuation magnitude. Only the fringe bias errors of the vertical and on-axis components are large enough to appear on the graph. For the same frequency shift, the vertical error is much more important than the on-axis component error. This is generally true for the velocities and frequency shifts found on towing tank LDV experiments. The velocity means and fluctuation characteristics are the same as in figure 8 for velocity bias. For fringe bias, the choice of frequency shift (affecting N_f) and M_f values are important. This is because fringe bias errors vary directly with the mean and the standard deviation of the ratio N_f/M_f that occur while measuring a component mean.

No direct formula can be given for uncorrected fringe bias errors. However, with some assumptions about the nature of the velocity fluctuations, the calculations behind figure 10 can be repeated (Appendix D). In this way an error estimate can be made.

Filter Bias Estimation It is very possible that the desire to reduce signal noise and increase data rates in the towing tank LDV system will rule against setting a large, safe (with respect to filter bias) range of unfiltered frequencies on the counter processor. Rather, the low pass and high pass filters will be set as close together as
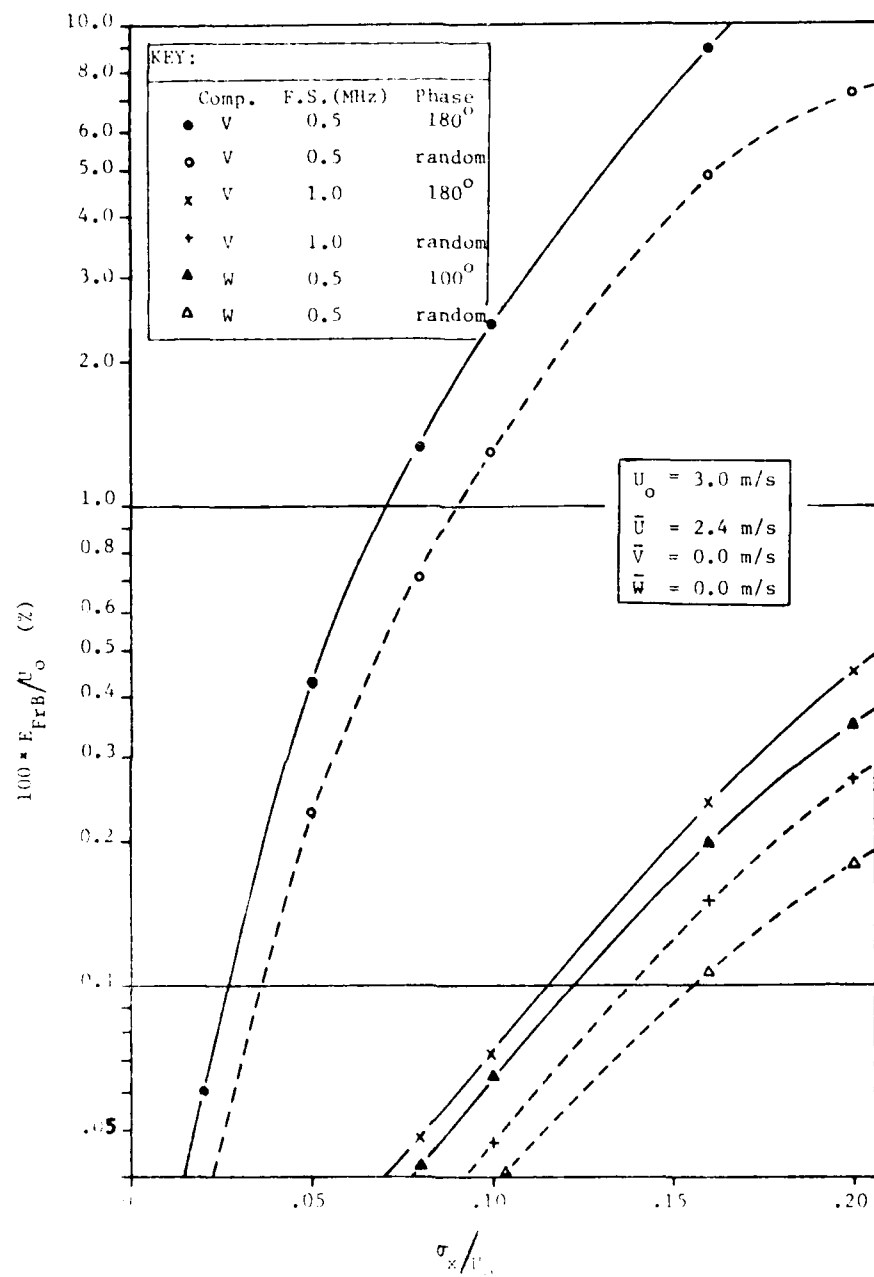
41

Figure 11: Example Fringe Bias Calculations

42

still allows measurement of all velocities that occur. Since high frequency noise is the most disruptive of counter processor operations, the low pass filter is particularly important. Appendix F estimates the amount of bias developed as the signal frequency approaches the low pass filter frequency. Counter processor specifications rate these filters with a minimum of 30 dB per octave rolloff.

Figure 11 represents the results of Appendix F under the following assummptions:

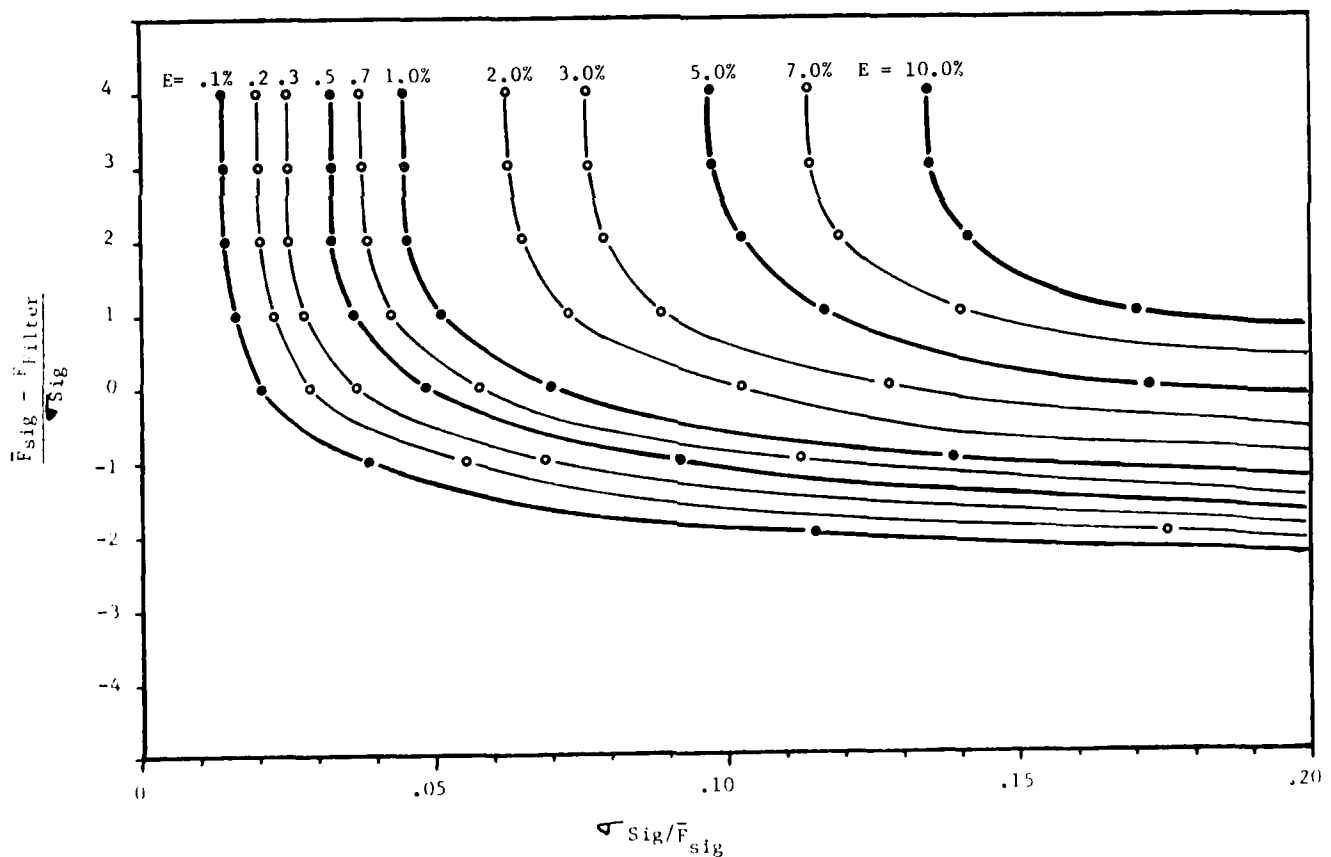1. low pass filter rolloff of 30 dB per octave starting at the filter frequency, F_{Filter}.

Figure 11: Filter Bias Error Calculations

2. signal frequencies have a mean, $\overline{F}_{Sig}$ and standard deviation σ_{Sig}

3. the signal frequencies have a normal distribution.

4. frequency measureability is directly proportional to the precent of the signal voltage passed by the low pass filter.

Note that the error given in the figure is a percentage of F_{Sig}. To get the filter bias velocity error as a percent of the towing speed, this number must be multiplied by:

$$K = \overline{F}_{Sig} * S_x / U_o \tag{19}$$

Summary of Mean Fluid Velocity Errors

All the errors in this section are assumed to be independent of each other and all previously defined errors. Formulas are developed for all the errors except for the three bias errors. These three can also be estimated from operating parameters and flow field characteristics. However, the nature of these calculations requires a computer program to do the long summations and to tailor the many flow field assumptions to the user's requirements. With the available velocity bias correction, the bias is "half" removed but a modified velocity fluctuation error, E_v', is required.

Two of the errors are "fast changing" and will be reduced by taking the mean of multiple samples of the particle velocity. This is a good assumption for the type of particle lag error formulated. However, particle lag error due to some persistant fluid flow structures is "slow changing" and will not be accounted for. The user must be on the look out for these situations and estimate his own particle accelerations and lag errors (using Appendix C formulas).

The uncorrected bias errors are "slow changing" errors. They will not be reduced in multiple sample means.

In most situations (if frequency shifts are properly chosen and

44

velocity bias correction is done), E_V' will be the only important error of this group. Table 5 conveniently displays this information.

TABLE 5 - MEAN WATER VELOCITY ERROR FORMULAS

| | Character | | Component Velocity Errors | | |
	Fast	Slow	Streamwise	Vertical	On-Axis
E_L:	X			$3.4 * 10^{-4} * ((\sigma_x/U_o)^2 + U_o^2)^{0.5}$	
E_V:	X		σ_U / U_o	σ_V / U_o	σ_W / U_o
E_{VB}:					
Uncor.		X	C.P.	C.P.	C.P.
Corr.	X		$E_V' = 1.06 * E_V$	$E_V' = 1.06 * E_V$	$E_V' = 1.06 * E_V$
E_{FrB}:	X		C.P.	C.P.	C.P.
E_{FiB}:	X		C.P.	C.P.	C.P.

KEY:

U_o : towing speed

$\sigma_x, \sigma_U, \sigma_V, \sigma_W$: standard deviation of velocity fluctuation

C.P. : computer program for estimation

σ_{Sig} : standard deviation of signal frequency

FINALIZED WATER VELOCITY DATA ERRORS

Mean water velocity components already analyzed are not the end result desired from typical wake surveys. Ideally the user seeks, at known positions, non-dimensionalized, velocity components that are orthogonally aligned to the ship model and undisturbed by the LDV strut. Velocities are usually non-dimensionalized by an independently measured free stream velocity magnitude (towing speed). Component directions are not exactly orthogonal due to optical alignment limitations. Velocity disturbances created by the LDV strut and

45

positioning inaccuracies cause measured velocities to be different from those sought. These four error sources and available correction techniques are treated in this section.

Carriage Speed Errors

This error is the result of towing carriage speed variation. It is not an error in fluid velocity measurement Rather, the error is introduced when the measured data is non-dimensionalized.

Many carriage passes will be required to take an entire wake survey. In order to use data taken on different carriage passes or even at different times on the same carriage pass, the measurements must all be non-dimensionalized by the carriage speed at the time of measurement.

The LDV measurement procedure records an average carriage speed for each pass. It uses that speed to non-dimensionalize every measurement made during the pass. Thus, this error is "position independent" and "slow changing". Speed variations during the same pass can, with care, be held to within +/- .1% of the mean speed. This is better than the carriage speed variation between different passes that can be +/- .3% or more when equal speed passes are sought. Assuming a normal distribution of towing carriage speed (during a pass) with a mean of U_o and standard deviation of $5*10^{-4}*U_o$, carriage speed error has a mean of zero and a standard deviation of:

$$E_c = 5*10^{-4} \tag{21}$$

Carriage speed measurement errors and flow field changes (from variation of model ship Froude number) have been neglected in this error estimation.

Flow Disturbance Errors

The configuration of the towing tank LDV system means that the partially submerged probe strut (figure 2) will always cause some

46

disturbance of the flow field. The strut's location and basic shape are mostly set by the optical requirements of the laser beams and scattered light that pass through it. In order to provide for rigidity and laser light passage, the underwater portion of the strut is basically a hollow aluminum column: 0.19 m. wide by 0.095 m. thick by as much as 0.90 m. tall. The lowest portion (0.18 m.) of the strut must accommodate the laser beam focusing lens and is 0.122 m. thick.

Plastic fairings are attached to the forward and rear faces of the strut to:

1. reduce separation for flow angles of -5° to 5°;
2. reduce strut drag;
3. reduce flow disturbance at the LDV measurement volume;

The faired shape appears in figure 12. The asymmetrical shape of the box fairing causes less flow disturbance on the flat side (side of LDV measurement volume) than the more curved side. However, it also produces a sideways force or lift that may cause strut deflection and
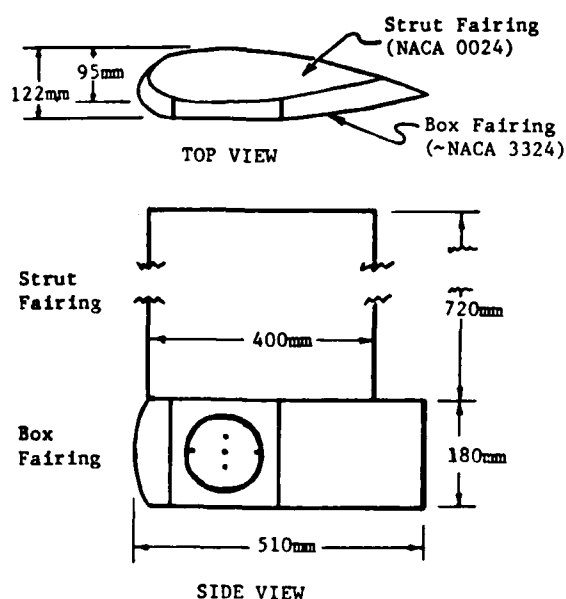

Figure 12: LDV Strut Dimensions

47

stability problems above the maximum checkout speed of 4.0 m/s.

Several experimental tests were run to quantify the flow disturbance of the strut. Basically they each consisted of putting another velocity sensing instrument (pitot static or 5-hole pitot tube) at the LDV measurement volume location. On a single carriage pass, the pitot tube measurement would be recorded, the LDV strut would be traversed out of the water (or 0.6 m to the side), and a second pitot tube measurement would be recorded. The difference between the first and second pitot tube measurements is reported here as the LDV probe strut flow disturbance.

The first series of measurements was done in the free stream with no ship model. Potential flow calculations indicated that the streamwise velocity component would be disturbed the most. A pitot static tube that sensed only that velocity component was used. The results appear in figure 13 for a range of strut depths. U_d is the pitot tube measurement of the disturbed flow with the LDV strut in place. All disturbance values are less than 0.4% of the tow speed, U_o.
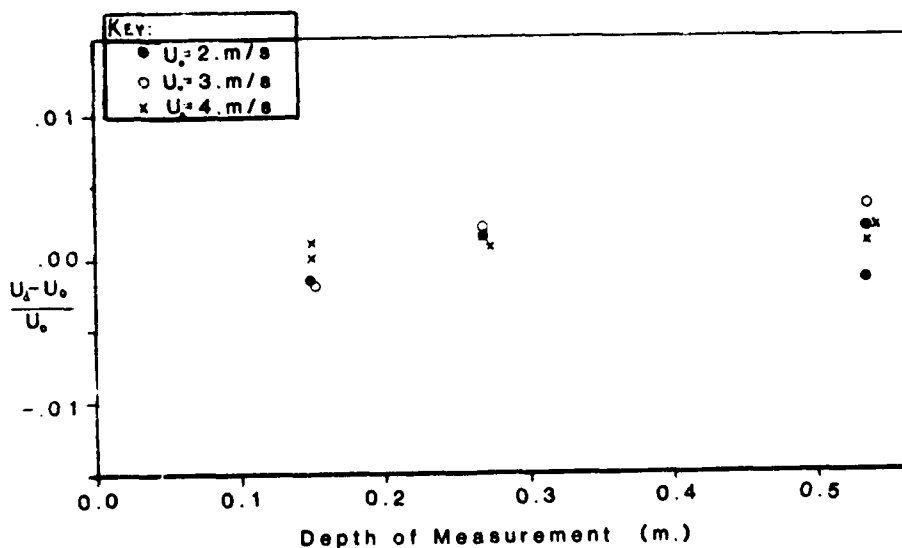

Figure 13: Flow Disturbance of LDV Strut (Free Stream)

A second series of measurements was done during a ship model bow flow survey. The ship model bow was fitted with pressure taps mounted flush with the bow surface. Bow pressures were recorded both with and without the LDV probe strut. Pressure differenc $\jmath$ ⸗ only a few tenths of a percent of the stagnation pressure ($\rho_w * U_o^2 / 2$) were measured. Figure 14 presents the results and measurement locations.
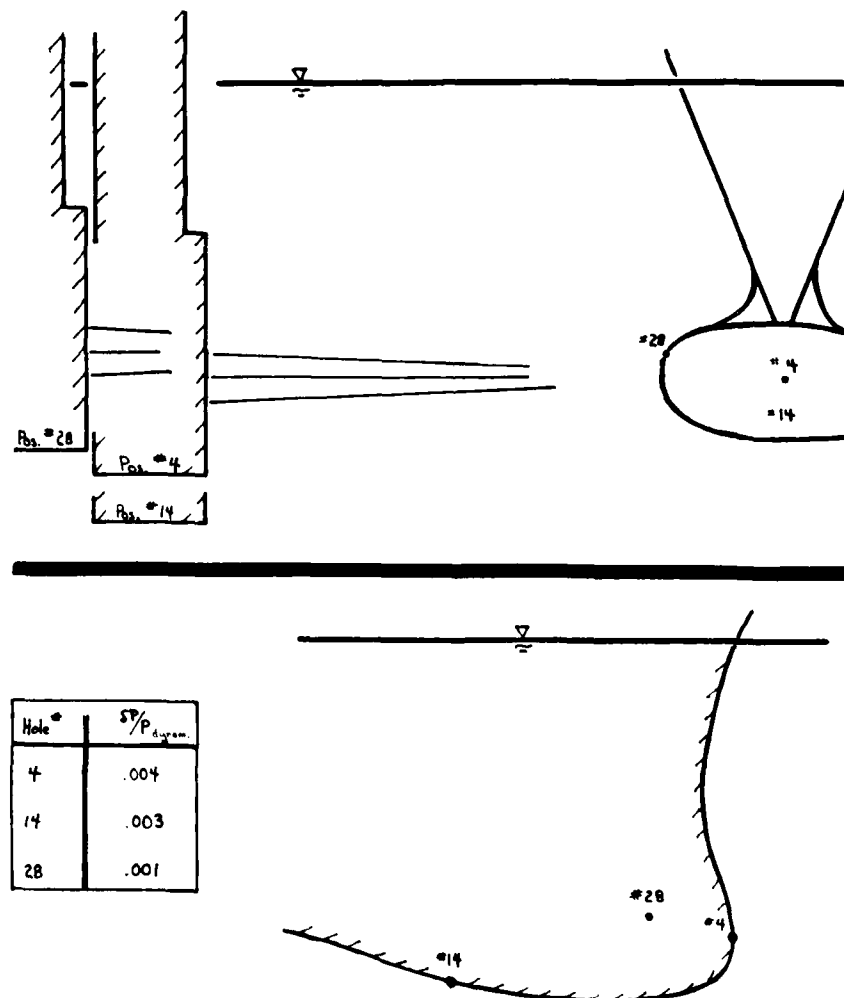

Hole #	$SP/P_{dynam.}$
4	.004
14	.003
28	.001

Figure 14: Flow Disturbance of LDV Strut (Bulbous Bow)

49

A final series of measurements was done in the propeller plane of a model with a particularly severe wake. A five-hole pitot tube was used but only the most disturbed component of velocity (streamwise) is presented in figure 15. This figure was done in a way to show the variation of pitot tube measurements of nominally the same
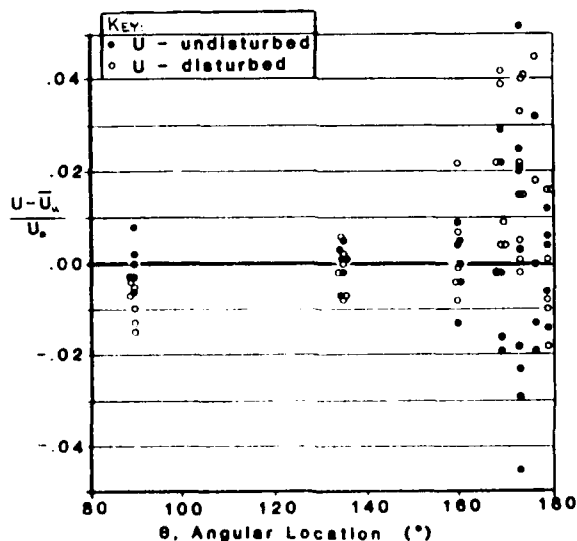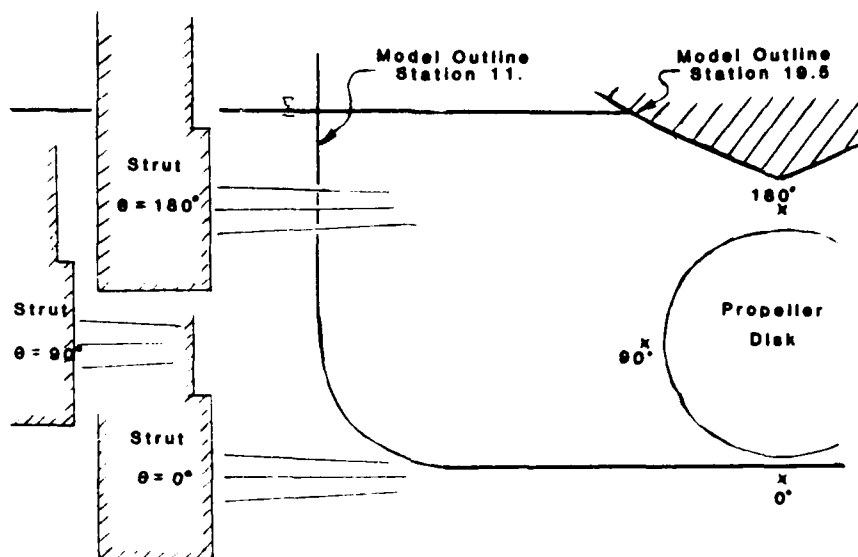

Figure 15: Flow Disturbance of LDV Strut (with Model)
R = .294 m.; Station = 19.5; 2.m/s

velocity for both the disturbed and undisturbed cases. Considering the data scatter (especially near the angular location of 180°), the undisturbed and disturbed data sets are essentially the same or at worst different by about $.01*U_o$. The very wide model (an auxillary oiler) and the strong ($U < 0.2*U_o$), unstable wake field at the 180° location were purposely chosen as a severe test of the potential for strut flow disturbance. Most wake survey positions will have flow disturbances closer in magnitude to those found in the free stream tests (figure 13).

Typical error magnitudes are illustrated in figures 13 - 15. It is suggested that the strut disturbance correction (discussed in the next section) always be used. This correction, based on free stream velocity measurements, eliminates free stream flow disturbances for all velocity components. For error analysis, the flow disturbance error will then be assumed to be zero. In reality though, the LDV user must still be wary of situations like measuring "unstable", "severe wake" flows that are well under "wide models".

$$E_i = 2*10^{-3} \qquad \text{(uncorrected)} \qquad\qquad (22)$$
$$= 0 \qquad\qquad \text{(corrected)}$$

Velocity Component Directional Errors

Despite careful alignment procedures, the three measured velocity components do not come out perfectly perpendicular and aligned to the ship model. Errors of as much as $.5^\circ$ are possible for the vertical and streamwise components. The on-axis component can be as much as 1.5° misaligned. These are "slow changing" and "position independent" errors. Special caution should be observed with the on-axis component because even the slightest change in optical alignment can have a large effect on this error. The correction scheme described in this section should be done after any optical change to the LDV system. As a further precaution it should be done every week of experimentation, even if there is no known optical change.

51

As long as the measured velocity components are not coplanar, the desired orthogonal velocity components can be calculated if the measured directions are known. Alignment procedures make all directional errors zero to the best of their limited precision. Further (but not complete) correction is possible from data taken on calibration runs with a constant carriage speed and no model.

For a perfectly aligned and otherwise accurate LDV system, the measured velocity components on calibration runs should be:

$$U = U_o * \cos(\emptyset) \tag{23a}$$

$$V = U_o * \sin(\emptyset) \tag{23b}$$

$$W = 0.0 \tag{23c}$$

where $\emptyset$ = vertical traverse angle

The difference of measurements from these values is the result of a number of errors:

1. transverse components not perpendicular to streamwise direction (E_a)
2. carriage speed determination (E_c)
3. streamwise fringe spacing determination (E_f)
4. strut flow interference (E_i)
5. frequency shift - signal mixing accuracy (E_s)

Of the five errors listed, only E_s should not be proportional to the towing speed (should change randomly with channel frequency shift). There is no way and little need to separate the proportional errors. If calibration runs are done for a range of tow speeds (expected U velocity component range), corrections proportional to tow speed and constant corrections can be separated resulting in six correction factors:

$$U_o * \cos(\emptyset) = A_U * U_r + B_U \tag{24a}$$

$$U_o * \sin(\emptyset) = V_r + A_V * U + B_V \tag{24b}$$

52

$$0 = W_r + A_W * U + B_W \tag{24c}$$

where U_r, V_r, W_r: raw, uncorrected velocity components

A_U, A_V, A_W: proportional correction factors

B_U, B_V, B_W: constant correction factors

In general the B correction factors should be small enough to neglect. Doing only one tow speed and assuming $B_x = 0$ is just about as good as calculating the more involved two parameter correction. If parameters are derived from many points on several runs, the effect of tow speed measurement errors (mean value of $E_c = 0$) will be reduced through averaging. If parameters are derived from points at various depths (in the range used during the experiment) then an average flow disturbance will be corrected. The experimental data correction formulae then are:

$$U = A_U * U_r + B_U \tag{25a}$$

$$V = V_r + A_V * U + B_V \tag{25b}$$

$$W = W_r + A_W * U + B_W \tag{25c}$$

This correction does nothing about streamwise component direction or vertical component and on-axis component directions within the transverse plane. Sizable alignment errors of this type are still possible (0.5° for vertical or streamwise and 1.5° for on-axis). The estimated directional alignment errors that follow are based on the alignments left uncorrected and on the repeatability of the calculated correction factors. Also, note that full alignment correction, means that previous error standard deviation magnitudes should be assumed zero (E_c, E_f - streamwise only, E_i, and E_s). Uncorrected and corrected alignment directional errors should have a mean of zero (over many optical system setups) and a standard deviation of:

<center>No Correction Factors Used</center>

$$E_a(U) = ((.005*V)^2 + (.005*W)^2)^{0.5} / U_o \qquad (26)$$

$$E_a(V) = ((.005*U)^2 + (.005*W)^2)^{0.5} / U_o$$

$$E_a(W) = ((.013*U)^2 + (.013*V)^2)^{0.5} / U_o$$

<center>Correction Factors Used</center>

$$E_a(U) = ((.005*V)^2 + (.005*W)^2 + (.001*U_o)^2)^{0.5} / U_o \qquad (27)$$

$$E_a(V) = ((.005*W)^2 + (.001*U_o)^2)^{0.5} / U_o$$

$$E_a(W) = ((.013*V)^2 + (.002*U_o)^2)^{0.5} / U_o$$

Traverse Positioning Errors

In a non-uniform velocity field, positioning errors result in measured velocities that are different from the velocity at the intended position. The velocity error depends on both the magnitude of the positioning error and the magnitude of the local velocity gradient. Five sources of positioning error are discussed below.

Minor Positioning Errors. The SONY Magnescale encoders incorporated into the LDV traverse system[13], have an accuracy of +/- .003 mm. Positioning is automatically checked by these encoders before and after each carriage pass.

During the carriage pass the traverse system stepping motors are relied on to make the correct position changes according to a calibrated ratio of motor steps to position change. Based on encoder checks after the carriage pass these positioning errors are consistently less than +/- .04 mm. in either the vertical or on-axis direction (the traverse is not moved in the streamwise direction during a carriage pass).

Since the LDV traverse system and ship model are attached separately to the towing carriage, some relationship between the traverse encoders and the model coordinate system must be established

<center>54</center>

for each test. This can be done by placing the laser beam crossing point on model surface points of known location. The encoders can be zeroed (or set to any given value) at these points. Encoder readouts then directly display distance from those ship model points. This procedure can be done best on black model surfaces. When low power green beams cross on the black surface, a Doppler signal (frequency equals the effective frequency shift) will be observed at the signal processors with an oscilloscope. Positioning accuracy better than +/- .1 mm is possible

These first three positioning errors are relatively minor in comparison to LDV measurement volume dimensions and the two errors that follow. Combining all three (they are independent), the positioning error is still less than +/- .11 mm.

Major Positioning Errors. The position encoders actually display relative movement between adjacent parts of the traverse structure. Bending of the traverse structure under its own weight or hydrodynamic forces does not change the relative position of adjacent parts. However, it can affect the relative position of the LDV measurement volume and the independently mounted ship model.

As traversing shifts the significant weight of the optics breadboard and support members, the whole traverse structure undergoes bending changes. Investigations have shown that most of the bending occurs near the top of the structure and is associated with the vertical traverse mechanism and the attachment to towing carriage members. Bending angles, though small, are transformed into significant displacements by the distance between the source of bending and the point of interest (the LDV measurement volume).

This bending is a fairly repeatable function of the absolute traverse location and therefore positioning corrections can be made. These errors were documented (Figures 16 and 17) by careful experimentation with a stationary towing carriage. In certain extreme cases the positioning error can be greater than 10 mm. Appendix G formulates how, when necessary, these errors can be reduced by
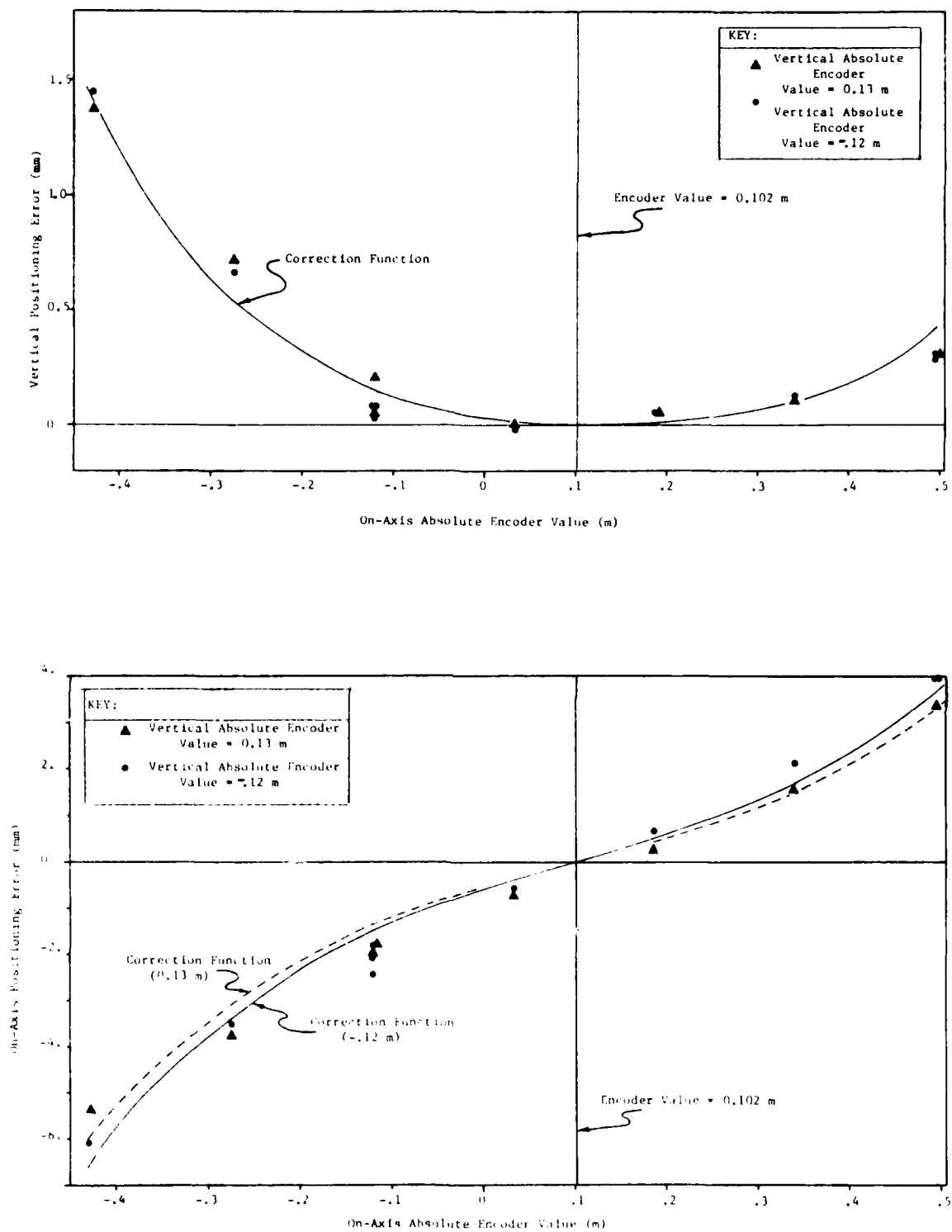
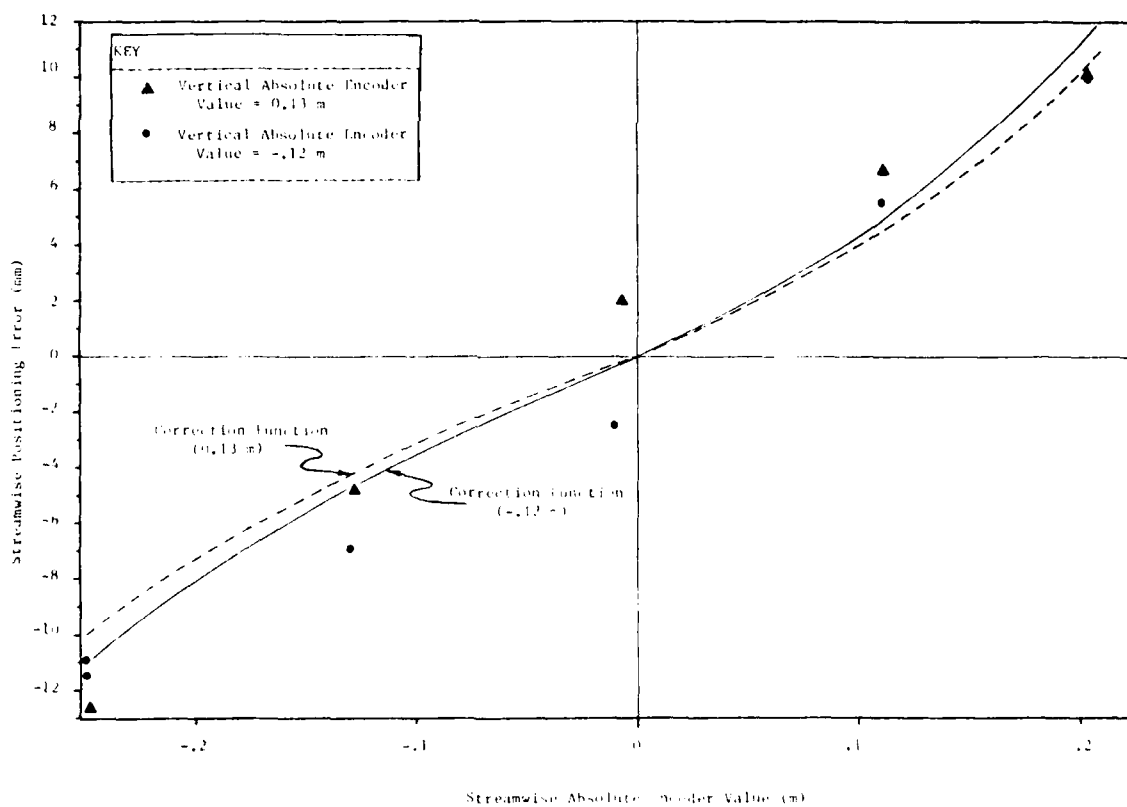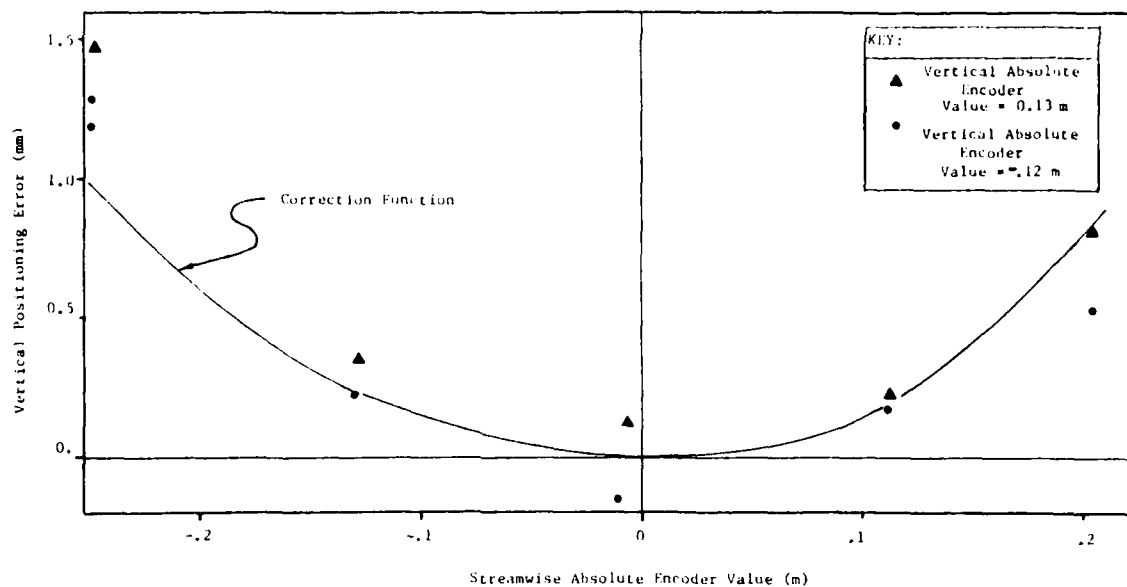Figure 16: Positioning Error Correction as a Function of On-Axis Location

56

Figure 17: Positioning Error Correction as a Function of Streamwise Location

57

correction factors that are incorporatated into the data taking computer software. Figures 16 and 17 also show the positioning error reductions possible when correction factors are used.

Traverse structure bending also results from the two main hydrodynamic forces exerted on the submerged strut. They are drag and side forces. Both are a function of towing speed, flow angle of attack (for strut), and the assymmetric probe box fairing. Thus, they are also a function of strut position in the flow field as modified by the towed model. Figure 18 shows strut position changes
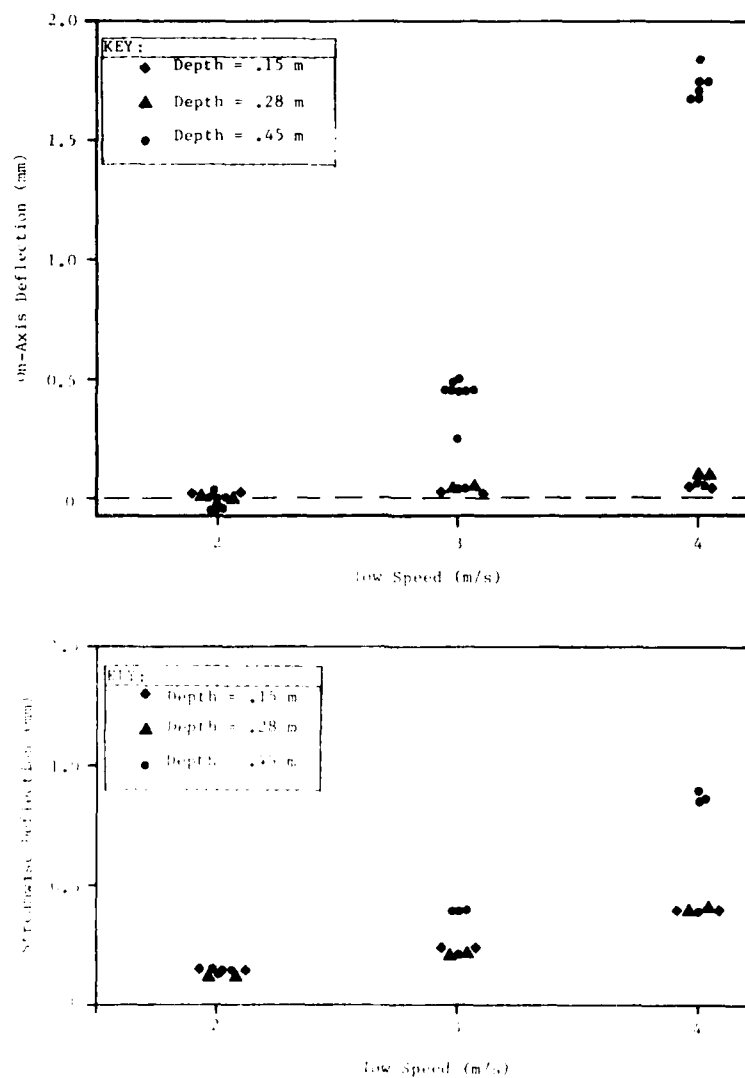

Figure 18. Dynamic Position Error Due to Drag and Side Forces

58

as a function of towing speed. These measurements were actually made on the strut (as far down as possible while still above the water surface), but they should closely approximate measurement volume deflections. Even under the freestream conditions of figure 18, the repeatability of deeply submerged strut deflections is disappointing. Unstable flow about the strut may be the reason. Appendix G shows how traversing calibrations under tow can correct for both static and some dynamic bending errors.

These last two positioning errors (due to bending) depend on which corrections are used and the measurement point's distance from model reference positions (where there is no positioning error).

Total Positioning Error. The five contributors to the positioning error are independent of each other. The total positioning error is "slow changing" and "position dependent". From setup to setup it should have a mean of zero and standard deviation of*:

Positioning Error With No Corrections

$$P_x = (((Y-Y_o)*3.0)^2 + (((Z-Z_o)*5.0)^2 + 0.011^2)^{0.5} \text{ mm.} \qquad (28)$$

$$P_y = (((Y-Y_o)*12.)^2 + 0.011^2)^{0.5} \text{ mm.}$$

$$P_z = (((Z-Z_o)*45.)^2 + 0.011^2)^{0.5} \text{ mm.}$$

Positioning Error With Bending Corrections

$$P_x = (((Y-Y_o)*0.3)^2 + (((Z-Z_o)*0.6)^2 + 0.011^2)^{0.5} \text{ mm.} \qquad (29)$$

$$P_y = (((Y-Y_o)*1.2)^2 + 0.011^2)^{0.5} \text{ mm.}$$

$$P_z = (((Z-Z_o)*4.5)^2 + 0.011^2)^{0.5} \text{ mm.}$$

where   X, Y, Z : vertical, on-axis, streamwise position (m.)

        X_o, Y_o, Z_o : model reference point location (m.)

----

* dynamic bending errors are assumed zero or accounted for by model position referencing during a carriage pass

Nothing has been said yet about the velocity gradient part of the positioning velocity error. The local velocity gradient is "position dependent" and "fast changing" but does not generally have a mean value of zero. Velocity gradients can only be guessed or estimated from the experimental results themselves. The highest gradients occur near forward ship model stagnation points and in thin model boundary layers. Users should be especially careful to establish nearby model reference points in these cases.

Velocity Error Due to Traverse Positioning

$$E_t(U) = ((P_x * \partial U/\partial x)^2 + (P_y * \partial U/\partial y)^2 + (P_z * \partial U/\partial z)^2)^{0.5} / U_o \quad (30)$$

$$E_t(V) = ((P_x * \partial V/\partial x)^2 + (P_y * \partial V/\partial y)^2 + (P_z * \partial V/\partial z)^2)^{0.5} / U_o$$

$$E_t(W) = ((P_x * \partial W/\partial x)^2 + (P_y * \partial W/\partial y)^2 + (P_z * \partial W/\partial z)^2)^{0.5} / U_o$$

Because of the difficulty in guessing or estimation the velocity gradient at each measured point, this error will be reported as positioning error (P_x, P_y, P_z) and not a velocity error. After the data has been taken, the user must determine if the estimated positioning error causes significant velocity errors.

Summary of Finalized Fluid Velocity Errors

All the errors in this section are assumed to be independent of each other and all previously defined errors. However, some of the suggested correction techniques reduce several error magnitudes at once.

None of these errors are "fast changing" and they will not be reduced by taking the mean of multiple samples of the particle velocity.

Table 6 summarizes the error formulations both with and without the described correction procedures. Uncorrected alignment errors are probably the most important among this group. Uncorrected positioning errors can also be important for either large velocity

60

TABLE 6 - FINALIZED WATER VELOCITY ERROR FORMULAS

| | Character | | Component Velocity Errors | | |
	Fast	Slow	Streamwise	Vertical	On-Axis
E_c:		X	$5*10^{-4}$	$5*10^{-4}$	$5*10^{-4}$
E_i:					
Uncor.		X	$2*10^{-3}$	$2*10^{-3}$	$2*10^{-3}$
Corr.		X	0	0	0
E_a:			$((a*U)^2 + (b*V)^2 + (c*W)^2 + (d*U_o)^2)^{0.5}/U_o$		
Uncor.		X	a = .000	a = .005	a = .013
			b = .005	b = .000	b = .013
			c = .005	c = .005	c = .000
			d = .000	d = .000	d = .000
Corr.		X	a = .000	a = .000	a = .000
			b = .005	b = .000	b = .013
			c = .005	c = .005	c = .000
			d = .001	d = .001	d = .002
P_x, P_y, P_z:			$((a*(Y-Y_o))^2 + (b*(Z-Z_o))^2 + 0.011^2)^{0.5}$ mm.		
Uncor.		X	a = 3.0	a = 12.0	a = 0.0
			b = 5.0	b = 0.0	b = 45.
Corr.		X	a = 0.3	a = 1.2	a = 0.0
			b = 0.6	b = 0.0	b = 4.5

KEY:

E : standard deviation of velocity error divided by U_o

P : standard deviation of position error in units of "mm."

U_o : towing speed

X, Y, Z : vertical, on-axis, streamwise position (m.)

X_o, Y_o, Z_o : model reference point location (m.)

gradients or large traversing ranges.

VELOCITY COMPONENT ERROR SUMMARY

Tables 4, 5, and 6 summarize the error calculation formulas developed in this section. In the case of a fluctuating velocity field, generally only:

1. E_n....Signal Noise Error
2. E_f....Fringe Spacing Determination Error
3. E_v....Velocity Fluctuation Error
4. E_{VB}...Velocity Bias Error
5. E_{FrB}..Fringe Bias Error
6. E_{FiB}..Filter Bias Error
7. E_a....Velocity Component Direction Error

can be significant. In non-fluctuating velocity fields, the calculated bias and velocity fluctuation errors are zero except when FS, M_f, and low pass filter settings mean a velocity is totally unmeasureable. However, despite the calculation, velocity bias can exist in a steady flow field if a sharp local velocity gradient causes the LDV measurement volume to see significantly different velocities at the same "position".

INITIAL OPERATING PARAMETER SELECTION

This section provides a guide for making an intelligent estimate of the velocities that will be measured in an LDV experiment. It then helps pick operating parameter options appropriate to those expected velocity component ranges. Finally a computer program is available to estimate the size of various error sources as a function of those velocity ranges and operating parameters. One or more iterations through this program can yield a good starting point of LDV operating parameter choices plus an idea of what experimental errors to expect.

MEAN VELOCITY COMPONENT RANGES

The primary determinant of velocity component range is the experiment's towing speed. This section will only discuss component ranges that are non-dimensionalized by this speed.

LDV error analysis calculates errors in each of the three component mean measurements. In a strict sense, each component error is a function of all three mean velocity components. However, the long thin measurement volume ellipsoid, enables very accurate error estimation for each component based on only two velocity components. Some of these estimates break down for velocity directions that are less than 15° from the on-axis direction. Vertical and streamwise component errors are primarily functions of both the vertical and streamwise mean velocities, "U" and "V". The on-axis component error is primarily a function of its own mean velocity, "W" and the cross-measurement volume component "T" or $(U^2 + V^2)^{0.5}$.

Figure 19 displays velocity "Scatter" plots for two different towing tank LDV experiments. There are two companion plots from each experiment. The first shows experimental mean velocity components needed for streamwise and vertical component error calculations. The second displays components for the on-axis error calculation. Appendix B contains a more complete compilation of these Scatter plots from LDV experiments.

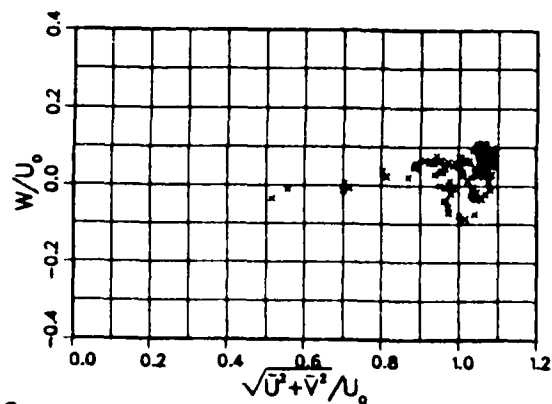In estimating mean velocity component ranges, the LDV user may
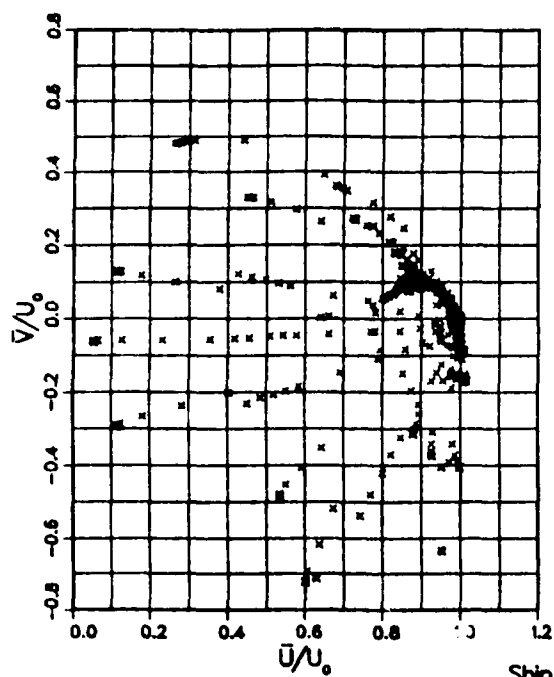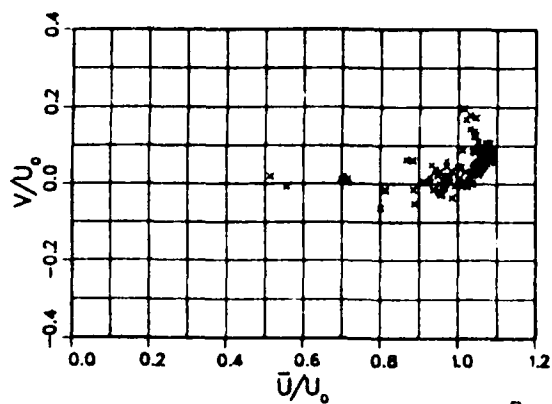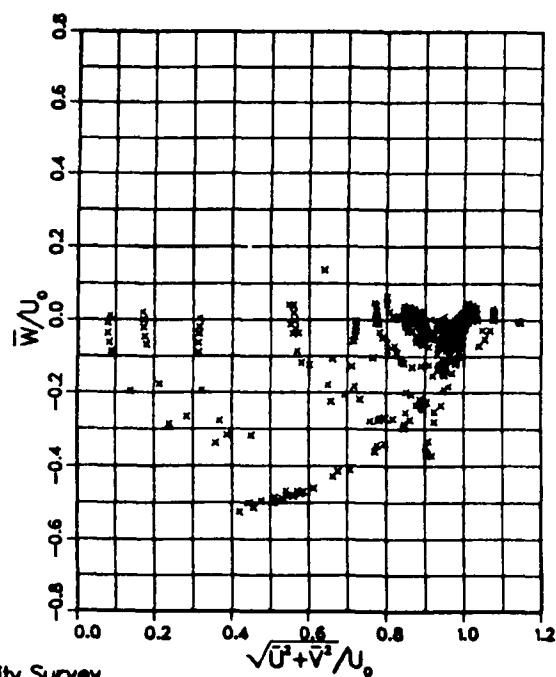
Figure 19   Two Examples of Scatter Plots

utilize the results of an experiment in Appendix H that has some similarity to his own. Pitot tube results from past wake surveys are another reference source. Whether either of these sources or just experience and intuition are used, the LDV user needs an estimated minimum and maximum mean value of the four velocity components: "U", "V", "W", and "T".

VELOCITY FLUCTUATION MAGNITUDE

Each velocity component has its own fluctuation magnitude reflected in the component standard deviation at a measurement point. In almost all situations, the fluctuation magnitudes will be nearly equal for each component.

Measured LDV standard deviations, which also reflect the signal noise level, for each component may not be equal. Figure 20 shows "Histograms" for the three measured components in a ship bow flow field where their was essentially no fluctuation of any velocity component. The width of the "Histograms" is due to each component's signal noise level. With proper operating parameters, the vertical velocity component will usually be the most noise-free of the three measured. Noise standard deviations of about 0.5% of the tow speed are common.

Figure 21 shows the distribution of the vertical velocity component standard deviation, σ_V for two experiments. The bow flow example indicates the complete absense of measured turbulent velocity fluctuations. The propeller inflow survey for a very clean destroyer hull shows both non-turbulent potential flow and turbulent flow entering the propeller. Appendix I displays more examples of these bar plots.

Since error estimation is very much a function of the velocity fluctuation magnitude, the LDV user should carefully choose one or two values that he wants to input to the error estimating computer program. The bar graphs presented in Appendix I, other experience, and intuition may all help determine the choice.
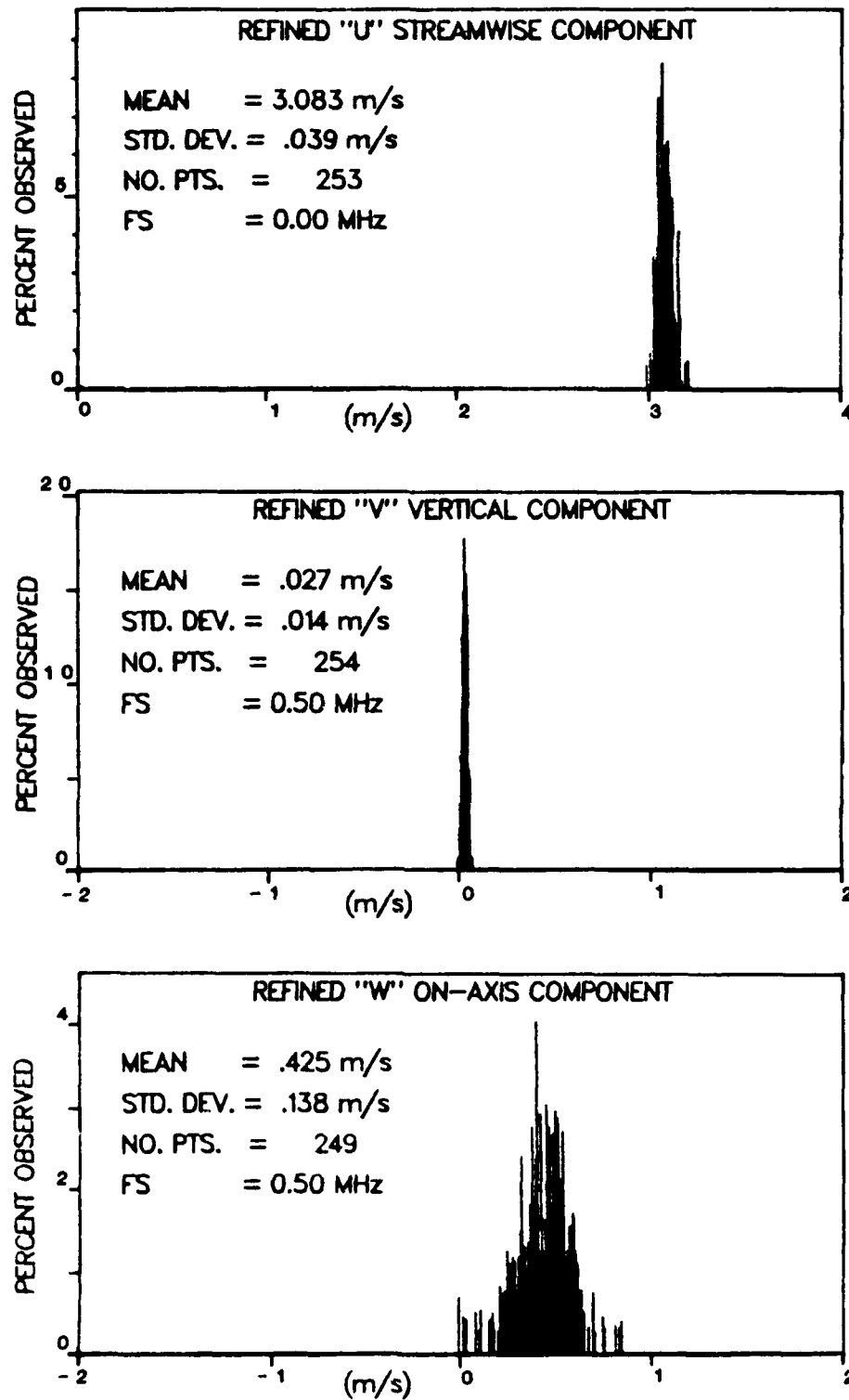
65

REFINED "U" STREAMWISE COMPONENT

MEAN = 3.083 m/s
STD. DEV. = .039 m/s
NO. PTS. = 253
FS = 0.00 MHz

REFINED "V" VERTICAL COMPONENT

MEAN = .027 m/s
STD. DEV. = .014 m/s
NO. PTS. = 254
FS = 0.50 MHz

REFINED "W" ON-AXIS COMPONENT

MEAN = .425 m/s
STD. DEV. = .138 m/s
NO. PTS. = 249
FS = 0.50 MHz

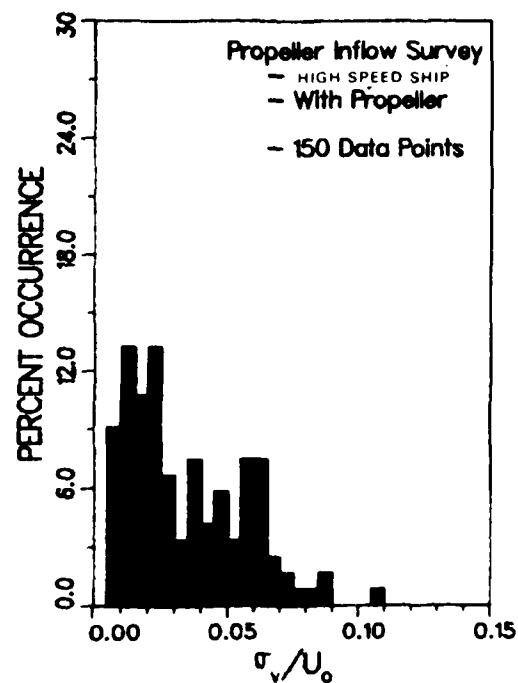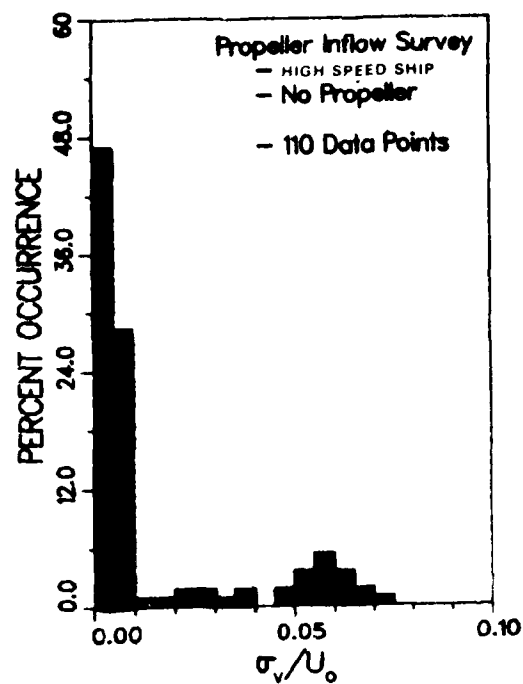Figure 20 Example of Steady Flow Histograms (Bow Flow; U_o= 3 m/s)
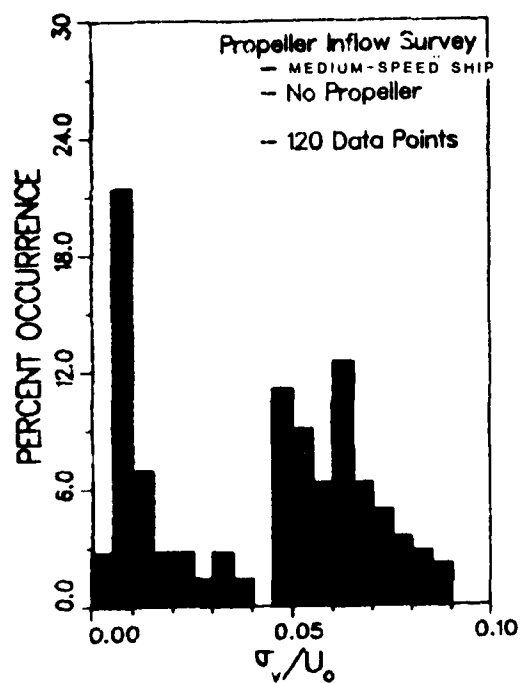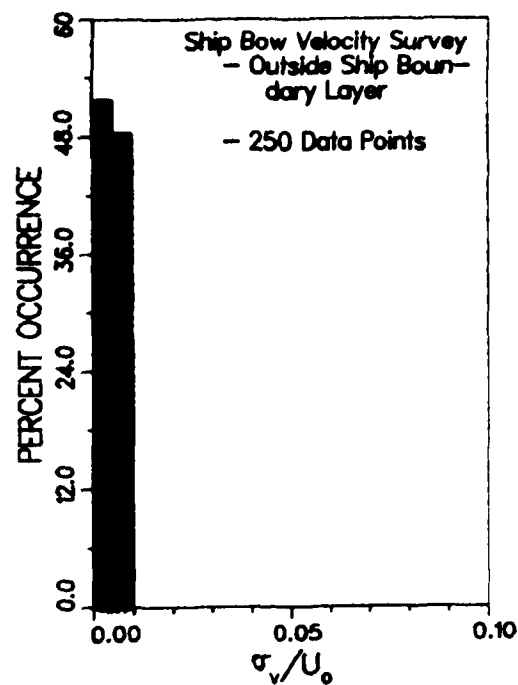
Figure 21   Bar Plots of Velocity Fluctuation Magnitude

LDV OPERATING PARAMETER CHOICES

Table 7 is a compilation of information previously listed in tables 1 and 2. It lists the LDV operating parameters and the errors on which they impact. Parameters, for which there is really no user choice to be made, are indicated. The rest are discussed below.

Frequency Shift

Experience has shown that only a few frequency shifts make sense at possible model towing speeds. Examples of these are:

Streamwise, "U":	0.0, 0.2, 0.5 MHz
Vertical, "V":	0.2, 0.5, 1.0, 2.0 MHz
On-Axis, "W":	0.2, 0.5, 1.0, 2.0 MHz

Figures 22a, 22b, and 22c provide more specific guidance in the choice of frequency shift for each component. Curves in velocity space indicate the velocities for which the indicated frequency shifts will produce 8 (or 16) fringe crossings for particles traveling through the measurement volume center. In other words velocities for which measurement is marginally possible. On one side of the line are velocity component combinations that are measureable (22a - to the right; 22b - above; 22c - left) at the labeled frequency shift and on the other side of the line those that are not measureable.

Depending on the mean velocity component ranges and fluctuation magnitude (discussed above), the LDV user should be able to narrow his frequency shift choices to one or two values for each component. Note that unworkable (too low) frequency shifts will result in the calculation of very high fringe bias errors, E_{FrB}. Frequency shifts that are higher than necessary have higher than needed noise error E_n.

Frequency Filters

From velocity component range, frequency shift, and fringe

Table 7 Operating Parameter - Measurement Error Relationship

MEASUREMENT ERRORS	CHARACTERISTICS				ERROR INPUTS		
	Fast	Slow	Pos. Dep.	Pos. Indep.	Operating Parameters	Flow Field	Equipment
INDIVIDUAL PARTICLE VELOCITY COMPONENTS:							
1. Signal Noise	X			X	I-A,II-A,II-B, II-D,II-E,II-F, III-K	d,e	-
2. Time Digitization	X	X		X	I-A,II-D,II-E	a	-
3. Fringe Spacing		X		X	-	-	3
4. Freq. Shift Vel.		X		X	I-A,III-G	-	1
MEAN FLUID VELOCITY COMPONENTS:							
5. Particle Lag	X		X		II-C	b,d	-
6. Velocity Fluctuation	X		X		II-D,III-C	a	-
7. Velocity Bias		X	X		II-D,III-A,III-H	d	-
8. Fringe Bias		X	X		II-B,II-D,II-E, III-A,III-I	a	-
9. Filter Bias		X		X	I-A,II-A,III-J	a	-
FINAL, DIMENSIONLESS, UNDISTURBED, MEAN FLUID VELOCITY:							
10. Carriage Speed		X	X		-	-	2
11. Velocity Component Direction		X	X		III-E	-	3
12. Flow Disturbance		X	X		III-F	c	4
13. Traverse Positioning Error		X	X		-	c	5

KEY TO ERROR INPUTS:

• Flow Field Characteristics:
a. Velocity fluctuation at measurement
b. Local velocity gradients
c. Towed model velocity field
d. Light scattering speed particles
e. Solid surface proximity to measurement point

• Equipment Characteristics:
1. Frequency shift - signal mixer calibration
2. Carriage towing speed measurement
3. Angle measurement of laser beams
4. Probe strut size and shape
5. LDV traversing accuracy

• Operating Parameters:
Frequency Shift Operating Parameters:
I-A   FREQUENCY SHIFT.........
Counter Processor Operating Parameters:
II-A   INPUT FREQUENCY FILTERS..........
II-B   INPUT GAIN.....
II-C   AMPLITUDE LIMIT.........
II-D   MODE OF OPERATION.........
II-E   Mf OR FRINGE CROSSINGS COUNTED.....
II-F   COUNT COMPARISON ACCURACY........AUTOMATIC
II-G   TIMER EXPONENT CONTROL.........
Computer System Operating Parameters:
III-A RANDOM OR COINCIDENT TRANSMISSION.......RANDOM
III-B TIME BETWEEN MEASUREMENTS.......NOT STORED
III-C TOTAL MEASUREMENTS PER LOCATION.......
III-D DISTRIBUTION OF MEASUREMENT AMONG COMPONENTS.....EQUAL
III-E VELOCITY COMPONENT DIRECTION CORRECTION........
III-F LDV PROBE STRUT FLOW DISTURBANCE CORRECTION.......
III-G FREQUENCY SHIFT - SIGNAL MIXER CORRECTION.......
III-H VELOCITY BIAS CORRECTION........
III-I FRINGE BIAS CORRECTION........NONE
III-J FILTER BIAS CORRECTION.......NONE
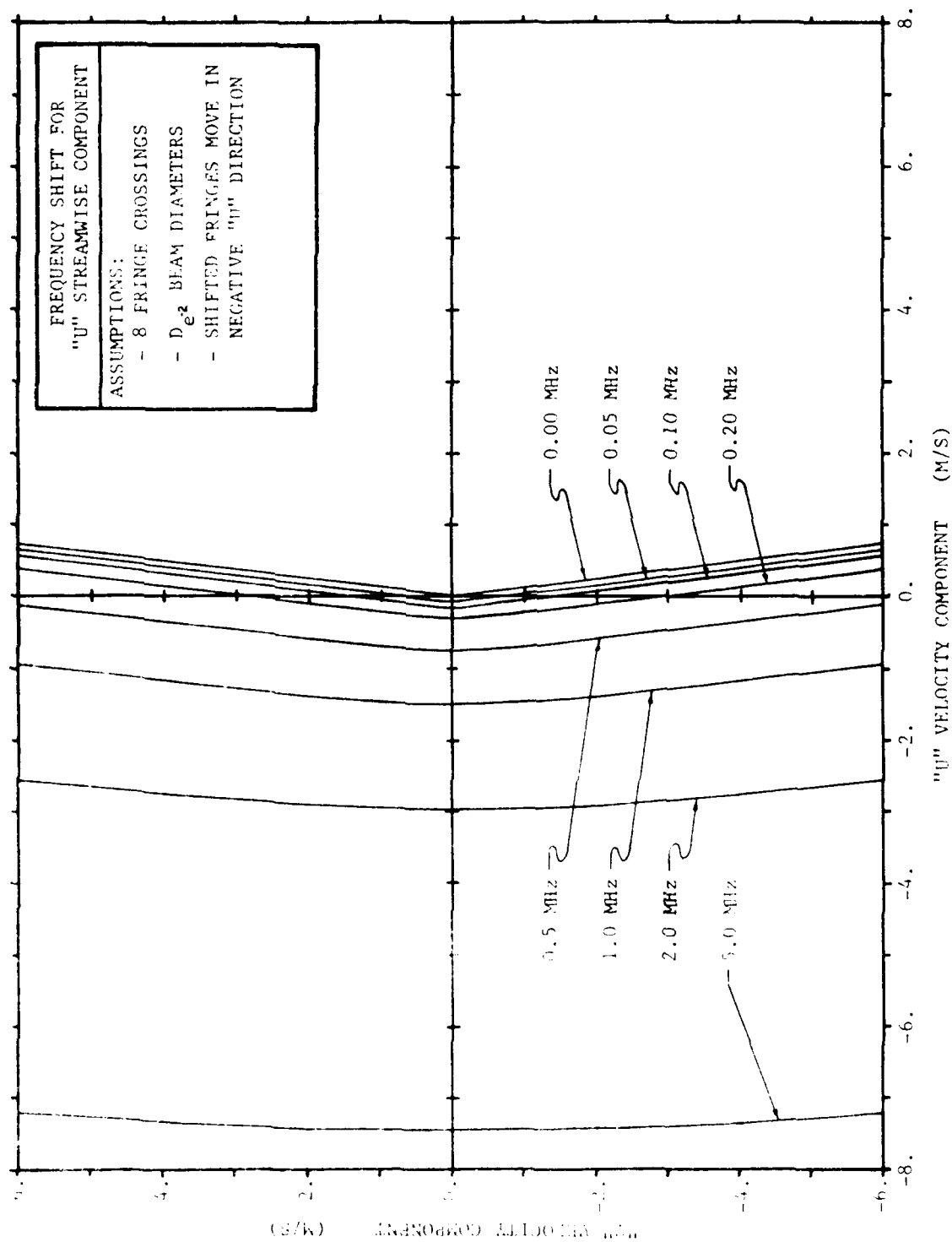III-K ERRONEOUS DATA ELIMINATION.........

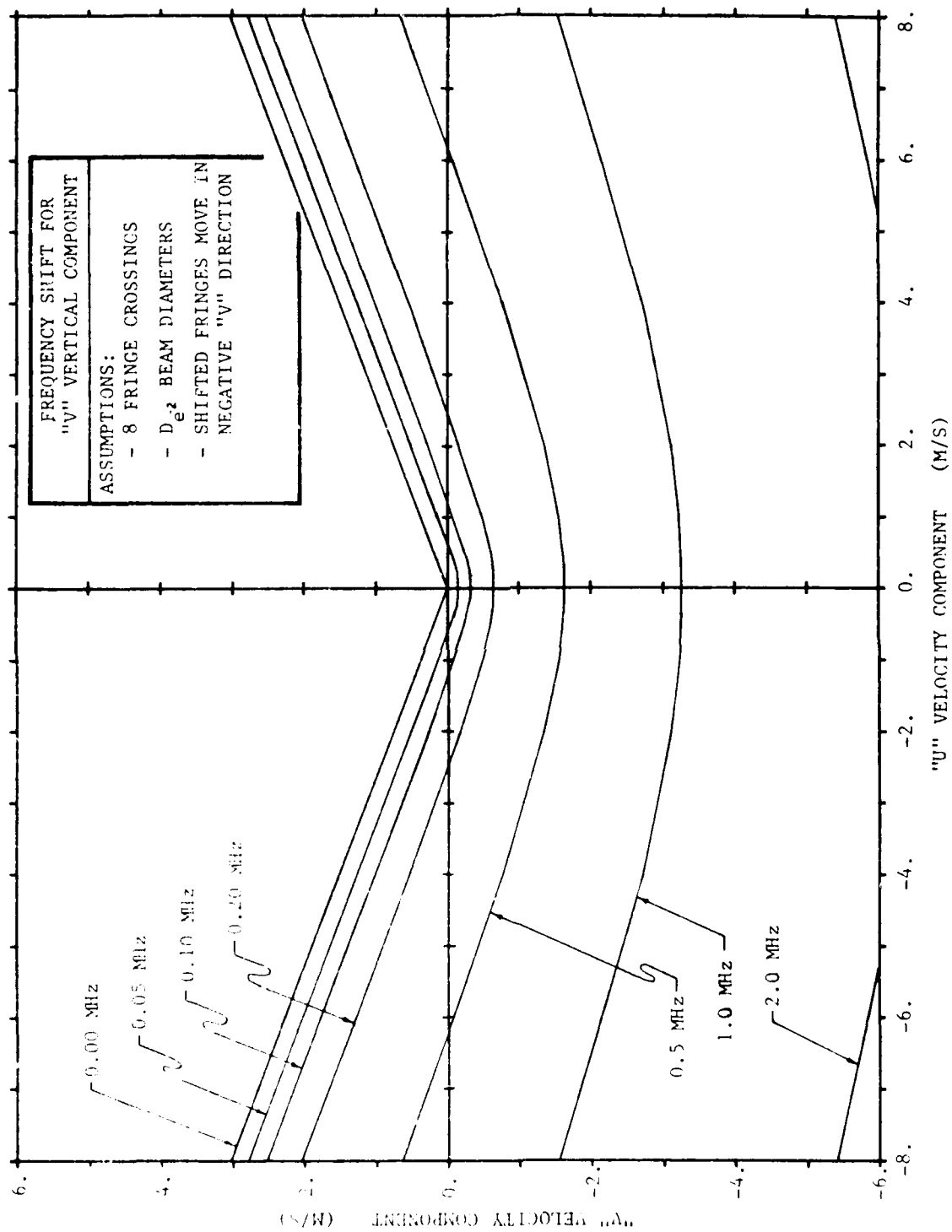Figure 22a   Measurement Ranges as a Function of Frequency Shift

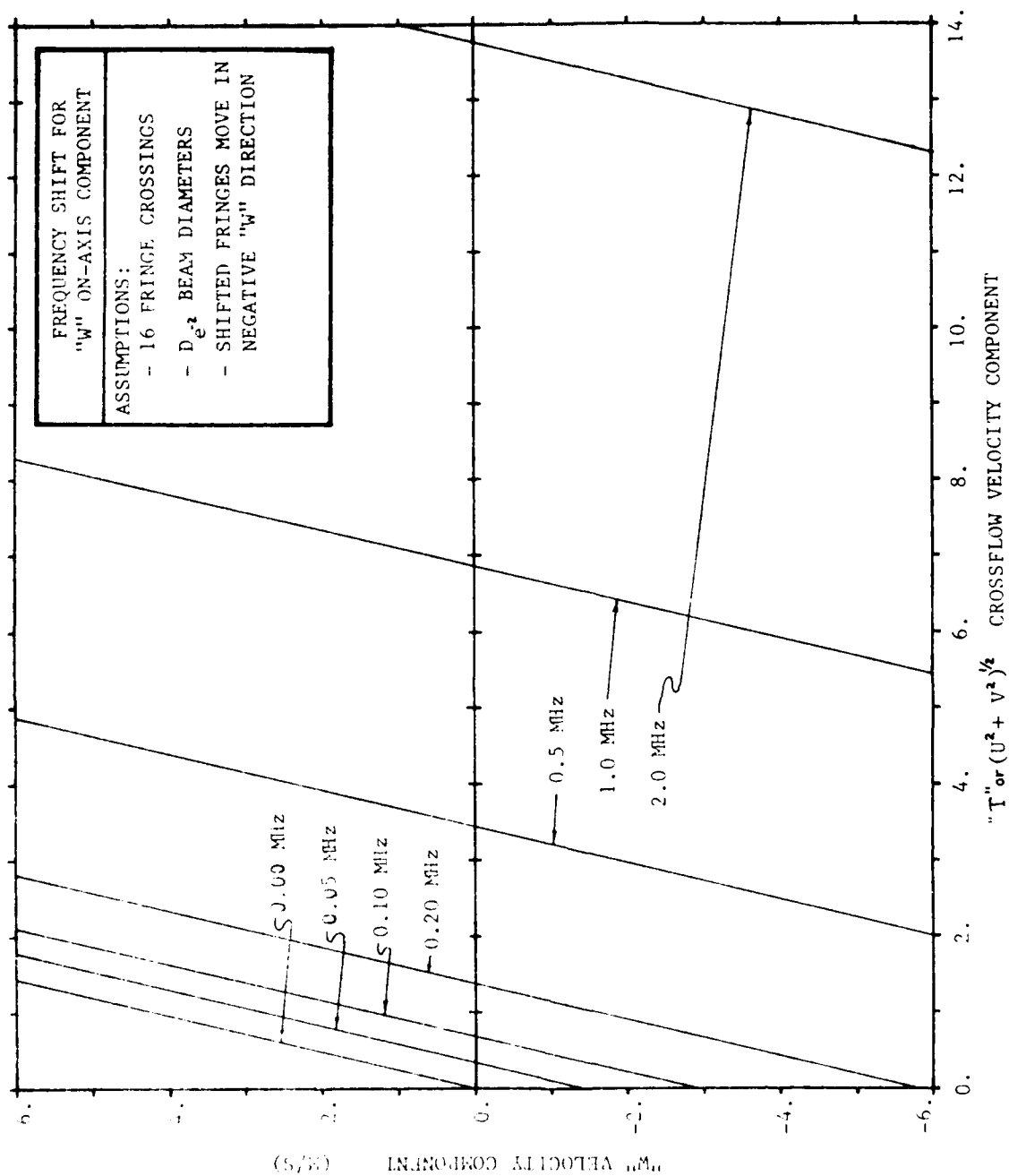Figure 22b Measurement Ranges as a Function of Frequency Shift

71

Figure 22c Measurement Ranges as a Function of Frequency Shift

72

spacing, the LDV user can calculate the signal frequencies that the signal processors will see. The formula for such a calculation is:

$$F = FS + U/S_U \qquad (31)$$

where   FS: Frequency shift (MHz)

        U : measured velocity component (m/s)

        S_U: component fringe spacing (μm.)

Note that a frequency range calculation is necessary for each frequency shift of each velocity component.

The high pass filter setting on the signal processor is not too important and can be set safely below the frequency range. The low pass filter is important in eliminating some signal noise, the LDV user should choose one or possibly two settings that are as close as possible to the maximum signal frequency. The lower the setting, the more noise elimination. If the setting is too low, error calculations of filter bias, E_{FiB} will be large and at least some LDV signals will be noticeably attenuated.

Input Signal Gain

This parameter is set during the experiment when real LDV signals can be observed. It sometimes adjusted during the course of measurements. Noise error, E_n calculations assume that it is adjusted so that the noise between signal bursts has a peak to peak amplitude of less than 50 mV. (or half the signal processor trigger levels).

Amplitude Limit

This adjustment should be turned off. Experience has shown that measured velocities come only from seeded particles. If particle lag error, E_L estimates are too large for the generally used particles (Figure 6), then use of this adjustment can be considered. However, a surer solution is to buy smaller seed particles or classify the seed on hand into a smaller size range. This should normally not be necessary.

Amplitude limit does not enter into the error calculations

except to perhaps change the assumed mean particle diameter of 6 m. used in the calculation of E_L. A key drawback in using the adjustment is that there is no easily determined relationship between setting and maximum measured particle size.

Signal Processor Mode

It is recommended that "TBC" or total burst count mode be employed on all signal processors. This allows the velocity bias correction (based on total cycles per burst) to be done. This mode also permits bad data elimination by comparing primary and secondary fringe crossing timings as assumed in signal noise error, E_n calculations.

"TBM" or total burst mode is the only other mode that allows velocity bias correction but it does not allow timing comparisons.

FRINGE COUNT, M_f

It is recommended that either 8 or 16 be chosen for all signal processors. If an M_f value lower than 8 is chosen then the superior 5 to 8 timing comparison cannot be done. The SNR value used in signal noise error, E_n calculations assumes such a comparison. Also, the higher the fringe crossing count, the greater the possibility that random noise spikes may interrupt proper counter processor threshold crossings. Such data would be invalidated (lowering data rates) or recorded erroneously.

Note that fringe count and frequency shift for each component should be chosen together. Frequency shifts must be high enough to allow all expected velocities to cross at least M_f fringes in the measurement volume. The best "FS" - "M_f" combination trys to:

1. Minimizes the component's noise error, E_n
2. Avoids large fringe bias errors, F_{FrB}
3. Puts the maximum signal frequency very close to a low pass filter choice.

74

Timing Comparison Accuracy

A setting of 1% is recommended for best erroneous data removal. The SNR value used in signal noise error, E_n calculations assumes this 1% comparison value (Table 4).

Velocity fluctuation frequencies are generally much lower than necessary to cause real fringe crossing frequency changes during a single burst timing. If the user is unsure, a comparison can be done between $1/T_{d2}$ (eq. #3) and the expected velocity fluctuation frequency.

Total Number of Measurements, "N"

A recommended value of 768 measurements (256 per component) is suggested unless a combination of tight accuracy requirements and high velocity fluctuation magnitudes warrant more. Note that E_n or E_v errors have to be major errors for an increase in "N" to significantly affect the total error. Also, note that the use of "N" in error calculations assumes that each measurement is independent. Experiment data rates faster than the frequency of velocity fluctuations do not supply completely independent measurements.

Five Data Corrections

Previously described data corrections for component direction, flow disturbance, frequency shift, velocity bias, and positioning errors are always recommended. Note that though these corrections are done during data analysis, they rely on certain measurements that must be taken during the course of the experiment.

Erroneous Data Elimination

The use of Chauvenets' Criterion is recommended in all locations except where velocity component distributions are expected to be far from guassian. Measurement locations that are crossed by the fluctuating edge of a turbulent boundary layer or wake are examples of when not to use any data elimination. Note that such a determination requires careful review of the velocity component histograms and

75

still is usually a judgement call at best.

ERROR CALCULATION COMPUTER PROGRAM

Two versions of an LDV measurement error program "ERROR1" were written. Both computer programs are in "Fortran" and use the error calculation formulas of this report to calculate a total error for each velocity component. They differ only in the sophistication of the output graphics and the computer on which they will run. All individual errors are assumed independent and combined on that basis.

The simplest ERROR1 version runs on the PDP 11-23 computer used in LDV data collection. It outputs error number tables. Error contour plots (in velocity space) are available from the second version written for a HDL-VAX computer generally used for LDV data graphics. The key to the VAX implementation is the availability of the DISSPLA plotting package (version 9.0).

Velocity range and LDV operating parameters are entered interactively by the ERROR1 user. The user also chooses which errors are to be calculated and summed. This allows looking at either individual errors or the total component error. Before any errors are calculated, the user is presented with two tables listing the choices he has made. This is a last chance for changes before calculation proceeds. Figure 23 displays example input tables as they are output by ERROR1.

ERROR1 does the error calculations, outputs the results, and then allows the user to change the velocity ranges, operating parameters, errors calculated, or all three. The calculations are redone as often as the user changes his inputs. The user must keep track of which are the largest errors, because only by improving them can the total error be significantly reduced. In general, fluctuating velocity fields, only:

$$E_n, \ E_f, \ E_v, \ E_{VB}, \ E_{FrB}, \ E_{FiB}, \ \text{and} \ E_a$$

can be significant. Of these E_f is fixed and E_a only responds to the directional data correction. In non-fluctuating velocity fields, the

	U Comp.	V Comp.	W Comp.	T Vel.
Minimum (m/s)	0.30	-1.00	-1.00	0.30
Maximum (m/s)	3.00	1.00	1.00	3.10
Std Dev (/Uo)	0.07	0.07	0.07	0.07
Freq Shift (MHz)	0.000	0.500	0.500	
LP Filter (MHz)	2.000	1.000	1.000	
Fringe Count Mf	8	8	16	
Meas. Count N	256	256	256	
Comb. Correction	X	X	X	
V Bias Correction	X	X	X	

Tow Speed = 3.000 (m/s)

```
Signal Noise Error...........E<n>      X
Time Digitization Error......E<d>      X
Fringe Spacing Error.........E<f>      X
Frequency Shift Error........E<s>      X
Particle Lag Error...........E<L>      X
Velocity Fluctuation Error...E<v>      X
Filter Bias Error............E<FiB>    X
Carriage Speed Error.........E<c>      X
Flow Disturbance Error.......E<i>      X
Velocity Bias Error..........E<VB>     X
Fringe Bias Error............E<FrB>    X
Vel. Comp. Direction Error...E<a>      X
```

```
X X X X X X / X X X X X X / X X X X . X X X X X . X X X
X X X X X X / X X X X X X / - - - - . - - - - - - . - - -
X X X X X X / X X X X X X / - - - - . - - - - - - . - - -
```

Figure 23 "Error1" Input Tables

calculated bias and velocity fluctuation errors are zero except when
FS, M_f, and low pass filter settings mean that a velocity is totally
unmeasureable.   However, despite the calculation, velocity bias is
possible if a sharp local velocity gradient causes the LDV measure-
ment volume to see significantly different velocities at the same
"position". Note positioning error is not addressed by ERROR1.

Example outputs for the three velocity component errors appear
in Figure 24a and 24b.   The simplier output (PDP 11-23 version) and
the contour output (VAX-DISSPLA Version) are displayed side to side
for the same inputs. The simpler output version is analogous to the
contour plot.   But instead of contours, error values on a regular

77

grid (in velocity space) appear. Note that the plot axes are exactly those used previously for Scatter plots (Figure 19) and for Velocity measureability (Figure 22). In fact a superposition of the error contour plot and a corresponding Scatter plot is suggested to visualize and keep track of experimental errors.

The user should carry away from his session with ERROR1, a set of error contour plots corresponding to his experiment's optimum (smallest total error) operating parameters. Actually there may be more than one such plot per component because of uncertainties in mean velocity ranges and velocity fluctuation magnitudes.

Several notes about the ERROR1's characteristics are helpful in making efficient use of the program. The first is that though the program is conveniently available on the small PDP 11/23, it just barely fits into memory and a special linking procedure is required to produce a executable file. In addition whenever velocity or fringe bias errors are calculated, the error calculation procedure takes 3 minutes or more to complete. It takes a few seconds if these two errors are not calculated. The VAX version (when the system is not overloaded with users) is several times faster in the calculations, but each contour plot takes about a minute to plot on the terminal screen. As a printed message explains, unchanged inputs do not have to be continually reentered for each error calculation. Finally both program versions keep track of what inputs have changed from one error calculation to the next. If nothing has been changed to affect a given error, the program simply uses the previously calculated value.
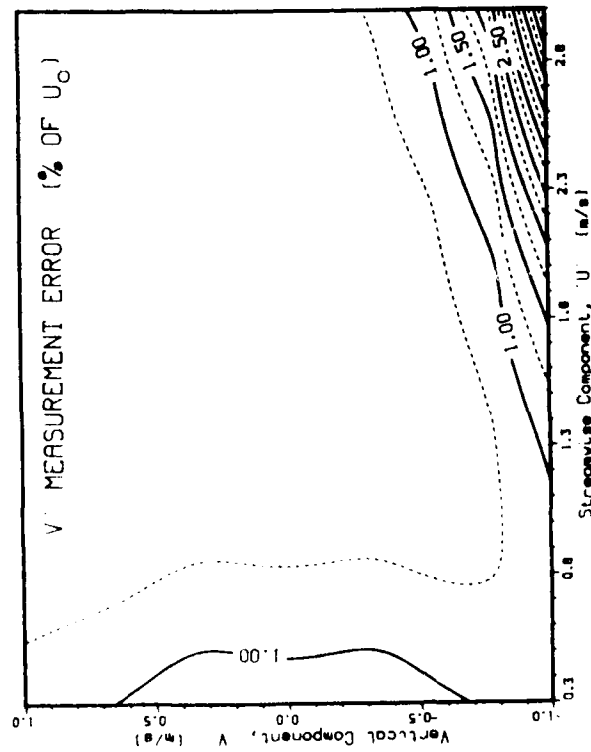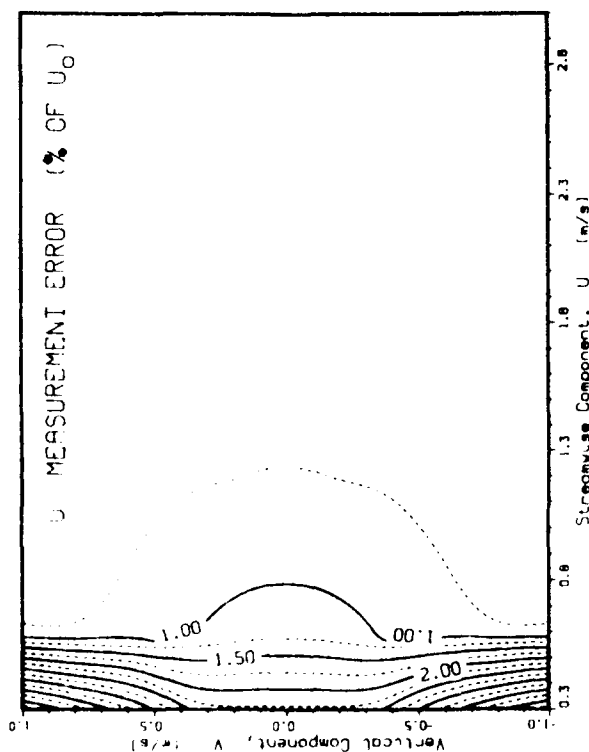
J - Component Measurement Errors
V = 1.0000

0.0441	0.0076	0.0066	0.0064	0.0063	0.0061	0.0060	0.0059	0.0058	0.0058	Filter Bias.........E<F1B>	X
0.0385	0.0076	0.0069	0.0066	0.0064	0.0061	0.0059	0.0058	0.0057	0.0056	Carriage Speed......E<c>	X
0.0320	0.0082	0.0076	0.0070	0.0065	0.0062	0.0059	0.0057	0.0056	0.0055	Flow Disturbance....E<1>	X
0.0238	0.0100	0.0084	0.0073	0.0066	0.0062	0.0059	0.0057	0.0055	0.0054	Velocity Bias.......E<VB>	X
0.0230	0.0114	0.0090	0.0076	0.0067	0.0062	0.0059	0.0057	0.0055	0.0054	Fringe Bias.........E<FrB>	X
0.0230	0.0114	0.0090	0.0076	0.0067	0.0062	0.0059	0.0057	0.0055	0.0054	Vel. Comp. Direction...E<a>	X
0.0238	0.0100	0.0084	0.0073	0.0066	0.0062	0.0059	0.0057	0.0055	0.0054		
0.0320	0.0082	0.0076	0.0070	0.0065	0.0062	0.0059	0.0057	0.0056	0.0055		
0.0385	0.0076	0.0069	0.0066	0.0064	0.0061	0.0059	0.0058	0.0057	0.0056		
0.0441	0.0076	0.0066	0.0064	0.0063	0.0061	0.0060	0.0059	0.0058	0.0058		

V = -1.0000
U = 0.3000   U = 3.0000

Signal Noise........E<n>   X
Time Digitization...E<d>   X
Fringe Spacing......E<f>   X
Frequency Shift.....E<s>   X
Particle Lag........E<L>   X
Velocity Fluctuation...E<v>   X

V - Component Measurement Errors
V = 1.0000

0.0082	0.0073	0.0065	0.0061	0.0059	0.0057	0.0056	0.0055	0.0054	0.0054	Filter Bias.........E<F1B>	X
0.0092	0.0076	0.0066	0.0062	0.0059	0.0057	0.0055	0.0054	0.0053	0.0053	Carriage Speed......E<c>	X
0.0107	0.0080	0.0070	0.0063	0.0059	0.0056	0.0055	0.0054	0.0053	0.0053	Flow Disturbance....E<1>	X
0.0123	0.0089	0.0072	0.0064	0.0060	0.0056	0.0054	0.0054	0.0053	0.0053	Velocity Bias.......E<VB>	X
0.0118	0.0089	0.0072	0.0063	0.0058	0.0056	0.0054	0.0054	0.0054	0.0056	Fringe Bias.........E<FrB>	X
0.0118	0.0089	0.0072	0.0063	0.0059	0.0056	0.0056	0.0056	0.0058	0.0062	Vel. Comp. Direction...E<a>	X
0.0123	0.0089	0.0073	0.0064	0.0060	0.0059	0.0060	0.0063	0.0068	0.0077		
0.0107	0.0080	0.0071	0.0066	0.0064	0.0066	0.0071	0.0079	0.0093	0.0114		
0.0094	0.0080	0.0072	0.0073	0.0077	0.0086	0.0102	0.0126	0.0163	0.0219		
0.0095	0.0090	0.0091	0.0102	0.0122	0.0154	0.0205	0.0287	0.0392	0.0509		

V = -1.0000
U = 0.3000   U = 3.0000

Signal Noise........E<n>   X
Time Digitization...E<d>   X
Fringe Spacing......E<f>   X
Frequency Shift.....E<s>   X
Particle Lag........E<L>   X
Velocity Fluctuation...E<v>   X

U MEASUREMENT ERROR (% OF U_o)
Vertical Component, V [m/s]
Streamwise Component, U [m/s]
1.00 1.50 2.00

V MEASUREMENT ERROR (% OF U_o)
Vertical Component, V [m/s]
Streamwise Component, U [m/s]
1.00 1.50 2.50

Figure 24a   "ERROR1" Calculation Outputs
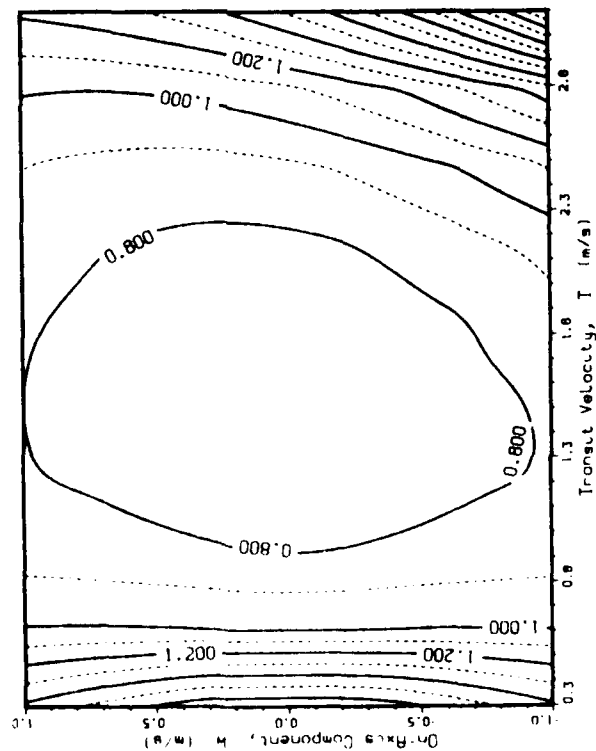
W - Component Measurement Errors

W = 1.0000

0.0142	0.0101	0.0101	0.0081	0.0080	0.0081	0.0084	0.0090	0.0101	0.0122
0.0151	0.0101	0.0101	0.0079	0.0077	0.0078	0.0082	0.0088	0.0100	0.0125
0.0159	0.0101	0.0101	0.0076	0.0075	0.0079	0.0079	0.0087	0.0101	0.0129
0.0166	0.0100	0.0100	0.0081	0.0074	0.0074	0.0078	0.0086	0.0102	0.0136
0.0168	0.0099	0.0099	0.0080	0.0073	0.0073	0.0077	0.0087	0.0106	0.0145
0.0168	0.0099	0.0099	0.0080	0.0072	0.0073	0.0079	0.0089	0.0111	0.0157
0.0166	0.0100	0.0100	0.0081	0.0073	0.0075	0.0079	0.0089	0.0111	0.0157
0.0158	0.0100	0.0100	0.0082	0.0073	0.0075	0.0081	0.0093	0.0117	0.0171
0.0150	0.0100	0.0100	0.0082	0.0076	0.0078	0.0085	0.0098	0.0125	0.0190
0.0142	0.0100	0.0100	0.0084	0.0079	0.0082	0.0089	0.0104	0.0135	0.0213
0.0142	0.0100	0.0085	0.0081	0.0082	0.0086	0.0094	0.0111	0.0147	0.0243

T = 3.1000

W = -1.0000
T = 0.3000

Signal Noise...........E$\langle n \rangle$	X		Filter Bias...........E$\langle F1B \rangle$	X
Time Digitization......E$\langle d \rangle$	X		Carriage Speed........E$\langle c \rangle$	X
Fringe Spacing.........E$\langle f \rangle$	X		Flow Disturbance......E$\langle 1 \rangle$	X
Frequency Shift........E$\langle s \rangle$	X		Velocity Bias.........E$\langle VB \rangle$	X
Particle Lag...........E$\langle L \rangle$	X		Fringe Bias...........E$\langle FrB \rangle$	X
Velocity Fluctuation...E$\langle v \rangle$	X		Vel. Comp. Direction..E$\langle a \rangle$	X

W MEASUREMENT ERROR (% OF U$_o$)

Figure 24b "ERROR1" Calculation Outputs

80

MONITORING EXPERIMENTAL ERRORS

During LDV experiments, a careful user should monitor to some degree the errors of the measurements he is taking. Also, he should complete all calibrations and error checks that will be needed later during data analysis. This section outlines the procedures involved.

PARAMETER SETTING AND ERROR TRACKING DURING EXPERIMENT

Position correction schemes are described in Appendix G based on either static (in drydock) or dynamic (towed LDV system) measurements. Dynamic corrections increase in importance for faster and deeper LDV struts. In addition to position corrections, the "in-tow" condition provides the best time to establish the traverse encoder location of some model reference point(s). Both LDV traverse and ship model strut bending can change with tow speed. Either way the establishment of model reference points is affected.

The user should take care in applying the position correction scheme. As a quick check of proper usage:

1. Traverse the full "Y" range (~1. m) using the LDV software and corrected positions; compare the encoder readout change to the corrected position change; the encoder readout should be on the order of 10 mm larger.

2. Traverse the full "Z" range (~0.5 m) using the LDV software and corrected positions; compare the encoder readout change to the corrected position change; the encoder readout should be on the order of 25 mm larger.

3. Compare software corrected "X" (vertical) positions to encoder readouts: the encoder readout should always be greater than or equal to the corrected position (i.e., higher) but by no more than 1 or 2 mm.

Each experiment should include some initial carriage runs at tow speeds that will be used during measurements. By observing the doppler bursts on an oscilloscope and the computer collected data, the validity of velocity range and operating parameter (arrived at in

81

the previous section) can be checked. The user should make sure:

1. Enough, but not too many, fringe crossings per Doppler burst

2. The next highest low pass filter setting does not noticeably increase burst amplitudes or data rates

3. Doppler bursts are pretty clean with nearly sinusoidal variation with fringe crossings

4. Measured mean velocity components are not out of the assumed range

5. Measured vertical component standard deviation is consistant with the assumed velocity fluctuation magnitude

6. The relationship between data rate and dispersed seed particles is consistent with past experience

Past experience has shown on carriage 2 that an average of 1 tablespoon of seed per pass can yield data rates for all components of $> 15*U_o$ (sec^{-1} where U_o is in m/s). The streamwise and on-axis component data rates are significantly slower than the attainable vertical component data rate.

If the previous "ERROR1" calculations are not applicable to the final parameters or velocity ranges found, then new calculations should be done. With these error contours, the user can start real measurements. He can locate by hand some of his data on the error contour plots. In doing so, he should be on the look out for:

1. Mean velocities exceeding plot ranges

2. Data points occurring in regions of unacceptably high error

3. Vertical Velocity standard deviations exceeding the assumed velocity component fluctuation magnitude

The occurrence of any of these may require operating parameter changes to minimize measurement error. Often the need for parameter changes is dramatically indicated by component data rates falling to zero or measured standard deviations becoming unexpectedly large.

82

RECORDS FOR FUTURE DATA ANALYSIS:

Fringe spacing for the streamwise and vertical components are determined by making measurements on a spinning wheel surface that travels at a very precise speed. An error estimate for this determination was made previously in the discussion of E_f. However, certain assumptions in this estimate may not be justified (a perfectly concentric rotating wheel, equal fringe spacing throughout the measurement volume, etc.). So, instead of one fringe spacing determination (always needed to begin taking data), the user should take four or more. Preferrably the determinations should be independent setups of the calibration wheel and, if possible, at both the beginning and end of any optical alignment.

The description of the velocity component directional error included a description of how LDV measurements taken with no ship model present could by used to wholly or partially correct for several errors. This procedure which consists of two or three carriage passes worth of data should be repeated for every optical alignment during the experiment. Table 8 displays data obtained from such a procedure. The non-zero values for the on-axis and vertical components are assumed due to their misalignment with the streamwise direction. The difference of the streamwise velcity from the tow speed is assumed to be due to fringe spacing measurement error, flow disturbance by the LDV strut, or both.

Finally a data repeatability test should be run at some time during the experiment. This means that data should be repeated at a few locations (at least 20 for every optical alignment) to allow later evaluation of measurement repeatability, as in Figure 25.

83

Table 8   TSI Output Table of Freestream Data

Prev/Velocity Data: [FREE] Tow Statistics
for the AUXILIARY OUTER WAKE SURVEY; PLANE #1: 3.25 KNOTS
.REF

Mpt #	Z (in)	X (in)	Y (in)	Vertical (VM/VT)	Turbulence Intensity (%)	On Axis (VM/VT)	Turbulence Intensity (%)	Stream-Wise (VM/VT)	Turbulence Intensity (%)	Raw Flt	Smp Grp
1	-8.00	-1.00	0.00	0.823355E-01	0.629730E+02	0.151955E+00	0.339133E+02	0.100449E+01	0.904301E+00	2	1
2	-8.00	1.00	0.00	0.854750E-01	0.596891E+02	0.144755E+00	0.332254E+02	0.100298E+01	0.107975E+01	-1	1
3	-8.00	1.00	0.00	0.845920E-01	0.572080E+02	0.145845E+00	0.344261E+02	0.100439E+01	0.107511E+01	-2	2
4	-8.00	1.00	0.00	0.802673E-01	0.583768E+02	0.144046E+00	0.332000E+02	0.100277E+01	0.103740E+01	-1	2
5	-8.00	0.00	0.00	0.843652E-01	0.596222E+02	0.141633E+00	0.341517E+02	0.100349E+01	0.997339E+00	-1	3
6	-8.00	0.00	0.00	0.823454E-01	0.573810E+02	0.143041E+00	0.341372E+02	0.100232E+01	0.100234E+01	2	3
7	-8.00	1.00	0.00		0.570684E+02	0.145575E+00	0.332500E+02	0.100171E+01	0.960099E+00	-1	4
8	-8.00	1.00	0.00		0.569113E+02	0.147291E+00	0.329755E+02	0.100066E+01	0.107752E+01	-2	4
9	-8.00	1.00	0.00		0.585728E+02	0.145166E+00	0.310496E+02	0.998813E+00	0.107045E+01	-1	5
10	-8.00	1.00	0.00		0.472430E+02	0.145202E+00	0.350715E+02	0.100060E+01	0.103667E+01	-2	5
11	-8.00	1.00	0.00		0.477552E+02	0.144471E+00	0.316787E+02	0.997667E+00	0.105699E+01	-1	6
12	-8.00	1.00	0.00		0.443000E+02	0.155994E+00	0.316054E+02	0.998464E+00	0.891453E+00	2	6
13	-8.00	1.00	0.00		0.502019E+02	0.149298E+00	0.329555E+02	0.998241E+00	0.107801E+01	-1	7
14	-8.00	1.00	0.00		0.515685E+02	0.156865E+00	0.291003E+02	0.999116E+00	0.102404E+01	-2	7
15	-8.00	4.00	0.00		0.481248E+02	0.147218E+00	0.292166E+02	0.999116E+00	0.122043E+01	-1	8
16	-8.00	4.00	0.00		0.483702E+02	0.142356E+00	0.294800E+02	0.997739E+00	0.975938E+00	-1	8

FREE STREAM ⟹

3/30/84

STREAMWISE FACTOR (All Pts) = U = .999 U
VERTICAL   FACTOR (All Pts) = V-V = .0093 U
ON-AXIS   FACTOR (All Pts) = W = W = .0491 U

84
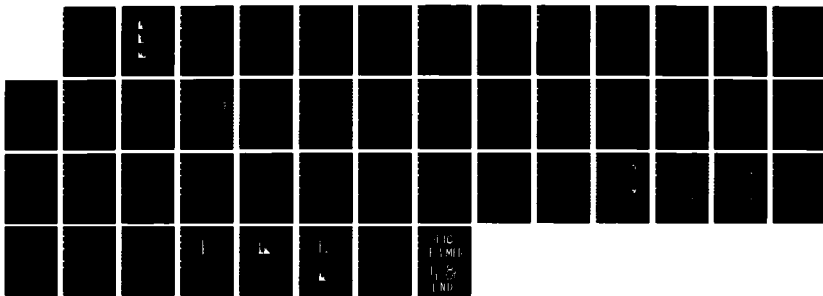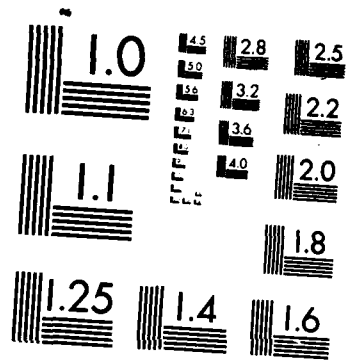
MICROCOPY RESOLUTION TEST CHART
NATIONAL BUREAU OF STANDARDS-1963-A
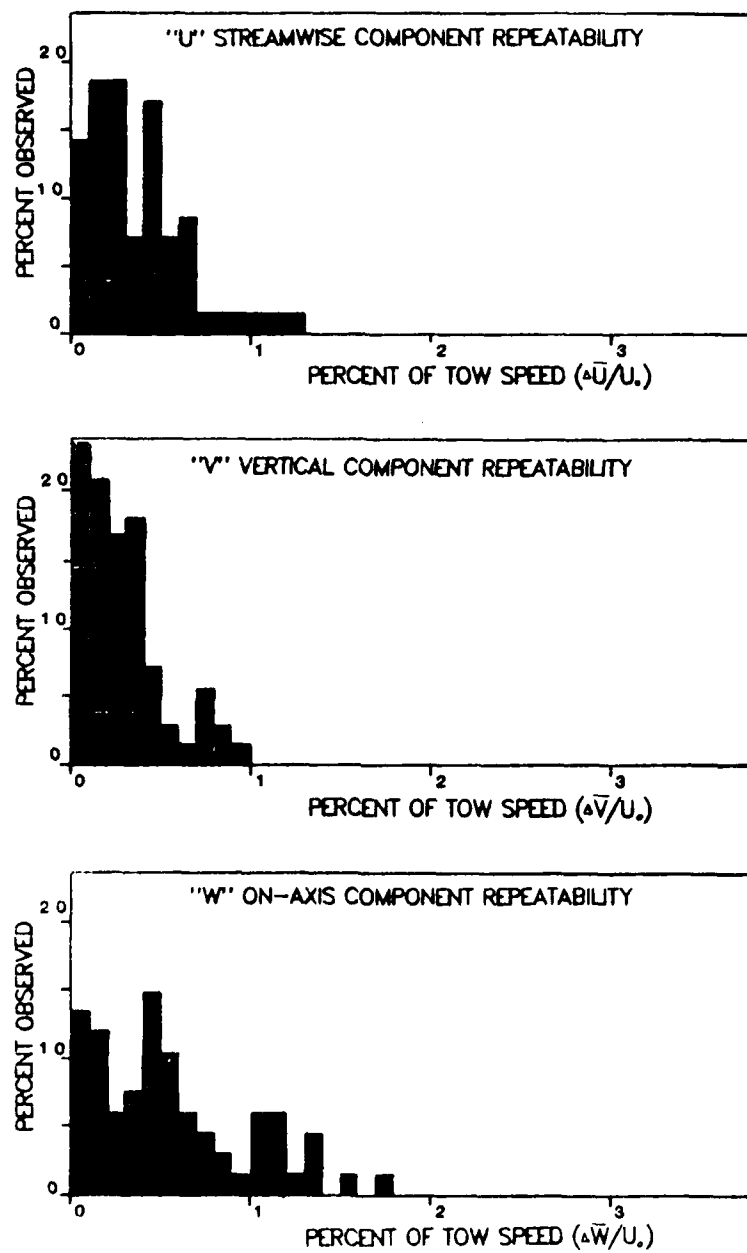
Figure 25 Velocity Component Data Repeatability

FINAL ERROR ESTIMATION

A recommended three component LDV data analysis procedure is detailed in Reference 13. This procedure contains many steps to correct for or evaluate measurement errors. This section will repeat the description of those data analysis steps that concern measurement errors.

HAND CALCULATIONS OF CALIBRATION DATA

The previous section on experimental procedures explained how both freestream LDV measurements and fringe spacing calibrations were to be taken. Assuming this information was properly recorded, it is relatively simple to extract the needed calibration factors.

Data like that displayed in table 8 can be averaged to calculate the correction factors (A_U, A_V, A_W, B_U, B_V, and B_W) as described in the Velocity Component Directional Errors section. As previously mentioned, the "B" factors are of marginal importance and can usually be assumed to be zero.

Freestream LDV measurements of velocity component standard deviations are unique for each experiment's optical alignment and operating parameters. The noise error for each component, E_n, is accurately estimated by the averaging component standard deviations obtained in the steady freestream flow.

The four or more fringe spacing calibrations done for each optical alignment, should be combined to estimate a mean and standard deviation of this measurement. The reliability of these estimates is directly related to the number of independent calibrations done during the experiment. A separate calculation is required for streamwise and vertical calibrations. Since the on-axis fringe spacing is calculated from the streamwise spacing, the means and standard deviations of the two are related (eq. #7 & 8).

COMPUTER PROGRAMS USEFUL IN DATA ERROR ANALYSIS

This section describes the computer programs used in the data analysis procedure[13] that deal with measurement errors. Listings of

the programs discussed appear in References 14 along with other data analysis and data display programs. Here, each program is discussed separately in terms of its purpose, user interaction, and program output.

NORMLZ: Data NORMaLiZation Program

NORMLZ takes any TSI Software Format data table (e.g. see Table 8) and performs certain user controlled corrections and/or normalizations. This includes the component directional error correction and adjustment of position coordinates by an additive constant and non-dimensionalizing length scale. The program is meant to run on the PDP 11-23 data taking computer or equivalent.

User Interaction. The user must create an input file: NORMLZ.DAT to contain the direction correction factors (A_U, A_V, A_W, B_U, B_V, B_W) and position coordinate additive constants and non-dimensionalizing lengths. The exact format of this file is shown in reference 13 and 14. While running the program, the user is asked to verify if each of these adjustments are actually to be used. If the user enters no, then that particular correction or adjustment is skipped.

The program is written to deal with a limited number of data adjustments. It can easily be rewritten to cover a variety of situations that can occur during data aquisition (e.g. erroneous fringe spacings or recorded carriage speeds).

Program Output. The program outputs a data file with table titles and data formats exactly the same as the input data file. Only the position and/or velocity values have been adjusted. A few table titles are also changed to reflect position coordinate non-dimensionalization if it has been chosen.

SCATR1 & SCATR2: Mean Velocity Component SCATteR Plots

These two programs take "Plot-able" LDV data files[13] and mark all data points on a graph whose axes are two velocity components.

SCATR1 plots data for "U" (streamwise component) and "V" (vertical component) axes. SCATR2 plots data for "T" ($[U^2+V^2]^{.5}$) and "W" (on-axis component). The program is written in Fortran, but includes calls to the plotting package, DISSPLA. The program has been run on the HDL VAX computer.

This program is useful in conjunction with error contour plots output by ERROR1 (described in Error Calculation Computer Program section). Together they show an estimate of the range of measurement errors for any component. Also, the plots may be used in establishing velocity component ranges for future, similar experiments. The required frequency shifts and other LDV operating parameters can be established when used with Figures 22a, 22b, and 22c.

User Interaction. The user copies the data file of interest to a file named "XWAKE.DAT" and then just runs the program on a Tektronix or other graphics display terminal. The axes are labeled in velocity components divided by the towing speed, U_o. If the user wishes other than the default axes' bounds, than he need only change the "Call GRAF(....)" program statement.[15]

Program Output. The program outputs a graph with "X"s marking the location of each data point in the LDV data file (Figure 19 and Appendix H). The axes are automatically set and labeled. An error should result if data points are far outside the plot boundaries.

BGRAF1: Velocity Fluctuation Magnitude Bar GRAph

This program looks at the standard deviations of any of the measured velocity components as found on a standard "Plot-able" data file. A bar graph is produced that shows the distribution of standard deviation values for any one velocity component. The program is written in Fortran, but includes calls to the plotting package, DISSPLA. The program has been run on the HDL VAX computer.

The plots (especially the vertical standard deviation) may be useful in establishing velocity component fluctuation magnitudes for

future, similar experiments. Derived values input to ERROR1 when future experimental LDV operating parameters are being determined, would increase the reliability of error calculation results.

User Interaction. The user copies the data file of interest to a file named "XWAKE.DAT" and then runs the program on a Tektronix or other graphics display terminal. The program asks for the component standard deviation to be plotted. The upper bounds of both the standard deviation and the percent occurrence axes are entered by the user after he is prompted by the computer with the maximum values that occur in the data set.

Program Output. The program outputs a bar graph like that shown earlier in Figure 20 and in Appendix I.

BGRAF2: Data Repeatability Bar GRAph

This program looks at the repeatability of the measured mean velocity components as found on any TSI Software Format data file. The file must contain some locations where two or more valid measurements were made. At a repeated location, the difference of each component measurement from the mean measured value is computed. A bar graph is produced that shows the distribution of the absolute value of these differences for a component chosen by the user. The program is written in Fortran, but includes calls to the plotting package, DISSPLA. The program has been run on the HDL VAX computer.

The plots are useful in demonstrating the quality of the velocity measurements and the steadiness of model conditions over different carriage passes, different days, or different experiments.

User Interaction. The user copies the TSI Software Format data file of interest to a file named "REPEAT.DAT" and then runs the program on a Tektronix or other graphics display terminal. The program asks for the particular velocity component to be plotted. The upper bounds of the both the repeatability and the percent occurrence axes are

entered by the user after he is prompted by the computer with the maximum values that occur in the data set.

Program Output. The program outputs a bar graph like that shown earlier in Figure 25.

BGRAF3: Streamwise Fringe Crossings Bar GRAph

This program looks at the frequency of occurrence of different numbers of fringe crossings for the streamwise LDV velocity component. The data is taken from calibration runs (no ship model) when the velocity direction is essentially streamwise. The plot is in the form of a histogram or bar graph. The program is written in Fortran, but includes calls to the plotting package, DISSPLA. The program has been run on the HDL VAX computer.

The input file called "FRINGE.DAT" must be obtained by examining the Raw Data files for a calibration run. The data must have been recorded with the streamwise signal processor in TBC or TBM mode.

User Interaction. The user cannot use any of the normal data table files, but must somehow decode the octal words of raw data files. He must extract from only streamwise words the total fringe crossing number [3,4]. A Fortran program FRINGE was written for the PDP 11-23 data taking computer to do this job. There is only a hard copy output from which the user must generate a FRINGE.DAT file formatted for input to BGRAF3[14]. Afterwards the user runs the program on a Tektronix or other graphics display terminal. The program asks for the particular component to be plotted. The upper bounds of the both the fringe crossings and the percent occurrence axes are entered by the user after he is prompted by the computer with the maximum values that occur in the data set.

Program Output. The program outputs a bar graph like that shown earlier in Figure 9.

ERROR2:   Final ERROR Estimation

This program takes "Plot-able" LDV data files[13] and estimates the component errors for each data point. The calculations are based on the error formulations of this report. Unlike ERROR1, velocity ranges and fluctuation magnitudes are not entered by the user. ERROR2 obtains the information from the measurements at each data point. The program is written in Fortran, but includes calls to the plotting package, DISSPLA. The program has been run on the HDL VAX computer.

This program gives the best possible estimate of the errors present in each velocity component at each measurement point.

User Interaction.   The user copies the data file of interest to a file named "LDA.DAT" and then runs the program on a Tektronix or other graphics display terminal. The user is asked to enter LDV system operating parameters and the errors to be summed (exactly as in ERROR1). The user is also asked for estimates of freestream component standard deviation magnitudes (assumed equal to E_n). Also, a standard deviation of the repeated fringe spacing calibrations is entered for each velocity component (assumed equal to E_f). The origin of both of these last two inputs was discussed earlier in this section under Hand Calculations of Calibration Data.

Program Output.   Output is in two possible forms. A bar graph can be displayed that plots any component's total error magnitude versus frequency of occurrence. Also, a revised data table (ErLDA.DAT) can be output with measured velocity standard deviations replaced by estimates of the total error. Total error means the standard deviation expected for measured component means about the true velocity component mean (as in ERROR1).

The data table ErLDA.DAT can be quite helpful in any LDV data plot. Reference to this table gives error "bars" or limits for each velocity component at each measurement point.

91

REPORT SUMMARY

There is essentially only one way to physically set up the towing tank LDV system. However, once it is in place, the user is confronted with many operating parameter choices before taking any data.

This report attempted to guide the user in making operating parameter choices as well as enable him to quantify the errors present in his measurements at various times. Capabilities and errors are first of all a function of the LDV equipment design and flow field characteristics. However, they are also highly dependent on operating parameters chosen by the user.

The sections of this report were of two types:

1. Background Information
2. Reference Information

Two sections initially supplied background information. The first listed the operating parameter choices for the Towing Tank system and described how they affect LDV measurements. The second listed all possible measurement errors and established their functional relationship to operating parameters, LDV equipment design, and flow field characteristics. Various appendixes supported and amplified the information given.

Three reference sections followed. The first provided guidance in making operating parameter choices and measurement error estimations _prior_ to an experiment. The second described how _during_ an experiment, the user can determine if proper parameters choices have been made. The last section detailed how final error estimates can be made _after_ an experiment for inclusion in written reports.

The main purpose of this report is to provide experimenters with the three reference sections on how to prepare for, execute, and analyze LDV data with the minimum of measurement error. Procedures and computer programs to facilitate proper use of the towing tank LDV system are detailed. The detail of the background section and most of the appendixes are for the user who wants to know more about the operation and errors of LDV systems. In making unusual measurements

92

by modifying the more or less standard mean velocity measurement procedures, this knowledge may be very important.

ACKNOWLEDGMENTS

REFERENCES

1. Fry, D.J., "DTNSRDC Three Component Laser Doppler Velocimetry: Towing Tank Equipment Setup," Report DTNSRDC/SPD 1163-04 in preparation, (Nov 1985).

2. "Towing Tank LDV System Manual," TSI Inc., St. Paul, Minnesota, (1984).

3. "Model 1990 counter Processor Manual," TSI Inc., St. Paul, Minnesota, (1982).

4. "Model 1998 Computer Interface Manual," TSI Inc., St. Paul, Minnesota, (1980).

5. "Standard Frequency Shift Manual," TSI Inc., St. Paul, Minnesota, (1980).

6. "Three Componnet Frequency Shift Manual," TSI Inc., St. Paul, Minnesota, (1982).

7. "LDV Data Reduction Program, DRP-3, User Guide," TSI Inc., St. Paul, Minnesota, (1983).

8. Drain, L.E., "The Laser Doppler Technique," John Wiley and Sons, Inc., New York (1980).

9. Thompson, H.D. and Stevenson, W.H., "Laser Velocimetry and

Particle Sizing," Hemisphere Publishing Corp., Washington, (1979).

10. "Short Course in Laser Velocimetry," TSI Inc., St. Paul, Minnesota, (1980).

11. Dimotakis, P.E., "Single Scattering Particle LDV Measurements of Turbulence," AGARD Conference No. 193 on Non-Intrusive Measurements, (1976).

12. Beers, Y. "Introduction to the Theory of Errors," Addison-Wesley Publishing Company, Inc., Cambridge, Mass, (1953).

13. Fry, D.J., "DTNSRDC Three Component Laser Doppler Velocimetry: Mean Velocity Data Analysis," Report DTNSRDC/SPD 1163-02, (Sept 1985).

14. Fry, D.J. and McGuigan, S., "DTNSRDC Three Component Laser Doppler Velocimetry: Computer Programs for Data Handling and Plotting," Report DTNSRDC/SPD 1163-01, (Sept 1985).

15. "Display Integrated Software System and Plotting LAnguage User's Manual," Integrated Software Systems Corporation, San Diego, California, (Version 9.0, Sept 1981).

APPENDIX A

TRANSMITTING AND RECEIVING OPTICS COMPONENTS
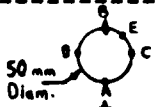
Appendix A: Towing Tank LDV Optics System
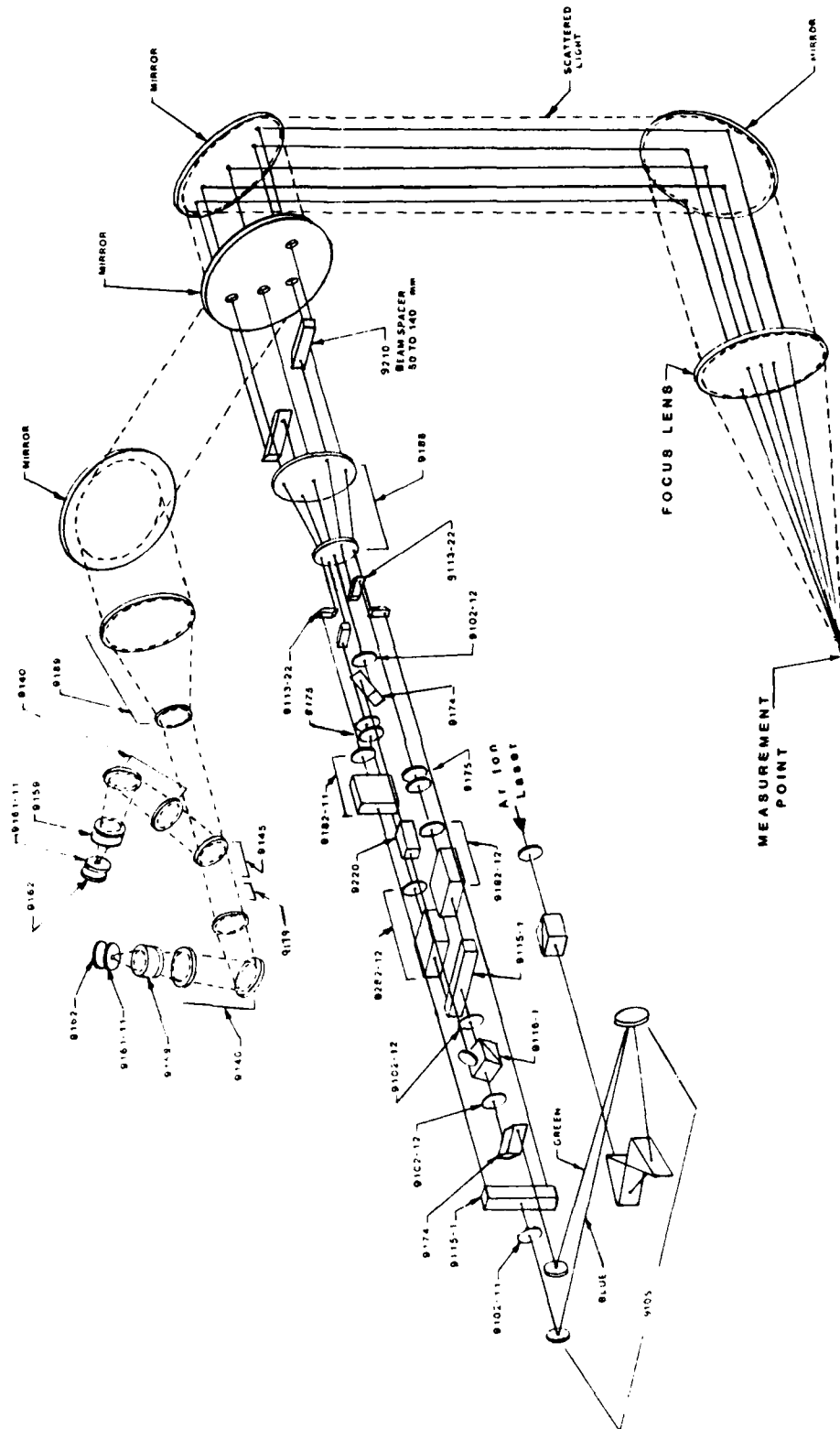
APPENDIX A   TRANSMITTING OPTICS COMPONENTS

Component Description	TSI Model No.	Affected Blue Beams		Affected Green Beams			Beam Pattern
		A	B	C	D	E	
Argon Ion Laser	9196-4	o	o	o	o	o	50 mm Diam.
Beam Collimator	9108	o	o	o	o	o	
Polarization Rotator	9105	o	o	o	o	o	
Beam Splitting Cube	9105	o	o	o	o	o	
Prism Pair	9105	o	o	o	o	o	
Mirror (25 mm Diam.)	9105	o	o	o	o	o	
Mirror (25 mm Diam.)	9105	o	o				
Mirror (25 mm Diam.)	9105			o	o	o	
Polarization Rotator	9102-11	o	o				
50 mm Beam Splitter	9115-1	o	o				
Displacement Prism	9174			o	o	o	
Polarization Rotator	9102-12			o	o	o	
Beam Splitting Cube	9216			o	o	o	
Polarization Rotator	9102-12			o	o		
50 mm Beam Splitter	9115-1			o	o		

98

APPENDIX A TRANSMITTING OPTICS COMPONENTS

Component Description	TSI Model No.	Affected Blue Beams		Affected Green Beams			Beam Pattern
		A	B	C	D	E	
40 MHz Bragg Cell	9182-11		o				
Beam Steering Wedges	9175		o				
40 MHz Bragg Cell	9182-12			o			
Beam Steering Wedges	9175			o			
60 MHz Bragg Cell	9282-12				o		
Beam Steering Wedges	9175					o	
Beam Spacing Adjuster	9220					o	
Displacement Prism	9174					o	
Beam Blockers	9181-3		o	o	o		
22 mm Beam Spacers	9113-22	o	o				
22 mm Beam Spacers	9113-22			o	o		
2.2x Beam Expander	9188	o	o	o	o	o	
140 mm Beam Spacers	9210			o	o		
Mirror (150 mm Diam.)	Special	o	o	o	o	o	
Mirror (150 x 80 mm)	Special	o	o	o	o	o	
Lens (F.L. = 600 mm)	Special	o	o	o	o	o	

APPENDIX A RECEIVING OPTICS COMPONENTS

Component Description	TSI Model No.	Blue Scattered Light	Green Scattered Light	Scattered Light Pattern
Lens (F.L. = 600 mm)	Special	o	o	
Mirror (150 x 80 mm)	Special	o	o	
Mirror (150 mm Diam.)	Special	o	o	
Mirror (200 mm Diam.) with 4 Holes	Special	o	o	
Mirror (200 mm Diam.)	Special	o	o	
3.75x Beam Contractor	9189	o	o	
Color Separator	9145	o	o	
Receiving Optics Module	9140	o		
488 nm. Color Filter	9159	o		
0.28 mm. Aperature	9161-11	o		
Photomultiplier	9162	o		
Receiving Optics Module	9140		o	
514 nm. Color Filter	9158		o	
0.28 mm. Aperature	9161-11		o	
Photomultiplier	9162		o	

APPENDIX B: LASER BEAM WAVELENGTHS

Laser beam wavelengths from transmission in air are well known and highly repeatable.   The two colors used in the towing tank LDV are specified to the tenth of a nanometer.

$$\lambda_{green} = 514.5 \text{ nm} \qquad \text{(in air)} \qquad \text{(B-1)}$$

$$\lambda_{blue} = 488.0 \text{ nm} \qquad \text{(in air)} \qquad \text{(B-2)}$$

The light wavelength in water is modified by water's index of refraction, n.   The index of refraction of water is most affected by water temperature.   Data from reference 13 shows this variation for pure water and 589.3 nm.   light.

$$\lambda_{water} = \lambda_{air} / n \qquad\qquad\qquad \text{(B-3)}$$

"T"	"n"
$14\,^{\circ}C$	1.33348
$15\,^{\circ}C$	1.33341
$16\,^{\circ}C$	1.33333
$18\,^{\circ}C$	1.33317
$20\,^{\circ}C$	1.33299
$22\,^{\circ}C$	1.33281
$24\,^{\circ}C$	1.33262
$26\,^{\circ}C$	1.33241
$28\,^{\circ}C$	1.33219

If the uncertainty in the basin water temperature is $2\,^{\circ}C$ then the uncertainty in the light wavelengths in water is .02% (if towing basin water refractive index follows the table above).

APPENDIX C: PARTICLE LAG ERROR CALCULATIONS

Given that Stokes Law (a "creeping flow" fluid-particle interaction) applies to the particle dynamics, the spherical particle equation of motion is:[8]

$$SG_p * Vol. * dV_p/dt = 3*\pi*\gamma*D_p*(U-V_p) \qquad (C-1)$$

where   Vol.: volume of particle = $0.1667*n*D_p^3$

γ : fluid kinematic viscosity

U : fluid velocity magnitude

D_p: particle diameter

V_p: particle velocity magnitude

Sinusoidal Velocity Variation

Assuming a fluid velocity with mean magnitude $\overline{U}$ and a sinusoidally varying component (amplitude u_o; frequency F_u), the particle velocity response can be derived:

$$V_p(t) = \overline{U} + (u_o*\cos(2*\pi*F_u*t - \emptyset)/(1 + (2*\pi*\tau_p*F_u)^2)^{0.5} \qquad (C-2)$$

where τ_p: $SG_p*D_p^2/ (18*\gamma)$

$\emptyset$: $2*n*F_u*\tau_p$

The error magnitude of interest is the standard deviation of the difference between V_p and $\overline{U}$. This is approximately:

$$E_L = (1/\pi) * (2*\pi*\tau_p*F_u)^2 * (u_o/ U_o) \qquad (C-3)$$

Turbulent Flow Field Accelerations

Using equation C-1, the particle lag velocity can be written:

$$(U-V_p) = (dV_p/dt)*SG_p*D_p^2/ (18*\gamma) \qquad (C-4)$$

102

In turbulent wake flows estimates of the acceleration, dV_p/dt, can be made for fluctuations of various length scales. First we assume that dV_p/dt and dU/dt are approximately equal (which will be true when lag errors are small) and then go on to estimate dU/dt.

For large scale turbulent eddies the length scale is   , the wake boundary layer thickness. The velocity scale is U_o, the towing speed. Thus the acceleration scale is:

$$dV_p/dt \approx dU/dt \approx U_o^2/\varsigma \qquad\qquad (C-5)$$

The smallest scale turbulent eddy that can be detected by the LDV is one whose length scale is equal to twice the LDV measurement volume size, D_{mv}. Turbulent scale arguments[14] assert that turbulent velocity, acceleration, and time scales are a function of only the eddy length scale of interest and the energy production rate ($E \approx U_o^3/\varsigma$) in the boundary layer. Thus the "small" scale acceleration magnitude are on the order of:

$$dV_p/dt \approx dU/dt \approx E^{2/3} * (2*D_{mv})^{-1/3} \qquad\qquad (C-6)$$

$$\approx U_o^2 / (\varsigma^{2/3} * (2*D_{mv})^{1/3})$$

Because the LDV measurement size will usually be smaller than ship model boundary layers, the "small scale" acceleration scale will be the larger of the two acceleration magnitudes. Indeed if it is not, we have no hope of detecting the boundary layer at all. The largest turbulence induced particle lag incorporates eq.#C-6 into its lag error estimation:

$$E_L = (U_o * SG_p * D_p^2) / (18 * \nu * (\varsigma^2 * 2*D_{mv})^{1/3}) \qquad\qquad (C-7)$$

103

APPENDIX D: BIAS ERRORS FOR FREQUENCY SHIFTED LDV

The equations in this appendix are a minor modification of equations found in reference 11. The modifications allow evaluation of biases for frequency shifted LDV systems with "moving fringes". Symbols correspond to those used in reference 11.

Stationary fringes require for a measurement that:

$$\Delta t > M_f * s \ / \ U_x \qquad\qquad (D-1)$$

where Δt: transit time of particle across measurement volume

M_f: fringe crossings needed for valid measurements

s : Fringe spacing

U_x: velocity component perpendicular to fringe planes

Moving fringes (with frequency shift, f_s) require for a measurement that:

$$M_f \leq f_s * \ t \ - \ U_x * \Delta t/s \qquad\qquad (D-2)$$

or

$$\Delta t \geq M_f/(f_s \ U_x/s) \qquad\qquad (D-3)$$

or

$$\Delta t \geq M_f' * s \ / \ U_x \qquad\qquad (D-4)$$

where M_f': $M_f * (U_x \ / \ (f_s * s \ - \ U_x))$

With this modified measurement fringe count, M_f', equation #18 in reference 11 becomes:

$$A/A_o = W * (1 \ - \ \epsilon'^2 * W^2 \qquad\qquad (D-5)$$

where ϵ': $M_f' \ / \ N_f$

N_f: $D_{mv}/ \ s$

Reference 11 develops an equation (19b) useful for calculating the sampling bias for any measurement, U. Modified for frequency

104

shifted LDV systems this equation becomes:

$$B(U; \epsilon') = \begin{array}{ll} |U_x|*W*(1 - \epsilon'^2*W^2) & \text{if } \epsilon'^2*W^2 < 1 \\ 0 & \text{if } \epsilon'^2*W^2 \geq 1 \end{array} \qquad (D-6)$$

where $\quad W^2: \quad 1 + ((U_y*\sin \emptyset/2)^2 + U_z^2) / ((U_x*\cos \emptyset/2)^2)$

$\emptyset$: beam crossing angle

This equation combines velocity and fringe bias into one equation. In an LDV setup (given ' value) with uniform particle concentration, the data rate for any particular velocity U is proportional to "B". Thus 1/B can be used as a weighting factor to determine mean values of the velocity component U_x from data acquired from all particles passing through the measurement volume. These bias effects can be simply separated:

$$B(U; \epsilon') = G_v(U) * G_f(U) \qquad (D-7)$$

where $\quad G_v: \quad |U_x|*W$

$\qquad G_f: \quad (1 - \epsilon'^2*W^2)$

On-Axis Component Bias

The equations in reference 11 and this appendix can be directly applied to biases in the streamwise and vertical components of the towing tank LDV system. Symbols subscripted: "y" are in the on-axis direction, "x" are in the direction of the component being considered, "z" in the remaining direction. For biases in the on-axis direction however, the following definitions must be used:

$$W^2 = (U_x^2 + U_z^2 + (U_y*\sin \emptyset/2)^2)/U_y^2 \qquad (D-8)$$

$$B(U; \epsilon') = |U_y|*W*(1 - \epsilon'^2*W^2) \qquad (D-9)$$

where $\quad$ y : on-axis direction

$\qquad$ x,z: streamwise and vertical directions

105

APPENDIX E: VARIATION OF MEASUREMENT VOLUME CROSSING TIME

The difference between the two schemes of velocity bias correction is the choice of weighting factors. One scheme uses a computed rate of arrival of particles (proportional to $1/\overline{T}_B$). The other scheme uses individual measurements of crossing times, T_{Bi}. The individual measurements vary around $\overline{T}_B$ according to the degree which:

1. a particle trajectory misses the measurement volume center

2. noise causes the signal processor to perceive a premature end of the LDV signal burst

This variation induces an additional source of variation of weighted velocities about their true mean.

An estimate of the standard deviation T_{Bi} can be calculated by assuming that every particle that passes through the measurement volume ellipsoid is measurable and there is no "on-axis" velocity. This is a conservatively high estimate of the T_{Bi} standard deviation because it includes the very short T_{Bi} values for trajectories that barely penetrate the ellipsoid (where in reality less than M_f fringes would be crossed). Figure E-1 illustrates the geometry of the calculation that follows. A crossing distance variation is calculated first and then a crossing time variation inferred.

on ellipsoid surface:
$$Y = \sqrt{\ell^2 - \left(x/a\right)^2 - \overline{z}^2}$$
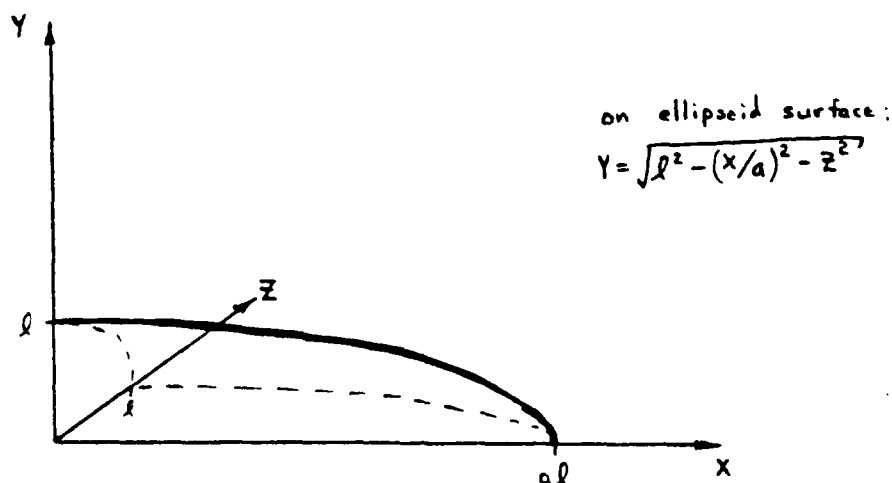
Figure E-1   Measurement Volume Ellipsoid Geometry.

Find the mean vertical crossing distance, $2*\overline{Y}$.

$$\overline{Y} = \int_0^{aL} \int_0^{\sqrt{L^2 - (X/a)^2}} (L^2 - (X/a)^2 - Z^2)^{0.5} \, dZ*dX \ / \ (\pi*a*L^2/4)$$

$$= \int_0^{aL} (\pi/4)*[L^2 - (X/a)^2]*dX \ / \ (\pi*a*L^2/4)$$

$$= [L^2*X - X^3/(3*a^2) \Big|_0^{aL}] \ / \ a*L^2$$

$$= 2*L/3 \hspace{4cm} or \ 2*\overline{Y} = 4*L/3$$

Find the mean vertical crossing distance squared, $\overline{(2*Y)^2}$

$$\overline{Y^2} = \int_0^{aL} \int_0^{\sqrt{L^2 - (X/a)^2}} (L^2 - (X/a)^2 - Z^2) \, dZ*dX \ / \ (\pi*a*L^2/4)$$

$$= \int_0^{aL} (2/3)*[L^2 - (X/a)^2]^{1.5}*dX \ / \ (\pi*a*L^2/4)$$

$$= [8/(3*\pi*a^4*L^2)] \ * \ (\int_0^{aL} (2/3)*[L^2 - (X/a)^2]^{1.5}*dX)$$

$$= [8/(3*\pi*a^4*L^2)] \ * \ [3*\pi*a^4*L^4/16]$$

$$= L^2/2 \hspace{4cm} or \ \overline{(2*Y)^2} = 2*L^2$$

The mean crossing distance then is $2*\overline{Y} = 4*L/3 = \overline{D}$. The standard deviation of crossing distance is:

$$\sqrt{2*L^2 - (4*L/3)^2} = 0.471*L = 0.354*\overline{D}$$

If the crossing distance has a standard deviation of 35% about its mean value, then the crossing times of particles will have a standard deviation about their mean of at least the same percentage.

107

The distribution about $\overline{T}_B(U)$ is an error in the weighting function $1/T_{Bi}$ that has a mean of 0 and a standard deviaition of $0.35*\overline{T}_B(U)$. The error is independent of the actual velocity U, and apparently increases the scatter of U about its mean.

$$\sigma_U' = [\sigma_U^2 + (.35*\sigma_U)^2]^{0.5}$$

$$= 1.06 \, \sigma_U$$

APPENDIX F: FILTER BIAS ESTIMATES

Assume that the measurability of any velocity is proportional to the signal voltage amplitude after filtering. As a simplified model of a low pass filter consider figure F-1.

Manufacturer specifications (TSI Inc.; see reference 3) call for a filter roll off of 30 dB/octave of signal voltage. So for every factor of 2 that F_{Sig} is above F_{Filter} the voltage is reduced by a factor of:

$$R = 10^{-(30 \ dB/20)} = .032 \qquad (F-1)$$

A more general formula is:

$$R = (F_{Sig} \ / \ F_{Filter})^{-4.98} \qquad (F-2)$$

Measured frequencies (F_{Sig}) are a function of the velocity component magnitude (U), the fringe spacing (S), and the component frequency shift (FS):

$$F_{Sig} = (U/S) + FS \qquad (F-3)$$
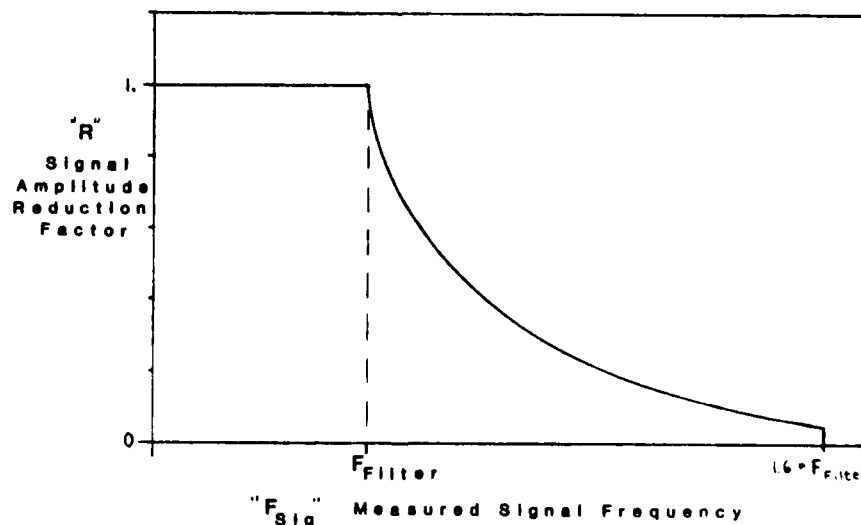
Figure F-1: Low Pass Filter Behavior Idealization

109

Substituting equation F-3 into equation F-2:

$(U/S + FS) > 1.6*F_{Filter}$:

$$R = 0.0 \tag{F-4a}$$

$F_{Filter} < (U/S + FS) < 1.6*F_{Filter}$:

$$R = [(U/S + FS)/ F_{Filter}]^{-4.98} \tag{F-4b}$$

$(U/S + FS) < F_{Filter}$:

$$R = 1.0 \tag{F-4c}$$

Thus for a given random sample of U values, the best estimate of the mean is:

$$\bar{U} = \sum_{i=1}^{N} U_i / N \tag{F-5}$$

while the arithmetic mean of the filter biased data is:

$$U' = \sum_{i=1}^{N} R_i *U_i / \sum_{i=1}^{N} R_i \tag{F-6}$$

$$\text{where } R_i = \begin{cases} 0.0 \longrightarrow FS + U_i/S > 1.6*F_{Filter} \\ 1.0 \longrightarrow FS + U_i/S < F_{Filter} \\ [(U/S + FS)/F_{Filter}]^{-4.98} \longrightarrow \text{otherwise} \end{cases}$$

The difference between the two mean velocity measurements is the filter bias "error" plotted in Figure 11. The curves in this figure were developed assuming a guassian distribution of the measured frequency about its mean (mean: $\bar{F}_{Sig}$ and standard deviation σ_{Sig}).

110

APPENDIX H: TRAVERSE POSITIONING ERRORS DUE TO BENDING

Positioning error values P_x, P_y, and P_z are defined as the traverse encoder reading minus the actual LDV measurement location. These errors can be significant and in a worst case may reach 25 mm or more. In this section (as previously), the positive traverse coordinate directions are: "X" - up; "Y" - south, on-axis; "Z" - east, streamwise. Careful measurements of the traverse system structural bending were made with a very accurate inclinometer (30 seconds accuracy). A mill table and calipers were also used to measure directly position errors. The following observations were made.

1. Over the range of possible "X" values (-.25 m. to +.25 m.) there is no evidence of structural bending changes or therefore direct position error changes. However there is a clear indication of an indirect effect on the Y - P_y and Z - P_z error relationships

2. Over the range of possible "Y" values (-.50 m. to +.50 m.) the P_x positioning error varies from 0.0 to +1.5 mm and the P_y error varies from -7.0 to +4.0 mm. The P_z position error does not seem to change significantly.

3. Over the range of possible "Z" values (-.25 m. to +.25 m.) the P_x positioning error varies from 0.0 to +1.5 mm and the P_z error varies from -12.0 to +10.0 mm. The P_y position error does not seem to change significantly.

4. Traverse structure inclination changes depend on where in the structure you measure it. The structure below and including the inner vertical traverse tube bends more than the outer fixed tube and structure attaching the traverse system to the carriage. Inclination variations of sections of the traverse rails are slightly larger than those measured on the strut or probe box.

5. There is indirect evidence of P_x, P_y, and P_z errors depending on the pivot position or distance of the vertical traverse tube from the carriage A-frame mount. In pivot

position 3 (close to the A-frame) the strut inclination changed by 12.5 minutes over the entire Y traverse range. In pivot position 11 (further from the A-frame) the strut inclination changed by 15.0 minutes over the entire Y traverse range. Pivot position 3 is recommended for all LDV tests to minimize structural bending and still accommodate all traverse vertical angles.

6. There is evidence that side to side bending angles (Θ_{SS} in X-Y plane) are substantially independent of X and Z position. There is also evidence that front to back bending angles (Θ_{FB} in X-Z plane) are substantially independent of X and Y position.

7. Both positioning error and bending angle measurements show evidence of errors due to hysterisis. This may account for much of the data scatter and represent the accuracy limit of the following correction scheme.

Simple Model of Positioning Error

Assume that the traverse structure is completely rigid except for bending at one point, a "bending point", somewhere along the axis of the vertical traverse. There is an axis or Y,Z position where ther are no moments or bending about this point. An approximate calculation and symmetry condition place this "balanced axis" at Y = .1 m. and Z = 0.0 m. (see figure G-1). The sign of the Y location depends on whether the strut is north (+) or south (-) of the measurement point.

Consider for each traverse location that a move is made from the balanced axis to that traverse location with <u>no bending allowed</u>. Then the structure is allowed to bend (at the bending point) in response to the moments created by the traverse. All movements of the LDV measurement volume caused by this bending are the positioning errors at that traverse location.

In this model bending moments and hence bending angles are only functions of Y and Z position. X position contributes only to the

112

Y_{Bal}:

    assume: 1. assymetric loading is caused only by probe
                strut which weighs 130 lbs.

             2. all other traversing loads are symmetric
                about the location Y = 0.0

             3. symmetric loads total 1000 lbs.
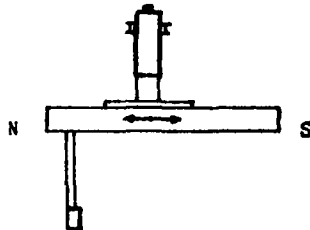
traverse system: idealized system:
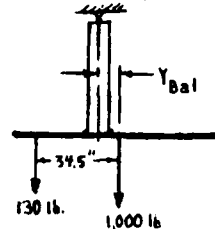
$$1000 * Y_{Bal} = 130 * (34.5 - Y_{Bal})$$
$$Y_{Bal} = 4.0 \text{ in.}$$

Z_{Bal}:

    assume: 1. since strut location is centered in the Z
                direction, there is no assymetric load. So:

$$Z_{Bal} = 0.0 \text{ in.}$$

Figure G-1: Location of Balanced Axis Calculation

positioning errors by changing the vertical distance from the bending
point to the measurement point. The positioning errors P_x, P_y, and
P_z are simple functions of the traverse geometry, the position
(X, Y, Z), and the two bending angles of the traverse $(\Theta_{SS}$ and $\Theta_{FB})$.
Figure G-2 presents a sketch of the simple traverse bending model and
the functional relationships for P_x, P_y, and P_z appear below.

$$P_x \quad (X_0 - X) * (1 - .5*\cos^2\Theta_{SS} - .5*\cos^2\Theta_{FB})$$
$$- (Y - 0.20m) * \sin\Theta_{SS} - Z*\sin\Theta_{FB} \tag{G-1a}$$

$$P_y = (X_0 - X) * \sin\Theta_{SS} - (Y - 0.20m) * (1 - \cos\Theta_{SS}) \tag{G-1b}$$

$$P_z = -(X_0 - X) * \sin\Theta_{FB} + (Z - 0.00m) * (1 - \cos\Theta_{FB}) \tag{G-1c}$$

113
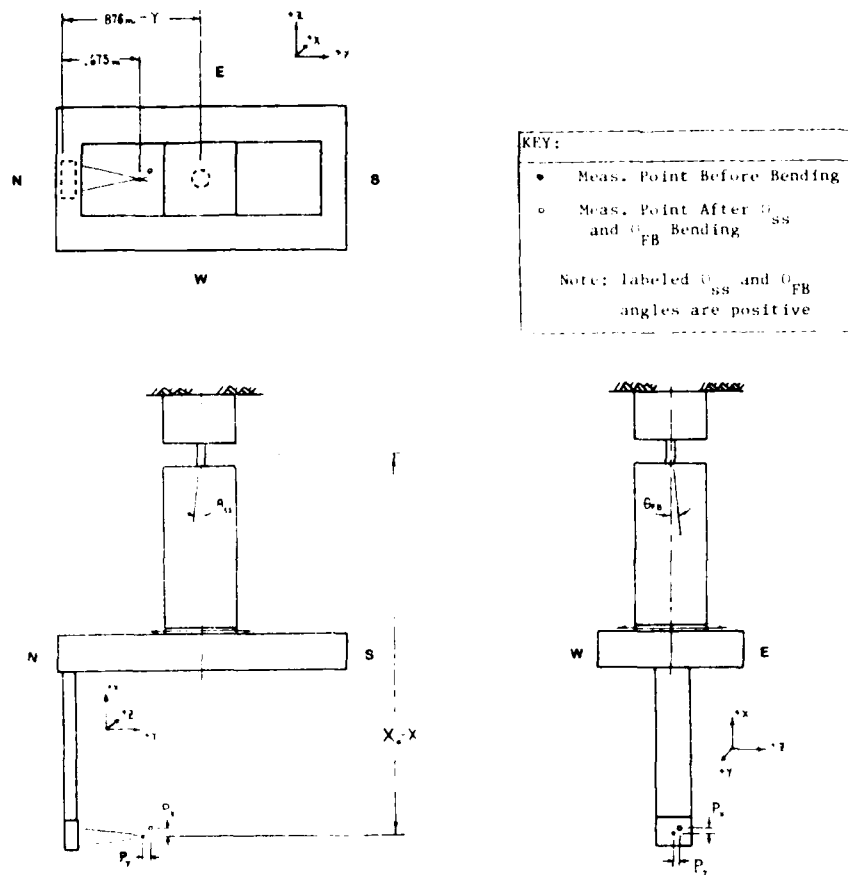
Figure G-2: Simplified Bending Model of LDV Traverse System

Positioning Error Predictions

Since measured magnitudes of Θ_{SS} and Θ_{FB} were not more than $0°\ 20'$, the following approximations are very good.

$$(1 - \cos \Theta_{FB}) = (1 - \cos \Theta_{SS}) = 0.000 \qquad (G-2)$$

$$\sin \Theta_{FB} = \Theta_{FB} \quad \text{(in radians)}$$

$$\sin \Theta_{SS} = \Theta_{SS} \quad \text{(in radians)}$$

So:

$$P_x = - (Y - Y_o)*\Theta_{SS} - (Z - Z_o)*\Theta_{FB} \qquad \text{(G-3a)}$$

$$P_y = (X_o - X)*\Theta_{SS} \qquad \text{(G-3b)}$$

$$P_z = -(X_o - X)*\Theta_{FB} \qquad \text{(G-3c)}$$

$$\text{where } \Theta_{SS} = f(Y)$$
$$Y_o = 0.201 \text{ m.}$$
$$\Theta_{FB} = g(Z)$$
$$Z_o = 0.000 \text{ m.}$$

There are three missing pieces of information that are needed to allow this model to predict positioning errors: $f(Y)$, $g(Z)$, and X_o. These can be empirically deduced from a set of data, part of which has already appeared in figures 16 and 17.

Based on optic's platform inclination measurements and traverse encoder readouts, preliminary functions $f'(Y)$ and $g'(Z)$ were obtained. A least square error fit to the data was made, assuming a relational form of angle (Θ'_{SS} or Θ'_{FB}) being a third degree polynomial of position (Y or Z respectively). Figure G-3 graphs these relationships and the utilized data. These optics platform inclination angles were assumed proportional to the needed inclination angles (Θ_{SS} and Θ_{FB}). The following multiplicative constants were defined:

$$K_{SS} = \Theta'_{SS} / \Theta_{SS}$$
$$K_{FB} = \Theta'_{FB} / \Theta_{FB}$$

The unknowns then became three unknown constants: X_o, K_{SS}, and K_{FB}.

The main data set included positioning error measurements as a function of the absolute traverse encoder readouts. It was obtained by careful, direct measurements utilizing a mill table and calipers. P_y and P_z resolutions of .1 mm were possible. P_x resolutions of .25 mm were also possible. The missing constant values were chosen as those that minimized the sum of the errors squared (difference

115
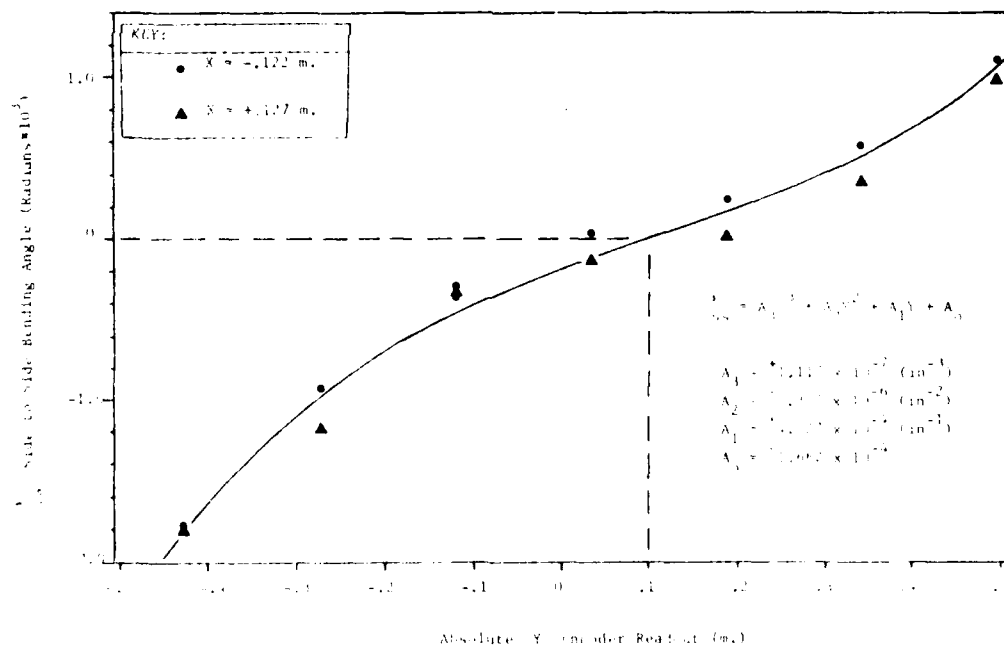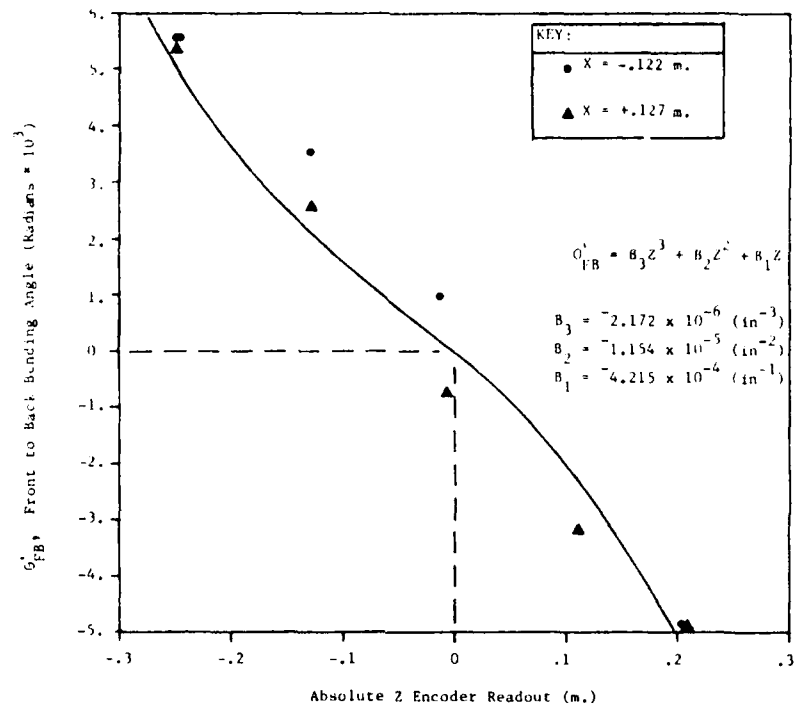
Figure G-3: Bending Angles as a Function of Traverse Location

between measured values of P_x, P_y, P_z and the formula predicted values).

$$X_O = 2.67 \text{ m.} \tag{G-4a}$$
$$Y_O = 0.201 \text{ m.} \tag{G-4b}$$
$$Z_O = 0.000 \text{ m.} \tag{G-4c}$$

$$K_{SS} = 1.273 \tag{G-4d}$$
$$\Theta'_{SS} = A_3 * Y^3 + A_2 * Y^2 + A_1 * Y + A_0 \tag{G-4e}$$

$$K_{FB} = 0.778 \tag{G-4f}$$
$$\Theta'_{FB} = B_3 * Z^3 + B_2 * Z^2 + B_1 * Z \tag{G-4g}$$

Implementing Traverse Positioning Error Corrections

Accelerometers have been permanently attached in the area of the probe strut to optics frame connection. These can be used to monitor Θ'_{SS} and Θ'_{FB} at that point. The initial data set of inclination angles, positions, and positioning errors has already been displayed along with the five derived constants, and two functional relationships (eq. G-4). These were all obtained with the carriage stationary and the strut entirely in the air.

The constant values (X_O, Y_O, Z_O, K_{SS}, and K_{FB}) will be assumed to be relatively unchangeable with time and dynamic strut loadings. They still should be checked every couple of years to ensure that traverse wear is not affecting them. This is also true of the traverse balance point derived in figure G-1 (absolute encoder readouts $Y = +/-0.1$ m.; $Z = 0.0$ m.). The functions for Θ'_{SS} and Θ'_{FB} (figure G-3) will only serve as default relationships because these functions should be rederived every measurement setup. This is possible because the inputs needed to derive these relationships are only the absolute encoder positions and the angle measurements of the permanently attached accelerometers. These inputs can be obtained as before with the carriage stationary. But the best corrections will result if they are obtained during preliminary carriage runs with the model ship attached. The derived functions will correct for the static

as well as dynamic effects.

In order for the towing carriage software to do the positioning corrections during data taking the parameters of this section must be entered into the computer. The "P" selection of the "U" towing tank menu brings up either a "left" or "right" parameter screen (Table G-1). The parameters can be entered directly into this displayed screen from the keyboard. Note that each entered number is at most 8 digits and a decimal point and that all dimensions are in inches. This can be a problem with with the 3rd Power polynomial coefficients which can be on the order of 10^{-7}. So in Table G-1, all polynomal coefficients are multiplied by 1000 and the proportionality constants are divided by 1000.

TABLE G1 - POSITION CORRECTION PARAMETER SCREENS (Right = North Probe Strut;
Left = South Probe Strut)

===

Traverse Deflection Parameters
Side = Right

Absolute Position of Relative Home in (in)	Absolute Position of Balanced Traverse (in)
X = ?.????	X = 105.2
Y = ?.????	Y = 7.91
Z = ?.????	Z = 0.0000

Angle Polynomial Coefficients Y - Axis	Angle Polynomial Coefficients Z - Axis
3rd Power = .0001117	3rd Power = .002172
2nd Power = -.001377	2nd Power = .01154
1st Power = .04527	1st Power = .4215
0th Power = -.1662	0th Power = 0.0000

Angle Proportionality Constants
Y-Axis = .001273
Z-Axis = -.000778

===

Traverse Deflection Parameters
Side = Left

Absolute Position of Relative Home in (in)	Absolute Position of Balanced Traverse (in)
X = ?.????	X = 105.2
Y = ?.????	Y = -7.91
Z = ?.????	Z = 0.0000

Angle Polynomial Coefficients Y - Axis	Angle Polynomial Coefficients Z - Axis
3rd Power = .0001117	3rd Power = .002172
2nd Power = .001304	2nd Power = .01154
1st Power = .04468	1st Power = .4215
0th Power = .1650	0th Power = 0.0000

Angle Proportionality Constants
Y-Axis = .001273
Z-Axis = -.000778

===

119

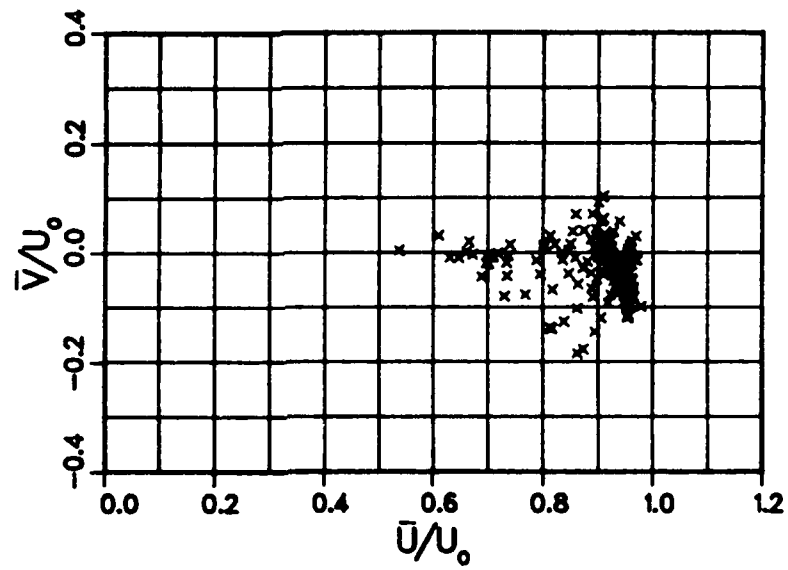APPENDIX H

EXPERIMENTAL MEAN VELOCITY SCATTER
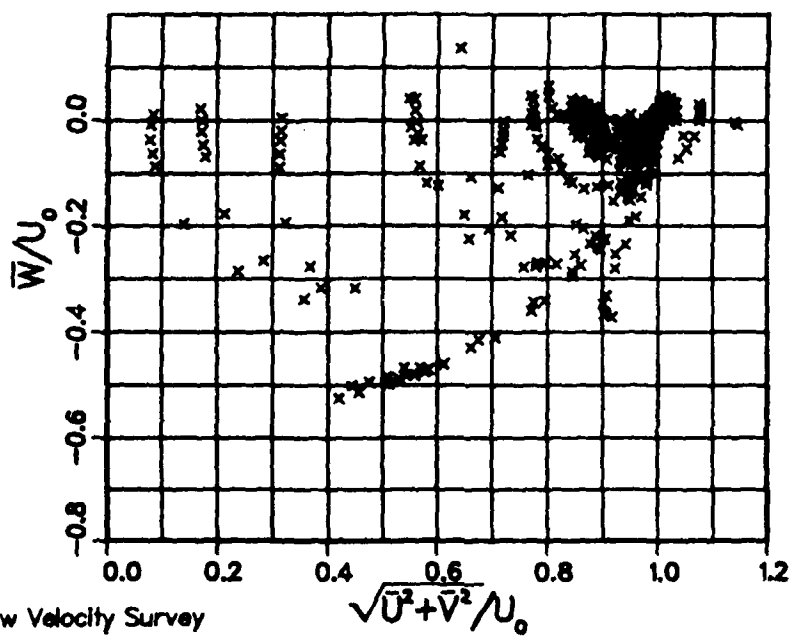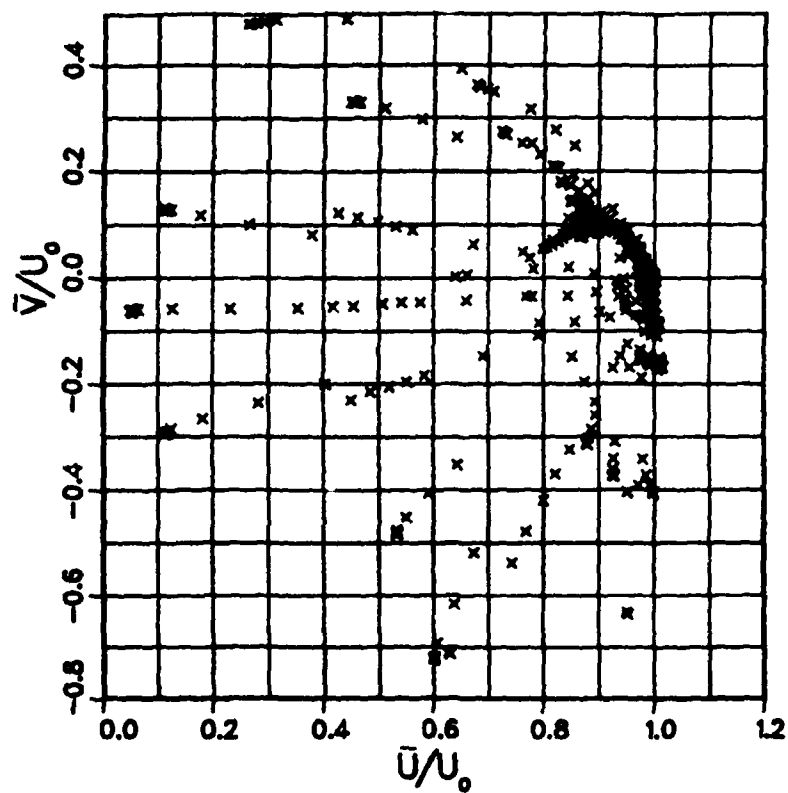
Ship Bow Velocity Survey
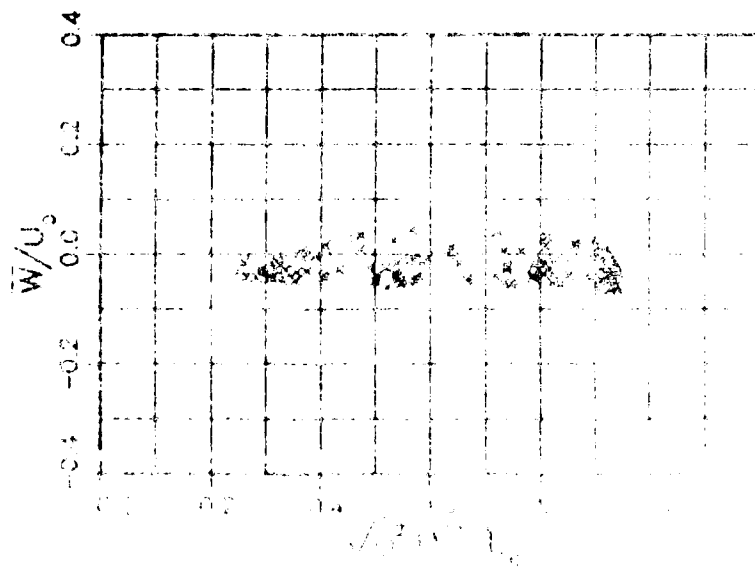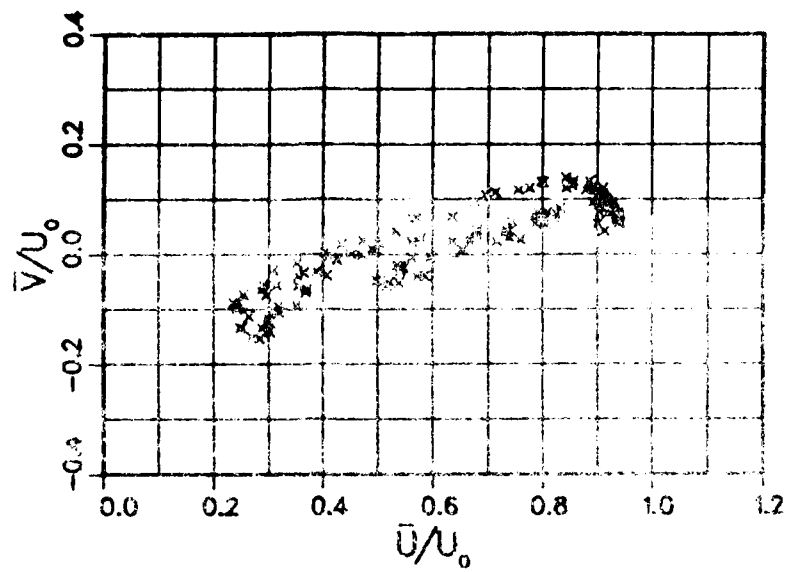− HIGH SPEED SHIP
− Fat, non−protruding
  bulbous bow

121

Ship Bow Velocity Survey
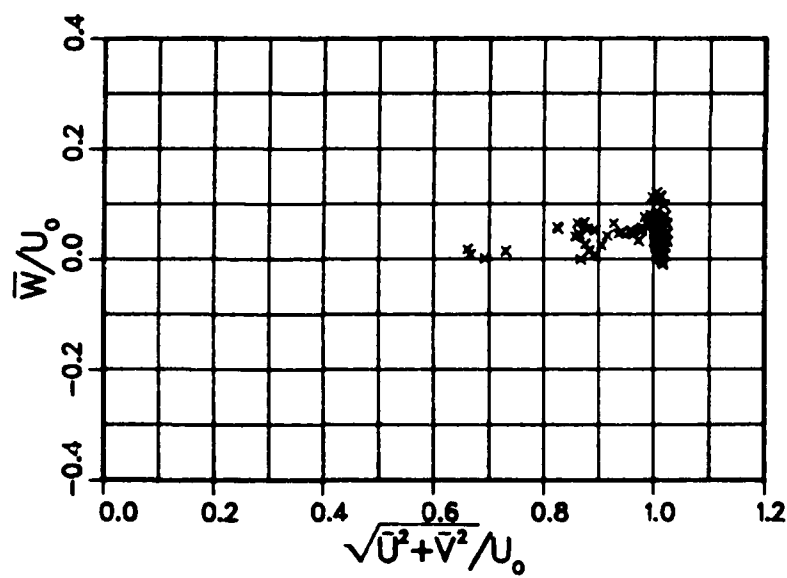- MEDIUM-SPEED SHIP
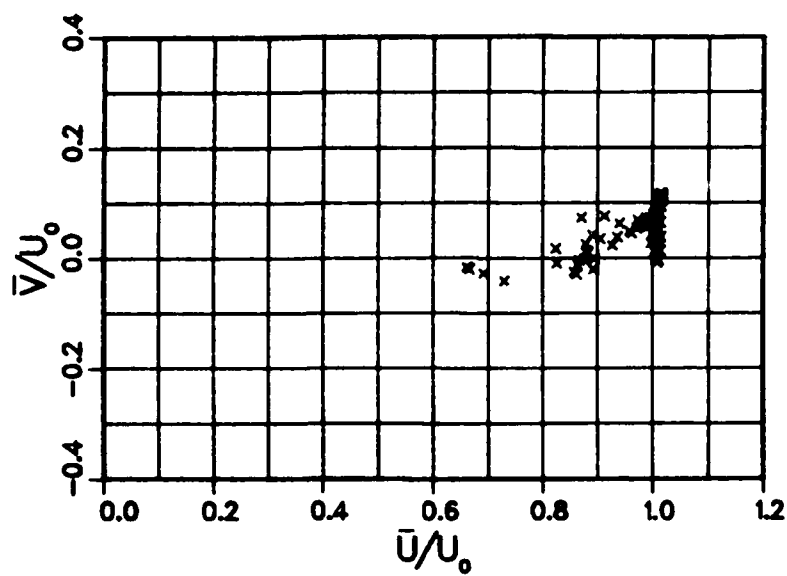- Thin, protruding
    bulbous bow
- Fr = 0.26
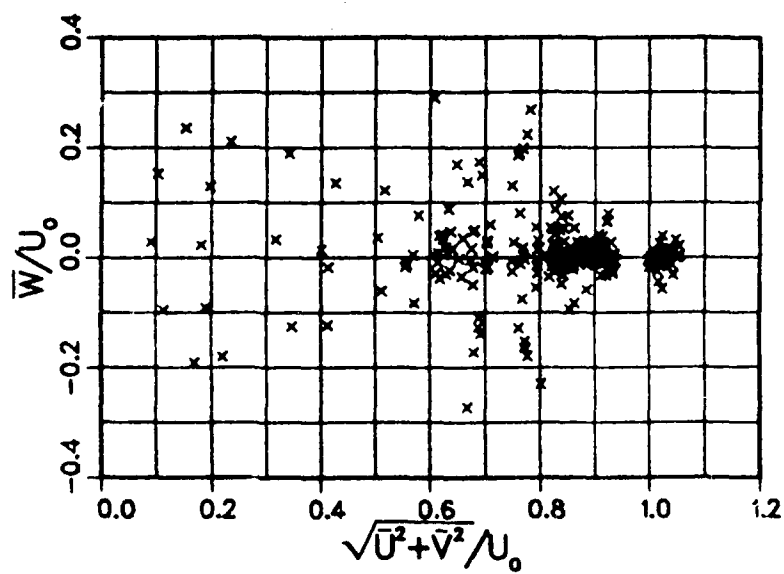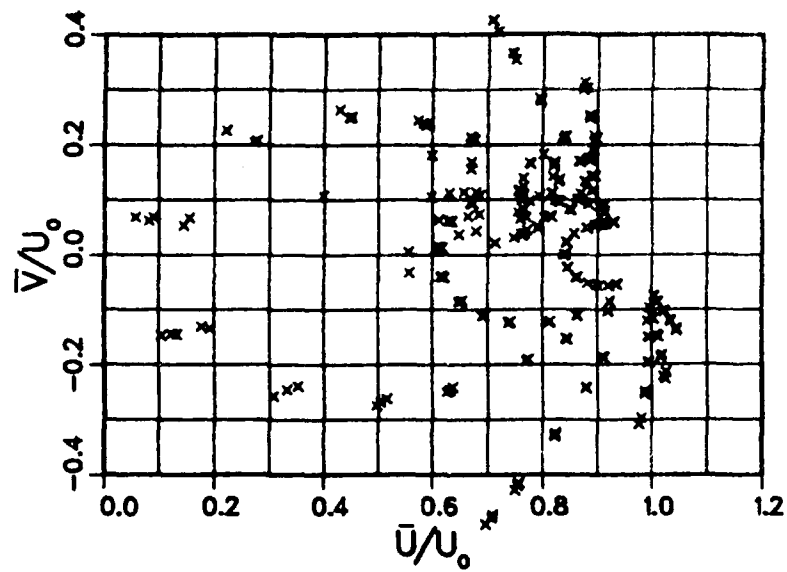
Ship Bow Velocity Survey
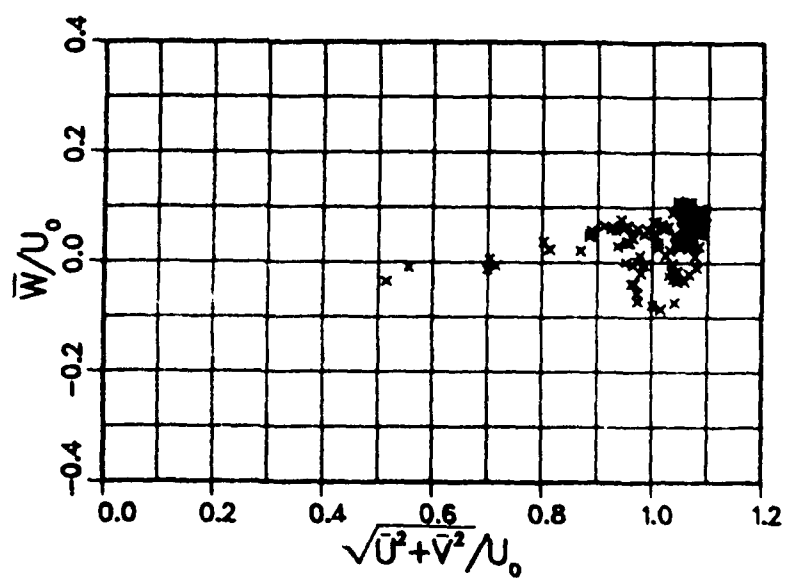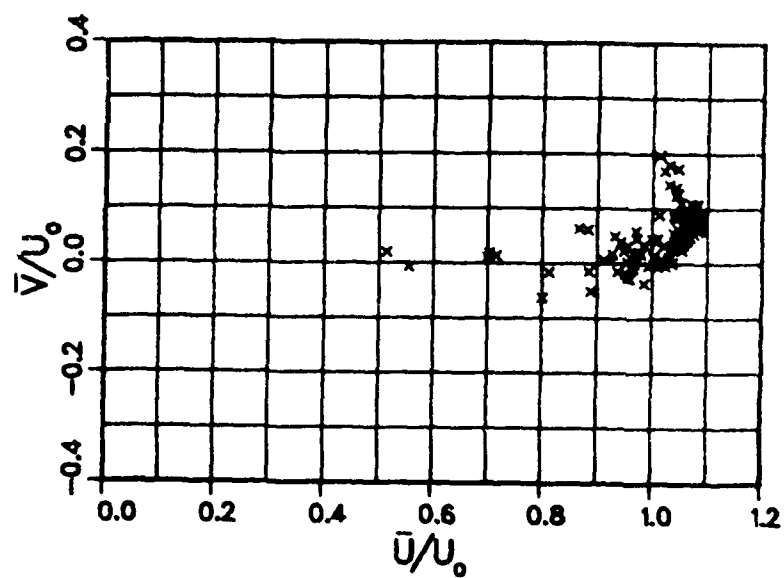— Series 60, Block
60 Hull
— No bulbous bow
— Fr = 0.32
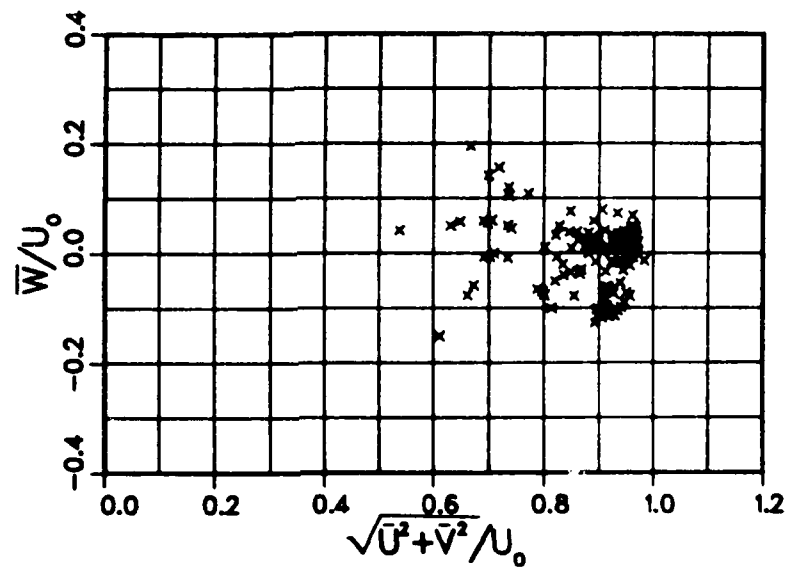
Propeller Inflow Survey
  – MEDIUM-SPEED SHIP
  – No Propeller
  – $U_0 = 2$ m/s

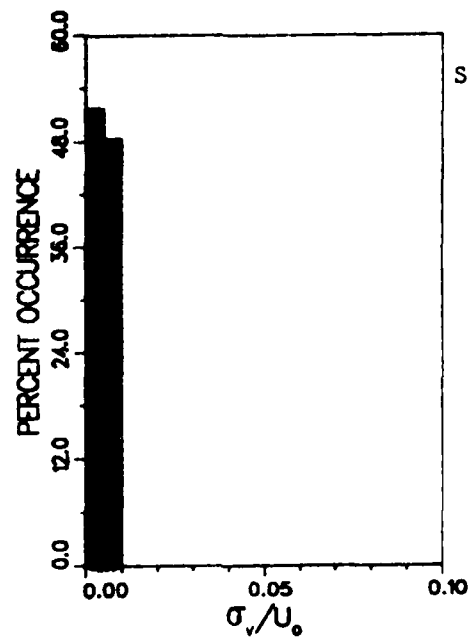Propeller Inflow Survey
  – HIGH SPEED SHIP
  – No Propeller

Propeller Inflow Survey
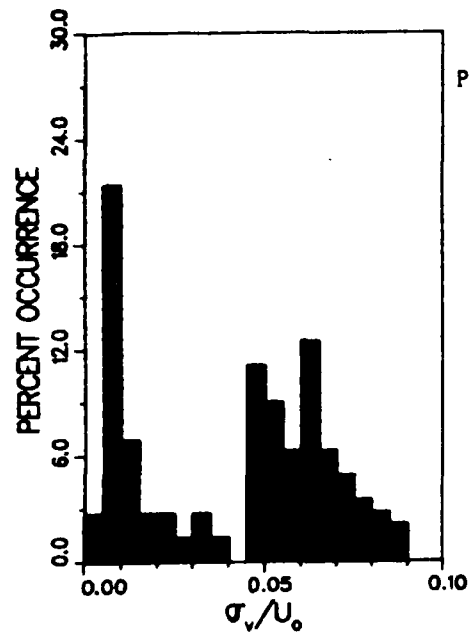 – HIGH SPEED SHIP
  – With Propeller

APPENDIX I

EXPERIMENTAL VELOCITY FLUCTUATION MAGNITUDES
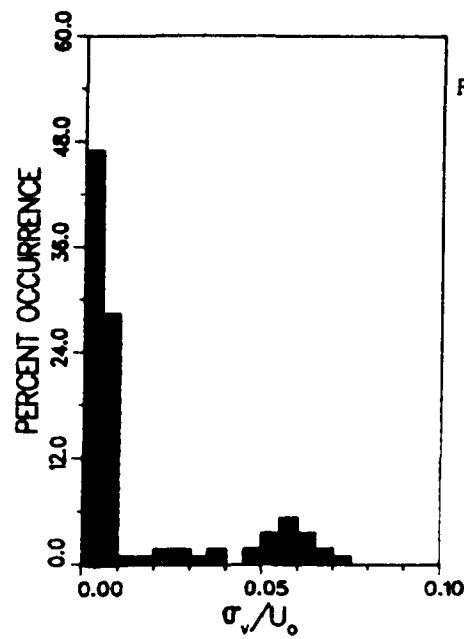
127

SHIP BOW VELOCITY SURVEY

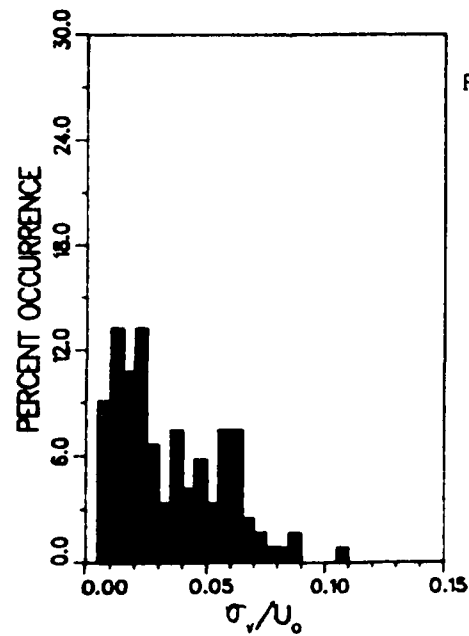- Outside Ship Boundary Layer
- 250 Data Points
- $U_o = 3$ m/s

128

PROPELLER INFLOW SURVEY
- **MEDIUM-SPEED SHIP**
- No Propeller
- 120 Data Points
- $U_o = 2$ m/s

PROPELLER INFLOW SURVEY

- HIGH SPEED SHIP
- No Propeller
- 110 Data Points

PROPELLER INFLOW SURVEY

- HIGH SPEED SHIP
- With Propeller
- 150 Data Points

130

DTNSRDC ISSUES THREE TYPES OF REPORTS

1. DTNSRDC REPORTS, A FORMAL SERIES, CONTAIN INFORMATION OF PERMANENT TECH-
NICAL VALUE. THEY CARRY A CONSECUTIVE NUMERICAL IDENTIFICATION REGARDLESS OF
THEIR CLASSIFICATION OR THE ORIGINATING DEPARTMENT.

2. DEPARTMENTAL REPORTS, A SEMIFORMAL SERIES, CONTAIN INFORMATION OF A PRELIM-
INARY, TEMPORARY, OR PROPRIETARY NATURE OR OF LIMITED INTEREST OR SIGNIFICANCE.
THEY CARRY A DEPARTMENTAL ALPHANUMERICAL IDENTIFICATION.

3. TECHNICAL MEMORANDA, AN INFORMAL SERIES, CONTAIN TECHNICAL DOCUMENTATION
OF LIMITED USE AND INTEREST. THEY ARE PRIMARILY WORKING PAPERS INTENDED FOR IN-
TERNAL USE. THEY CARRY AN IDENTIFYING NUMBER WHICH INDICATES THEIR TYPE AND THE
NUMERICAL CODE OF THE ORIGINATING DEPARTMENT. ANY DISTRIBUTION OUTSIDE DTNSRDC
MUST BE APPROVED BY THE HEAD OF THE ORIGINATING DEPARTMENT ON A CASE-BY-CASE
BASIS.

DTIC
FILMED

4-86

END